ACETYLACETONE AS A LIGAND IN GAS-PHASE EXTRACTION OF GOLD AND IRON

Gareth David Wood

A dissertation submitted to the
Faculty of Engineering and the Built Environment
in partial fulfilment of the requirements
for the degree
Master of Science in Engineering

UNIVERSITY OF THE
WITWATERSRAND,
JOHANNESBURG

August 2022

Declaration

I declare that this dissertation is my own unaided work. It is submitted for the degree of Master of Science in Engineering at the University of the Witwatersrand, Johannesburg. It has not been submitted before for any other degree or examination at any other university.

Abstract

Gas-phase extractions using acetylacetone as a ligand are reported to be a promising alternative method – particularly in gold extraction as an alternative to cyanide leaching. Extraction work has focussed on iron, aluminium, vanadium, and other transition metals. It has most recently targeted gold extraction. While previous extraction work focussed on metal recovery, the fundamental mechanism of extraction is not understood. This dissertation set out to improve the fundamental understanding of gas-phase extractions with acetylacetone as a ligand.

An *ab initio* study of potential gold complexes with density functional theory (DFT) suggested that Au(III) acetylacetonate or **$[Au(acac)_2]^+$** would be the most stable complex out of the following complexes considered: Au(I) acetylacetonate or **Au(acac);** Au(I) thioacetyl acetonate or **Au(Sacac);** Au(I) β-ketiminato substituted variant of acetylacetone or **Au(Nacac);** Au(III) acetylacetonate or **$[Au(acac)_2]^+$;** Au(III) acetylacetonate or **$Au(acac)_3$;** Au(III) thioacetyl acetonate or **$Au(Sacac)_3$;** Au(III) β-ketiminato substituted variant of acetylacetone or **$Au(Nacac)_3$**.

DFT work showed good agreement with previous DFT work on Au β-ketonato complexes. However, the work did not agree with empirical evidence. A gold-acetylacetonate complex synthesis from $AuCl_3$ did not yield any gold-acetylacetonate.

Gas-phase extraction work at 170-190 °C for 30-180 min, on 99.99 % gold beads ranging from approximately 1.0-1.7 g did not yield any detectable gold extraction, measured on ICP-MS, despite the gold samples being several orders of magnitude larger than that of previous gold extraction work with acetylacetone. The extraction work did reveal that acetylacetone may decompose during the process at 165-167 °C – supported by thermodynamic equilibrium modelling and the presence of free carbon detected on the samples in Raman spectra.

Further attempts to replicate some of the earliest previous acetylacetone extraction work on iron followed a similar outcome to gold. No iron extraction could be detected with ICP-MS on extractions from hematite at 220 °C for 200-210 min in both air and nitrogen atmosphere. Pyrite extraction attempts revealed that there is a surface reaction between pyrite and acetylacetone; however, no extraction was measured by mass difference or in concentrations of the condensate measured with ICP-MS.

A full investigation and discussion of previous acetylacetone extraction work found that cumulative summation for plotting extraction curves imposed a linear bias on the curve. Measurement of changes in baseline metal content of acetylacetone condensate could have produced the impression of metal extraction as starting baseline metal content in the acetylacetone was not considered in previous work.

Acknowledgements

I would like to thank my supervisors: Professor Herman Potgieter, Professor Adam Luckos, and Mr Paul den Hoed. Their guidance and expertise has been indispensable in the completion of this dissertation, it has further shaped my approach to problem solving forever.

I would also like to offer my deepest gratitude to Professor Alfred Muller and Dr Rudolph Erasmus for their assistance with X-ray diffractometry and Raman spectroscopy, respectively.

Thank you to DRDGold Ltd. for funding this research and to Professor Herman Potgieter for giving me the financial means to pursue this research.

Finally, I would like to thank my family for always listening to my rambling and acting as a springboard for new ideas and theories. I am grateful.

Contents

CHAPTER ONE

Current landscape of gold extraction

The extraction of precious metals has been, and continues to be, a lucrative business. The most famous of the metals, gold, has been extracted by the dominant cyanide process for the last 100 years (Gökelma *et al. 2016)*. The hydrometallurgical process has seen little change for much of the 20th century as it has had sufficiently high extractions to cover the costs with good profits. However, the cyanide process performs poorly on ores where sulfide minerals such as pyrite (FeS_2) and arsenopyrite (FeAsS) – that are not extracted by cyanide (refractory) – are dominant. This is the case for ores and reprocessed tailings in South African ores from the Witwatersrand basin (Fleming 1992).

The price of gold has risen over 2600 % in the last 50 years from $64/oz to around $1800/oz – driven by new and valuable uses for such metals in electronics, medicine, jewellery, and speculative value. This has led to a move by the mining industry to pursue lower-grade ores and even reprocess tailings and refractory ores in search of profits as high-quality reserves diminish (Teimouri *et al.* 2020). The high prices of gold have made it ever more important to consider waste streams and the possibility of recovering as much as possible from them.

Environmental impact of waste streams has also become an increasingly more influencing factor in gold extraction due to the "polluter pays" approach that has been employed in many countries (South Africa included). Non-cyanide processes have been investigated to prevent harmful effects of waste streams and slimes dames on the environment. An example is bird deaths that are often under reported, which lowers the perceived risk (Donato *et al.* 2007).

Chlorine roasting has been used as an alternative to cyanide for processing low-grade and refractory ores. In this process, gold ore is roasted with calcium chloride at

temperatures between 1000 and 1200 ˚C. High extractions (>79%) from alluvial material have also been demonstrated, at 600^{o} C at laboratory scale (Panias *et al.* 2009, Ojeda *et al.* 2009).

Thiosulfate leaching of gold has also been identified as a possible replacement to cyanide. It is favoured over chloride (highly corrosive) and thiourea which is expensive and a suspected carcinogen (Xu *et al.* 2017). Thiosulfate leaching comparably has low environmental risk and uses cheap reagents. However, the leaching rate is very slow. Whereas catalysed reactions have more promise, high thiosulfate consumption, challenges recovering dissolved gold and uncertainty in its leaching mechanisms require further investigation before full industrial adoption can take place (Xie *et al.* 2014).

More recently, alternative techniques for gold extraction from low-grade and refractory ores have been under investigation. These techniques include ionic liquids, supercritical CO_2, and gas-phase extraction.

Ionic liquids have shown to be highly selective towards gold and silver in a study by Whitehead *et al*. (2009), with extractions using a combination of thiourea and $BmimHSO_4$ (1-butyl-3-methylimidazolium) extracting upwards of 70 % of both metals in a 48-hour period. A similar study by Teimouri *et al.* (2020) considering refractory sulfide ores from South Africa, found that ionic liquid extraction with $BmimHSO_4$ and thiourea was lower than that of cyanide for gold. Nevertheless, ionic liquids still are promising as a more environmentally friendly option, or as the only option in countries have banned cyanide.

Gas-phase extraction of metals has been investigated using β-diketone ligands. β-diketones can form co-ordination complexes with most metals and are promising because of the increased stability from strong hydrogen bonding and their ability to chelate (Carmerman *et al.* 1983). Acetylacetone has extracted iron, vanadium, chromium, and aluminium from oxides (Potgieter *et al.* 2006). Acetylacetone is the simplest β-diketone and has promise to form the basis of an economical gas-phase extraction process. An advantage of the technique is that it is reported to extract metals faster than either cyanidation or ionic liquids (Van Dayk *et al.* 2010).

While gold separation from its acetylacetonate complex has not been demonstrated in the context of extraction processes, gold β-diketone complexes have many potential uses that are under investigation for direct use. However, complexes studied in literature have focussed on liquid-phase synthesis (Zharkova *et al.* 2006, Zharkova and Baidina 2008, Zharkova *et al.* 2010). Some of the most notable applications are the use of gold (III) β-diketone complexes to treat tumours as part of anti-cancer research (Marcon *et al.* 2002), and Metal Organic Chemical Vapour Decomposition (MOCVD) to form ultra-thin metallic films on complex geometric surfaces for use in electronics and as a protective layer (Basova *et al.* 2019).
Gas-phase extraction of gold using β-diketones is in its infancy, and the technical literature is silent on several aspects of the process. Currently there are indications that β-diketones such as acetylacetone can extract gold from low-grade ores in gas-phase (Machiba 2020, Ali 2021). However, the coordination chemistry of the complex remains unclear, and the selectivity of the ligand has not been investigated.

Problem statement and proposition

Traditional cyanide leaching of gold has been an attractive option for many years. As high-quality reserves are depleted, pursuit of the remaining refractory ores has pushed further research into alternative extraction techniques. New techniques have the goal of accessing refractory (to cyanide) gold particles that are surrounded by sulfide minerals such as pyrite. The Global moves towards greater environmental responsibility for waste streams have also placed additional pressure to find alternatives to cyanide as tailings dams can create lasting pollution and degradation of the surrounding environment and harm those that depend on it (Donato *et al.* 2007). This greater environmental conscience – with additional economic motivation – encourages new processes to target all gold within a given source, rather than only the free gold that is targeted by cyanide.
Processing tailings and refractory ores by an alternative process will require high extractions of low-grade material. Gas-phase extraction is proposed to be a suitable solution as greater access to gold can be achieved with a suitable ligand. It may also

be possible to break down pyrite and arsenopyrite simultaneously in gas-phase with the same ligand.

β-diketones are a promising gas-phase extracting ligand as they can form organometallic complexes (Von Hoene *et al.* 1958, Skopenko *et al.* 2004) and there is indication that they are also able to extract iron from oxides (Van Dyk *et al.* 2010), and possibly break up pyrites (Ali 2021). While it is reported that some β-diketones (such as acetylacetone) can extract gold, knowledge is lacking about the process, the complexes formed, and extraction selectivity of gold present with other metals while using β-diketones in gas-phase reactions. Furthermore, knowledge on separation of these unknown gold organometallic complexes from other metal complexes is incomplete – with gas and liquid chromatography being the main area of separation studied so far (Sievers *et al.* 1963, Huber and Kraak 1972, Masłowska and Starzyński 1989, Wai and Wang 2000).

Aim and objectives of this study

This study aims to achieve the following:

- Replicate gas-phase extraction of gold using acetylacetone.
- Gain an understanding of what the products of gold-acetylacetone extraction are.
- To investigate if pyrite presence has any impact on gold extraction in gas-phase.
- To confirm the initial indications by Ali (2021) that pyrite could be broken down by acetylacetone vapour.
- Demonstrate effectiveness of fractional condensation for separation of gold from other metal acetylacetonates.
- Use findings of this work to add design constraints to a new potential gas-phase gold extraction process.

Hypothesis

It is proposed that gold will be oxidized to either its aurous form (+1) or its auric form (+3) and complex with acetylacetone by the following reactions:

$$4Au + 4(acac)H + O_2 = 4Au(acac) + 2H_2O$$

$$2Au + 6(acac)H + 3O_2 = 2Au(acac)_3 + 6H_2O$$

Acetylacetone is reported to break down pyrite (Ali 2021) and this means that iron might be co-extracted with gold. It is also proposed that many other transition metals (especially silver from electrum found in the tailings) will be extracted and each will form its own complexes with acetylacetone. Different metal acetylacetonates have varying stabilities and volatilities (Von Hoene *et al.* 1958, Sievers *et al.* 1963) that can be exploited to separate the metal complexes and recover unreacted acetylacetone via fractional condensation as done in the past with acetylacetone extractions (Tshofu 2014).

Scope of the investigation and layout of the dissertation

This study will focus on two major elements. The first element will be a study on theoretical coordination chemistry through Density Functional Theory (DFT) to identify the structure of the gold complex that is thought to form. This will be coupled with a synthesis from a high-quality source of gold to aid analysis. The theoretical coordination chemistry and laboratory synthesis of the gold compound in a liquid-phase synthesis serve their purpose in creating a benchmark for the empirical work that follows. If our understanding of the complexation of gold and acetylacetone is correct, the analytical signatures from both liquid-phase synthesis products and predicted DFT should agree — becoming an analytical reference for empirical work to possibly identify which complex forms in gas-phase extraction. The second element will bring forward gas-phase extraction of both gold and pyrite and use this to either confirm or contradict whether complexation during gas-phase extraction at elevated temperatures behaves similarly to the theory (and possibly liquid-phase synthesis).

Investigation will follow the following objectives:

1. To confirm or deny the previous findings that indicate gold extraction with gas-phase acetylacetone is possible.
2. To identify the specific gold acetylacetonate complex that forms using DFT and confirm the findings empirically.
3. To determine gold extraction efficiency of acetylacetone from a high-grade gold sample.
4. To measure the extent of coextraction of gold and iron when gold and pyrite are exposed to acetylacetone together.
5. To confirm or deny repeatability of iron extraction using gas-phase acetylacetone from pyrite and hematite, and verify that $Fe(acac)_3$ is the complex that forms.
6. To determine if acetylacetone decomposes in the temperature range above its boiling point from 140 °C to 220 °C.
7. To assess the possibility of oxygen in the carrier gas influencing acetylacetone extractions.
8. To use the findings of this work to further constrain conditions for further development of a commercial extraction process for gold and iron.

Contribution and impact of the investigation

To develop an alternate extraction process to cyanide, there are certain things that are crucial to understand before moving forward with production. One of the most important, is to know the selectivity of the alternative extraction method as only a high gold extraction is not enough for a viable process. Further refining steps, required by processes with poor selectivity, may erode profit margins and can quickly render a process designed to extract gold from old tailings as economically unfeasible. However, no extraction is perfectly selective. Gold extraction will inevitably require further separation and purification. This forms the second major information that is required for a new process.

Separation of gold is not the end of a process. Many alternate gold extraction reagents are expensive. Recovery and recycling of reagents is essential for the design

of an economical gold extraction process (Van Dyk *et al.* 2010). Recovery and recycling is the third major piece of information required, however, this topic would be best investigated once separation efficacy is known as recycling is closely related to separation.

Finally, with selectivity, separation characteristics, recovery and recyclability known; investigation towards energy consumption, technical feasibility, environmental impact, and economic feasibility can take place. It is also important to note that forward thinking towards the aforementioned points should take place when considering choices in early development such as extraction methods, reagents and operating conditions.

CHAPTER TWO
Literature review

To begin an investigation of a new potential ligand for gold extraction, it is important to review the current technologies surrounding gold extraction. This will provide context to the investigation and construct the performance characteristics required for this new process.

Cyanide Process

Gold aurous (+1) or auric (+3) are the two most common ionic forms of gold. When forming a complex with a ligand, the molecule's overall stability decreases with increasing ligand electronegativity (Aghamirian 1997).

Gold extraction is a dissolution process with cyanide according to the following reactions:

$$2Au + 4NaCN + O_2 + 2H_2O = 2NaAu(CN)_2 + 2NaOH + 2H_2O_2$$

$$4Au + 8NaCN + O_2 + 2H_2O = 4NaAu(CN)_2 + 4NaOH$$

This is an electrochemical process where cyanide concentration affects anodic dissolution and oxygen concentration controls the cathodic reduction. Effective recovery using cyanide can only be achieved following a pre-oxidation step. This is because natural gold is insufficiently amenable to cyanide for an economical rate of leaching (Ellis and Senanayake 2004).

Dissolution occurs with the following steps, according to Crundwell and Godorr (1997):

1. Diffusion of reactants through liquid film to unreacted gold surface.
2. Reaction with metallic gold in surface reaction.
3. Diffusion of reaction products through boundary film, away from surface.

Ideally, diffusion limitation can be avoided by using agitation. This will allow the surface reaction with gold to be the limiting factor in rate equations (Ellis and

Senanayake 2004). However, sulphide ions inhibit the rate of gold dissolution (Crundwell and Godorr 1997) as they consume dissolved oxygen during the cyanidation step – leading to oxygen starvation and reduced metallurgical recovery (Nunan *et al.* 2017). Aghamirian (1997) found that sulphide ions had the worst impact on gold's anodic dissolution, followed by antimony. Conversely, galena and low concentrations of lead ions enhanced gold dissolution.

Cyanide leaching is a pH-controlled process, requiring alkaline conditions of ideally pH 11 (Xie *et al.* 2014). If pH levels drop then more cyanide is consumed by the following reaction to make HCN gas (Ellis and Senanayake 2004):

$$CN^- + H_2O = HCN + OH^-$$

$$CN^- + H_2O + CO_2 = HCN + HCO_3^-$$

HCN gas is not only an extremely toxic gas that has serious occupational health and safety implications, but its production increases cyanide waste – further consuming water in the process.

The established process of gold cyanide leaching uses large volumes of water. This challenge is particularly important to highlight in a South African context as South Africa is a water scarce country. Not only does the regular leach process consume water in the dissolution of gold, if conditions are sub-optimal (such as lowered pH), then additional water consumption can occur through side reactions such as the production of HCN gas.

Tailings management is another drawback of cyanide leaching as residual cyanide in the tailings can leak into the surrounding environment. The true environmental impact is difficult to monitor as Donato *et al.* (2007) pointed out in their work. The true number of deaths, especially in avian populations, is often severely underreported due to the challenges with tracking down and reporting deaths caused by a particular dump. Donato *et al*. (2007) also mentioned in their review article that the toxicity of cyanide to avian populations can vary with diet. Avian species that eat flesh were more sensitive to cyanide as their digestive system operates at lower pH – leading to a faster liberation of cyanide before metabolic breakdown and an increase in absorbed cyanide.

Ellis and Senanayake (2004) investigated gold leaching with cyanide and found that particles with a P_{80} = 45 μm initially leached faster in shorter leach times up to 8 hours. However, smaller particles with P_{80} = 38 μm ultimately had the highest extraction with leach times up to 32 hours. They also noted that smaller particle sizes, while giving the highest gold extraction, are not the optimal size as smaller particle sizes led to a large increase in NaCN consumption. They found the optimal particle size to be P_{80} = 63 μm. This gave good gold extractions of approximately 90 % with 32 hours of leaching. It must be noted that these values are all for ore treated in a pre-oxidation step of 8 hours. Without pre-oxidation, the gold recovery dropped to approximately 79 %.

Gold deposits in the Witwatersrand basin in South Africa are known to contain uranium-bearing minerals. It contains an approximate uranium content of 300 ppm as U_3O_8 – which is comparably low to other international deposits of uranium (Lottering *et al.* 2008). The uranium presence gives two methods of gold extraction via cyanide. The first is forward leaching, where gold is leached directly. Some of the uranium will compete with the gold and cause higher cyanide consumption. The other method is reverse leaching. This is a process where uranium is leached first using H_2SO_4 and following the acid leach, the gold is leached with cyanide. Reverse leaching was shown by Lottering et al. (2008) to improve gold recovery a further 3-4 %, resulting in an increased extraction from ~94 % to ~98 %. However, the recovery was investigated on an ore containing 8-12 g/t gold. For low grade ore such as tailings, it is unknown if pre-treating acid leach of uranium will yield significantly higher recoveries of gold in cyanide or other extraction processes.

Pre-oxidation and floatation pre-oxidation have been used to increase gold recovery of cyanidation of low-grade and refractory sulphidic ores. Hydrogen peroxide has been used for effluent treatment for many years and in pre-oxidation to increase gold recovery by oxidizing sulphides found in refractory ores (Nunan *et al.* 2017). This lowers the dissolved oxygen consumption of sulphides during cyanidation and allows for improved reaction kinetics and can improve gold recovery on smaller cyanidation tanks.

Nunan *et al.* (2017) performed an industrial trial of hydrogen peroxide pre-oxidation at AngloGold Ashanti's Serra Grande gold plant in Brazil where hydrogen peroxide was fed into the first three tanks (oxidation tanks) in the cyanide circuit. The plant performed pre-oxidation with only oxygen prior to the study. They found that a hydrogen peroxide dosage rate of 0.24 kg pure H_2O_2 per tonne of dry ore increased dissolved oxygen in the first three tanks from an average of <1 ppm to 7.2 ppm, and decreased cyanide consumption 23%. Cyanidation with pre-oxidation can yield recoveries of as high as 93 % - compared to approximately 91 % without pre-oxidation (Nunan *et al.* 2017). However, the primary benefit of pre-oxidation is reduction of cyanide usage.

Roasting cyanidation has been used as an alternative to H_2O_2 that can improve gold recovery of regular cyanidation. The roasting process uses high temperatures and oxygen to oxidize sulphides and carbonaceous material in the ore. Yang *et al.* (2015) achieved a gold recovery of 82.37 % using roasting cyanidation on gold concentrate. However, this process produces toxic waste gasses and has very high energy consumption and is additionally not suited to very low-grade ores such as tailings that are seeing renewed interest as a gold source (Falagán *et al.* 2017). This process is unlikely to be favoured in future processes as high energy use and pollutants production will be moving against global environmental drives.

Thiosulphate leaching

Thiosulphate leaching is a promising alternative to gold cyanidation as it has good selectivity, low corrosivity and is a cheap reagent. It is also more environmentally friendly than cyanide (Xu *et al.* 2017).

Thiosulphate leaching typically uses ammonia thiosulphate, catalysed by copper, to leach gold ore in a carefully controlled system. It requires specific concentrations of thiosulphate, copper, oxygen, and ammonia in the leach solution for practical operation. The thiosulphate reaction with gold occurs with the following reaction (Alymore and Muir 2001):

$$4Au + 8S_2O_3^{2-} + O_2 + 2H_2O = 4[Au(S_2O_3)_2]^{3-} + 4OH^-$$

A similar reaction also forms $Au(S_2O_3)^-$ but it is less stable than $[Au(S_2O_3)_2]^{3-}$ (Alymore and Muir 2001).

Traditional cyanidation is vulnerable to high consumption when ores containing copper or carbon are leached (Dong *et al.* 2017). However, thiosulphate is catalysed by copper – making it a very desirable ligand for use with some refractive ores such as chalcopyrite. Thiosulphate leaching has been studied for many years now, but with poor commercial adoption; attributed to the difficulty of recovering gold from pregnant thiosulphate leach solutions (Dong *et al.* 2017, Xu *et al.* 2017).

The presence of ammonia in the system improves the rate of gold dissolution by preventing a sulphur build-up caused by thiosulphate breaking down on the gold surface. The absence of ammonia may be desired in some cases, as an absence of ammonia in the thiosulphate leach solution allows for better silver recovery (Alymore and Muir 2001).

Chlorine roasting

Chlorine roasting is a high temperature process used to extract precious metals. The use of calcium chloride ($CaCl_2$) exploits the high affinity of chlorinating agents towards gold and silver. Whilst use of chlorides does allow relatively lower temperatures of extraction when compared to other oxidation or reduction processes (Li *et al.* 2018).

The chlorination of gold and silver with Cl_2 is enabled by the dissolution reaction of $CaCl_2$ that takes place first:

$$CaCl_{2(g)} + \frac{1}{2}O_{2(g)} = CaO + Cl_{2(g)} \qquad T \leq 1020\ °C$$

Following the dissolution of $CaCl_2$, the produced chlorine gas can chlorinate gold and silver to the following major reactions (Li *et al.* 2018):

$$2Au + 3Cl_{2(g)} = 2AuCl_{3(g)} \qquad T \leq 235\ °C$$

$$2Au + Cl_{2(g)} = Au_2Cl_{2(g)} \qquad T = 782\ °C$$

$$2Ag + Cl_{2(g)} = 2AgCl_{(g)} \qquad T \leq 2225\ °C$$

The normal oxidative roasting process operates at 600 °C – 700 °C on refractive ores such as pyrite (Fraser *et al.* 1991). Chlorination of alluvial gold was investigated by Ojeda *et al.* (2009). They investigated different roasting temperatures from 400 °C – 600 °C in a small-scale lab test bed. The highest gold extractions of approximately 98

%, were obtained at the highest temperatures of 600 °C for one hour. Tests that were operated at 400 °C yielded approximately 19 % gold extraction.

Li *et al.* (2018) found that chlorination roasting of cyanide tailings, at higher temperatures than those used by Ojeda *et al.* (2009), is aided by the presence of SiO_2 Fe_3O_4 and Fe_2O_3 as these compounds promote $CaCl_2$ decomposition – increasing production of chlorine gas. Li *et al.* (2018) achieved gold recoveries of >90 % and silver recoveries of >60 % whilst operating at 1050 °C for two hours. There was no significant increase in recovery of gold or silver when temperature was increased past this point in their study. Increasing dosage of $CaCl_2$ at 1050 °C suggested an optimal $CaCl_2$ dosage of 4 wt.% for gold recoveries.

A similar study by Li *et al.* (2020) investigated gold recovery from cyanide tailings, but using NaCl, $MgCl_2$, KCl and $CaCl_2$ as sources of chlorine for a roasting process. They found $CaCl_2$ to be the most effective due to its high chlorine production and slag reduction in roasting processes.

β-Diketones

β-Diketones are a class of chemicals that have been widely studied for many years for their various bonding capabilities. They have been utilized for their chelating ability with metals and form the functional base for some classes of polydentate ligands (Aromi *et al.* 2008).

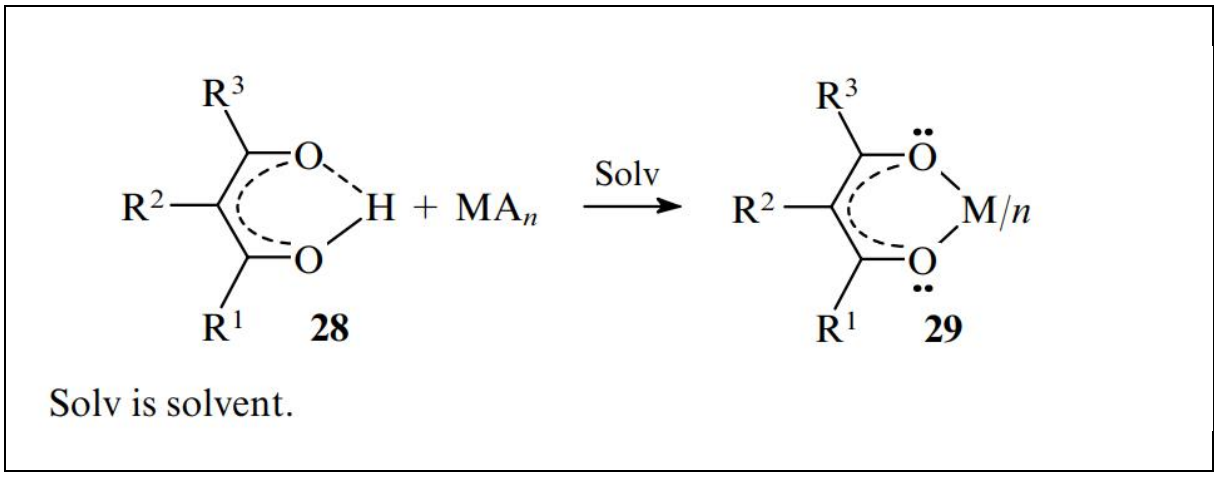

Figure 1: Reaction diagram of bidentate β - diketone complex formation with a metal (Aromi *et al.* 2008)

Acetylacetone (acac)

Acetylacetone or 2,4-pentanedione (hereafter referred to as acetylacetone) has been studied in metal coordination chemistry for many years. Acetylacetone is the simplest β-diketone structurally and was first synthesized by L. Claisen and E. F. Ehrhardt (1889). This synthesis is depicted in Figure 2 and is now more commonly referred to as the Claisen condensation (Aromi *et al.* 2008).

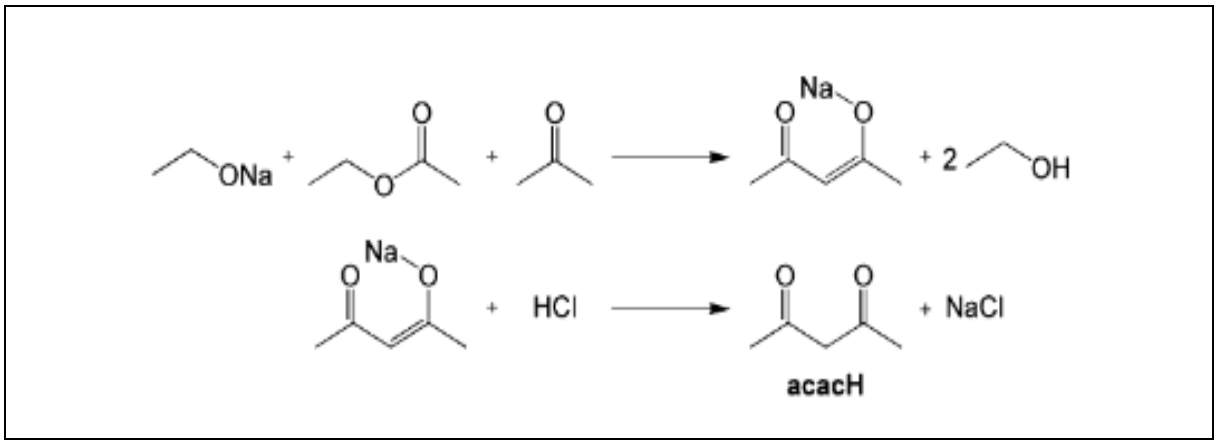

Figure 2: Claisen condensation reaction scheme (Aromi *et al.* 2008)

A more efficient and economical reaction scheme was developed by Meerwein (1933) and is the dominant production method used today. The reaction (depicted in Figure 3) uses BF_3, acting as a Lewis acid catalyst, for the condensation between acetone and acetic anhydride (Aromi *et al.* 2008). Acetylacetone can form a wide variety of metal chelates according to the expression: $M(acac)_x$ where x = 1,2,3 and M = a transition metal, this structure is also expressed in Figure 4 (Von Hoene *et al* 1958).

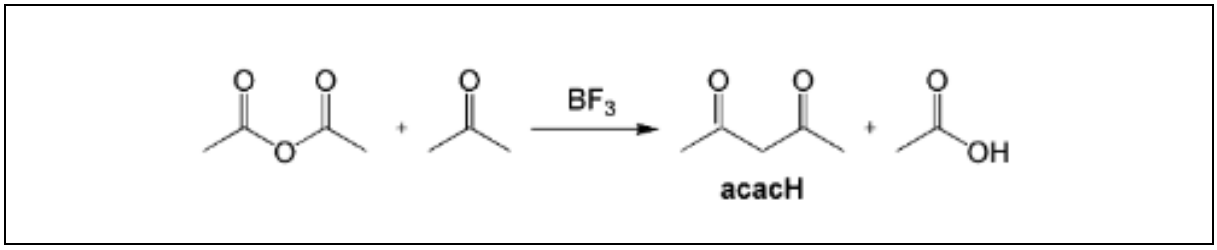

Figure 3: Acetylacetone synthesis route developed by Meerwein in 1933 (Aromi *et al.* 2008)

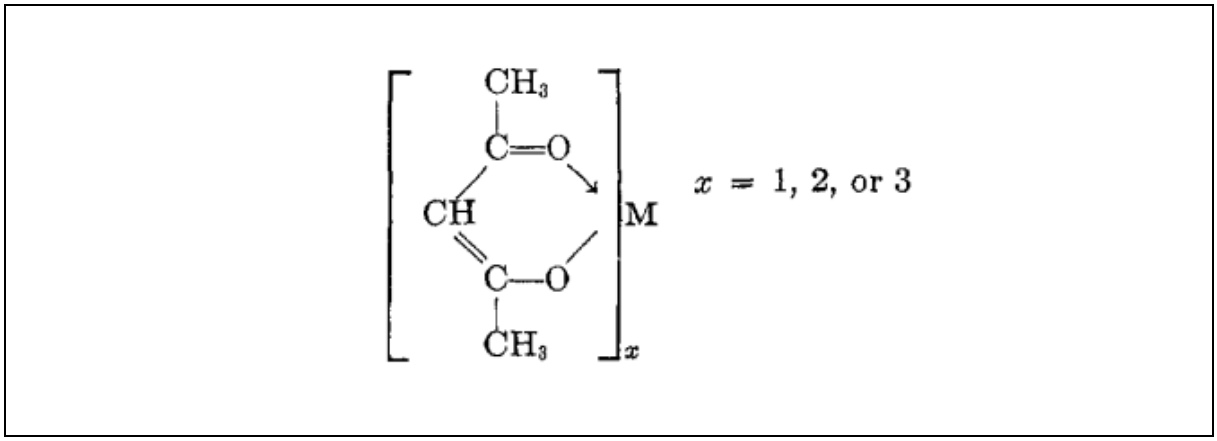

Figure 4: Structure and bonding of metal acetylacetonates (Von Hoene *et al.* 1958)

Acetylacetone has been found to form unidentate complexes through the middle carbon atom or undergo bidentate chelation, through the oxygen atoms as expressed in Figure 5. Whilst both bonding mechanisms are possible, Komiya and Kochi (1977) reported that metal bonding with acetylacetone more commonly forms a chelation through the oxygen atoms.

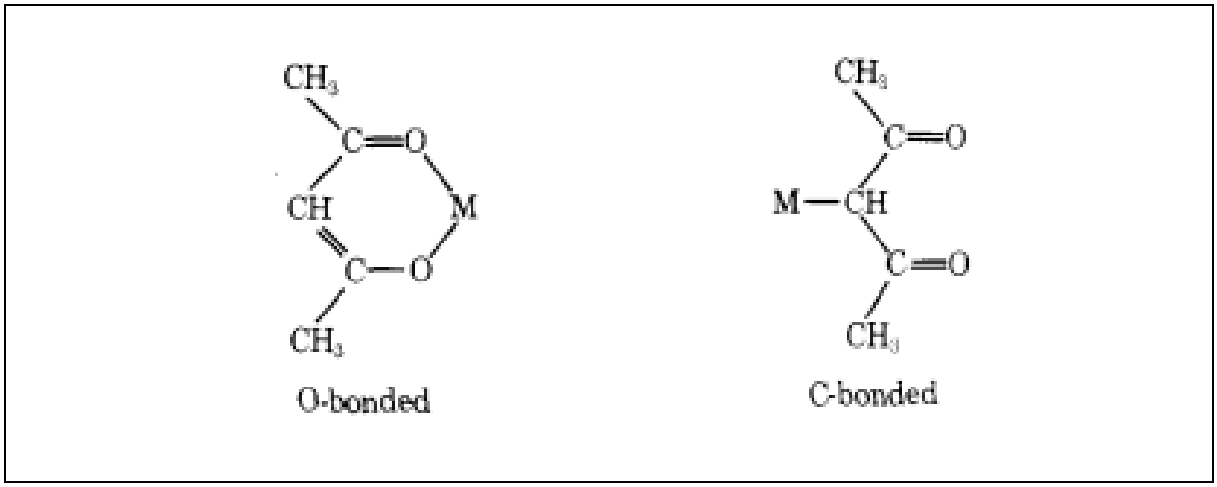

Figure 5: Bidentate and unidentate acetylacetone (Komiya and Kochi 1977)

Zharkova *et al.* (2006) were the first to report on a crystallographic study of a gold (III) acetylacetonate complex, namely dimethylgold (III) acetylacetone or $(CH_3)_2Au(acac)$, presented in Figure 6. They report that the gold acetylacetone complex was highly volatile (melting point 82-84 ^oC, decomposition in He 145 ^oC) and noted that the coordination around the gold atom is that of a slightly skewed square. They prepared the samples from dimethylgold (III) iodide, and the synthesis reaction was liquid-phase.

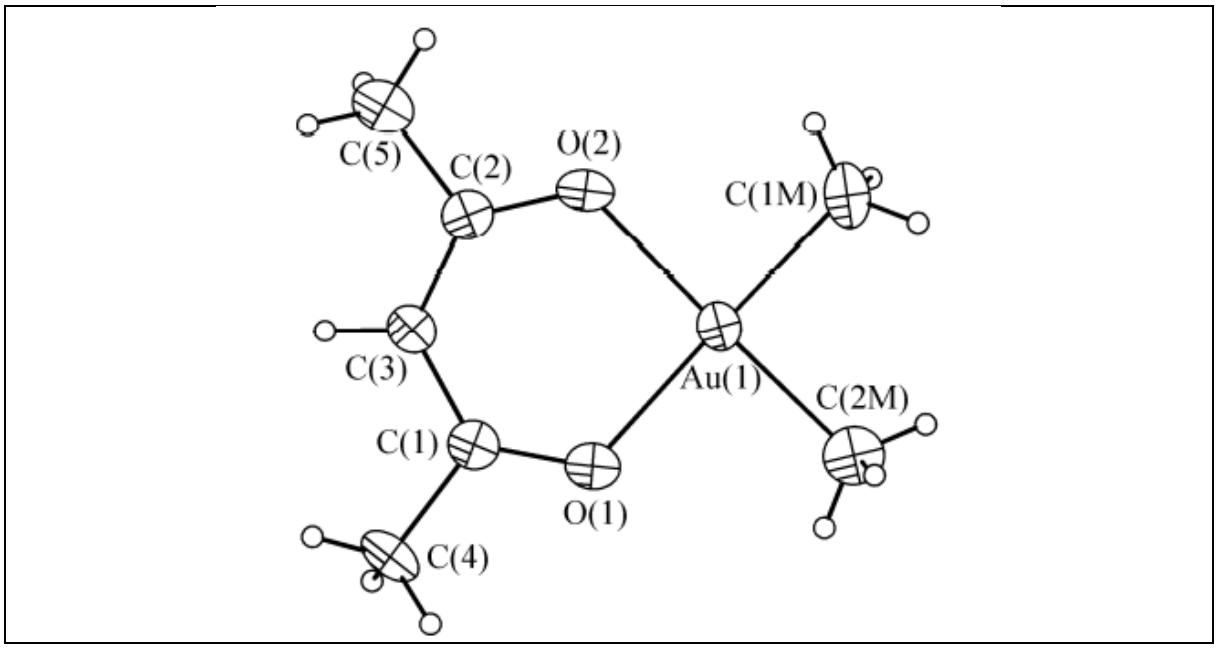

Figure 6: Structure of $(CH_3)_2Au(acac)$ complex (Zharkova *et al*. 2006)

No other gold-acetylacetone complex has been studied with X-Ray Diffraction.

CHAPTER THREE

The modelling and synthesis of gold acetylacetonate complexes with Density Functional Theory

When investigating new extraction techniques, there are some things that are essential to know to develop a thorough understanding of a new potential process. Perhaps, one of the most important things to know about a potential gold extraction process with acetylacetone, is the composition of the products formed during an extraction. If the reaction products can be determined, investigation of possible reaction pathways can follow.

Understanding more about the base chemical reaction involved is a crucial first step to understanding physical and chemical properties of the product, constrain the operating conditions to sensible parameters, understand and develop kinetic models, and examine high-level feasibility (both economically and technically).

Previous understanding of gold extraction using acetylacetone, conducted by Ali (2021), indicated that gold extraction is possible. However, the research only measured for gold presence in extraction condensate via AAS, and no understanding into the complexation of gold with acetylacetone could be obtained from this work. There was some investigation in the work also conducted by Ali (2021) into potential gold complexes forming by using Density Functional Theory (DFT) to compare relative stabilities of a group of selected theoretical complexes.

This section will further the work on DFT and attempt a synthesis of a potential gold acetylacetonate complex for comparison and analysis properties.

Density Functional Theory

Density Functional Theory (DFT) is a quantum-mechanical method favoured for its good price to performance ratio when calculating the electronic structure of atoms

and molecules. It is the dominant electronic structure method used around the world and has advantages over other methods such as Møller-Plesset perturbation theory or coupled cluster (Van Mourik *et al.* 2014).

The basis of almost all electronic structure calculations is the Schrödinger equation:

$$\mathrm{H}|\Psi\rangle = E|\Psi\rangle$$

Where H represents the Hamiltonian of the molecular system. E represents the total energy and $|\Psi\rangle$ is the total eigenstate. The total molecular Hamiltonian (H_{tot}) can be expressed as (Malloum 2021):

$$\mathrm{H}_{tot} = \mathrm{T}_n + \mathrm{H}_\mathrm{e} + H_{mp}$$

Where T_n represents the nuclear kinetic energy operator, H_e represents the electronic Hamiltonian and H_{mp} is the mass polarization due to the mass centre system (Malloum 2021). However, the Schrödinger equation cannot be solved in this form without simplifying assumptions.

DFT makes use of the framework developed by Hohenberg, Kohn and Sham in the 1960s, that proves the total electron density determines all the ground state properties of a system with a specified number of electrons. This allows the use of density as the core variable in electronic structure calculations (Malloum 2021).

DFT is one of two exact theories of electronic structure; the other being wave function theory (WFT) – a method that provides guaranteed convergence to the Schrödinger equation. The primary advantage DFT has over WFT is the far lower computational requirement. This does come at the cost of accuracy (that has been shown to be acceptable) but has the benefit of being able to evaluate much larger systems rather than being restricted to single particle systems with WFT (Bartlett *et al.* 2005).

Another reason DFT is highly attractive in computational chemistry is that it can be used predictively (*ab initio*) with reasonable accuracy. This allows one to predict properties of theoretical and novel compounds without experimental input (Bartlett *et al.* 2005). It is precisely this quality that this work seeks to utilize. It is important to note that convergence on DFT methods is not guaranteed to converge on a correct

answer. Where possible, one should search for confluence between DFT predictions and empirical data.

Objectives of DFT work

Ab initio DFT study of gold organometallic complexes can provide predicted structural and physical data with reasonable accuracy for selected atoms or complexes (Bartlett *et al.* 2005). Unfortunately, it is not feasible to exhaust all possible gold complexes with β-diketonato ligands such as acetylacetone (the greater focus of this study) – there are nearly infinite possibilities if one considers the possibility of multiple atoms of gold bonding to each ligand in different ratios and geometries. Some constraints will be applied to this work to narrow the possibilities to a select group of gold β-diketonato complexes based on current understanding of β-diketonato complexes with other metals. β-diketonato metal complexes are well known to chelate with a single metal atom in the nucleus. The number of ligands bound to the nucleus will depend on the metal itself and its oxidation state (Aromi *et al.* 2008, Von Hoene *et al.* 1958).

Pioneering work by Von Hoene *et al.* (1958), Chaudhuri and Ghosh (1983), Zharkova *et al.* (2006, 2010), Zharkova and Baidina (2008), Carmerman *et al.* (1983), and many others, has shown that β-diketonato ligands – namely acetylacetone (and similar sulphur & amine substituted versions) – regularly and consistently form chelate compounds with multiple ligands around a single nucleus.

This *ab initio* study will firstly, consider optimized geometry stability of the following complexes of Au(I): Au(acac), Au(Sacac), Au(Nacac); and the following complexes of Au(III): $[Au(acac)_2]^+$, $Au(acac)_3$, $Au(Sacac)_3$, $Au(Nacac)_3$ where acac = acetylacetone, Sacac = thioacetyl acetone, Nacac = β-ketiminato substituted variant of acetylacetone. Thereafter, a more detailed investigation into potential reactions with acetylacetone (acac), gold and oxygen, and the predicted IR spectra of each. The data obtained in this DFT study will attempt to predict potential gold complexes that could form during gas phase gold extraction with acetylacetone. Later in this chapter, the predicted IR spectra will be compared to measured IR spectra from material generated in a synthesis attempt to find concurrence if any.

Computational details

Initial modelling and calculation of gold complexes was performed on Gaussian03 in Windows 10 compatibility mode (Frisch *et al.* 2004) using Becke's three parameter exchange with Lee, Yang and Parr correlation functional (B3LYP) DFT and Stuttgart Dresden triple zeta Effective-Core Potential (SDD) basis sets. These computational settings are recommended for systems with heavy metals (Mohammed and Abbood 2017). The initial modelling was used to converge an approximate geometry of each complex studied, thereafter, the optimized geometry was used on a more recent version of software at the Centre for high performance computing (CHPC). Calculations on the CHPC used Gaussian16 on Linux (Frisch *et al.* 2019) using generalized-gradient approximation (GGA) function with Perdew-Burke-Ernzerhof (PBEPBE) and triple zeta valence plus smaller sets of polarization functions (Def2TZVP) basis set (Weigend and Ahlrichs 2005), converged on similar structures to the initial calculations on B3LYP/SDD. Calculations on PBEPBE/Def2TZVP were used for all results shown in this work.

Geometry optimized structures

The optimized geometries of (a) Au(acac), (b) Au(Sacac), (c) Au(Nacac) are presented for Au (I) in Figure 7, and (d) $[Au(acac)_2]+$, (e) $Au(acac)_3$, (f) $Au(Sacac)_3$, (g) $Au(Nacac)_3$ for Au (III) in Figure 8 and following Figure 9. Where Au=bright yellow, Sulphur=dark yellow), Nitrogen=orange, Oxygen=red, Carbon=grey and Hydrogen=blue. All calculations were performed with four different spin multiplicities to find the most stable spin multiplicity. For acetylacetone class of compounds, an overall spin multiplicity of 1 was found to have the lowest Gibbs energy and hence, the most stable. For both sulphur and nitrogen substituted variants (Sacac and Nacac groups respectively), the most stable overall spin multiplicity was 5.

Structures (a), (b), and (c) all present similar geometries and the bond angles on the Au (I) atom range from 103.74˚ to 114.44˚ – the O, O ligand had perfect symmetry and the introduction of either a N, O or a S, O chelate appeared to skew the bond toward the nitrogen and sulphur – with sulphur displaying the greatest skewing.

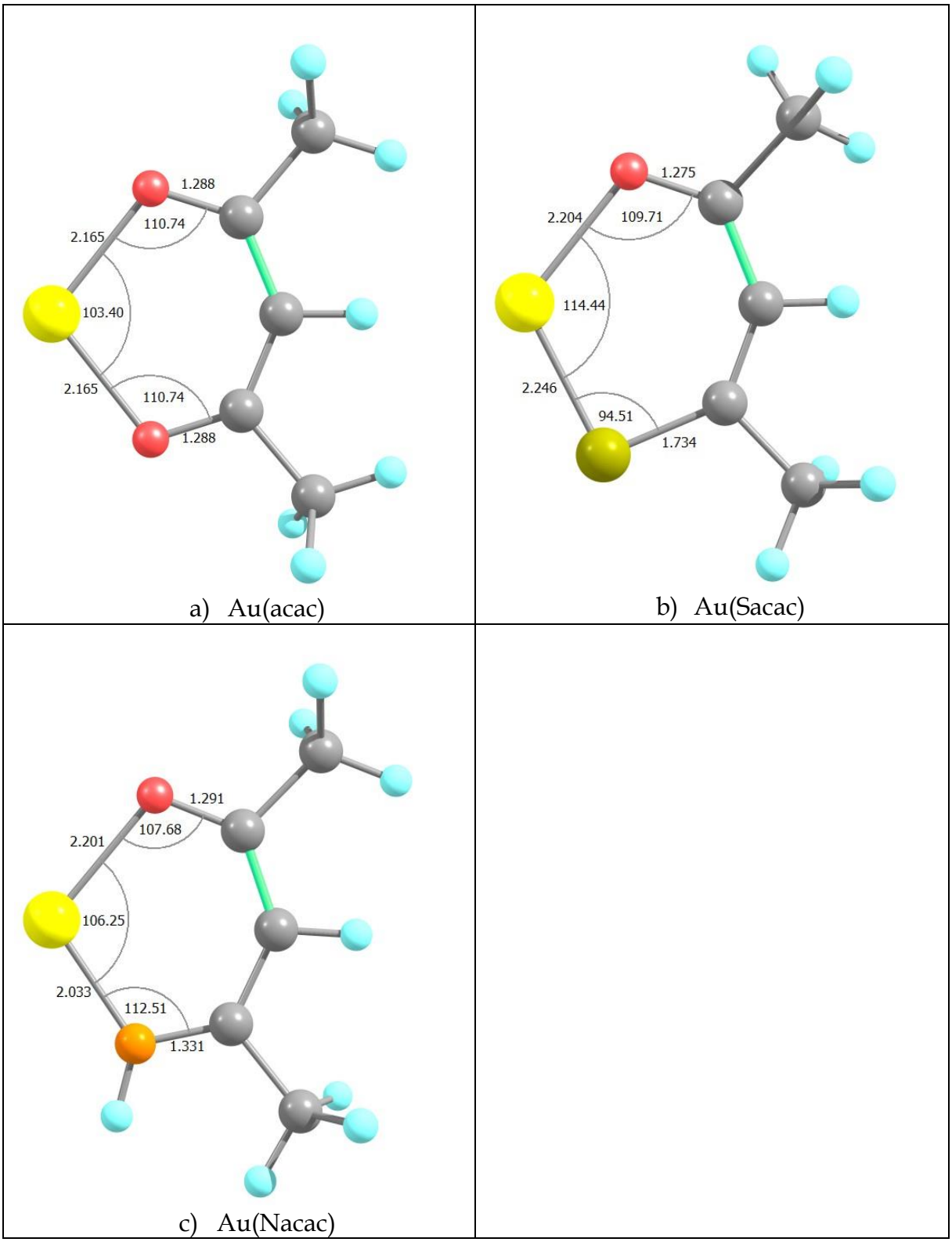

Figure 7: Optimized geometry of Au(I) acetylacetonate-style structures with sulphur (S, O chelate) and nitrogen (N, O chelate) substituted. a) Au(acac), b) Au(Sacac), c) Au(Nacac)

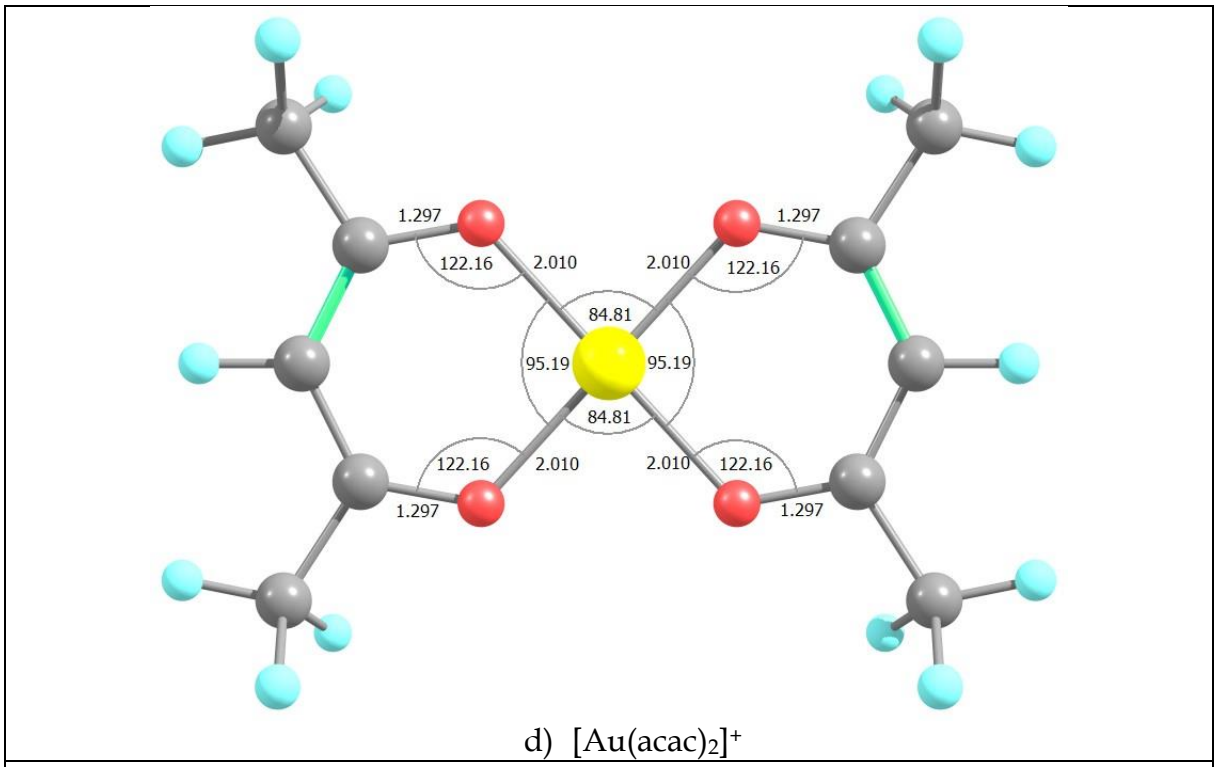

d) $[Au(acac)_2]^+$

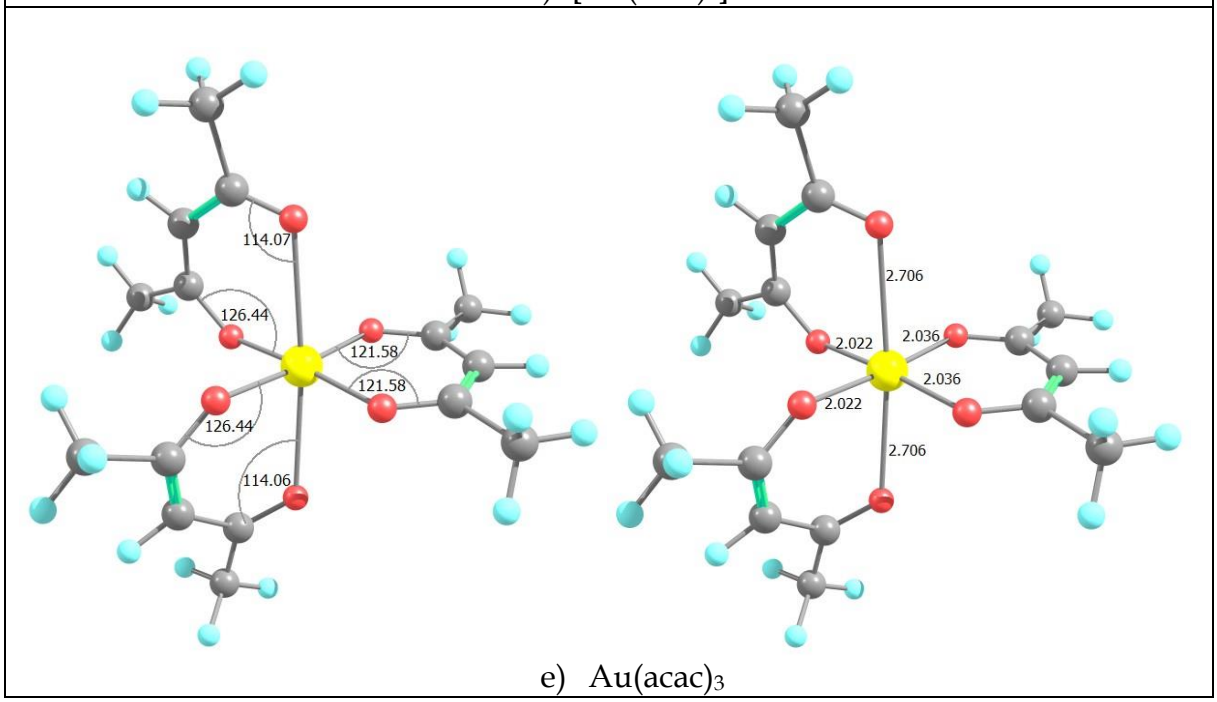

e) $Au(acac)_3$

Figure 8: Optimized geometry of Au(III) acetylacetonate structures of d) $[Au(acac)_2]^+$ and e) $Au(acac)_3$

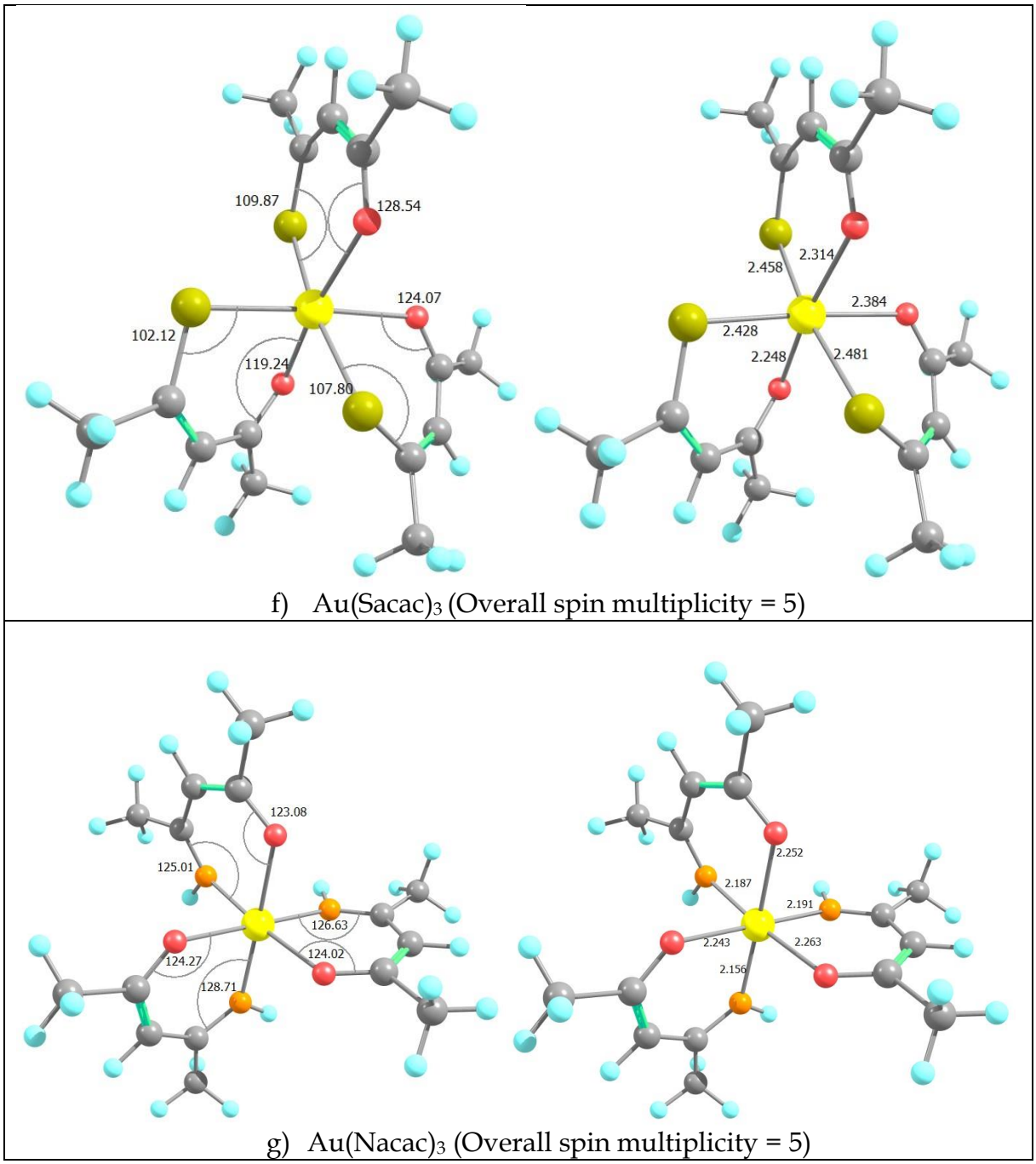

f) $Au(Sacac)_3$ (Overall spin multiplicity = 5)

g) $Au(Nacac)_3$ (Overall spin multiplicity = 5)

Figure 9: Optimized geometry of Au(III) acetylacetonate-style structures with S, O chelate f) $Au(Sacac)_3$ and N, O chelate g) $Au(Nacac)_3$

Structures (d) and (e) compare two possibilities for gold complexation with acetylacetone (acac), the former with two acac groups and the latter with three. $[Au(acac)_2]^+$ had four-coordination between the oxygen atoms – with bond angles of approximately 90˚ – in a shape close to square planar. Au (III) bond angles of 95.19˚ and 84.81˚, and Au-O bond lengths of 2.010 Å, are similar to O–Au–O bond angles of 89.7-93.7° and 2.07-2.108 Å found in an XRD study of $(CH_3)_2Au(acac)$ by Zharkova *et*

al. (2006). It also showed agreement with previous DFT calculations performed on B3LYP/SDD (Ali, 2021). Similarly for $Au(acac)_3$, the Au (III) bond angles varied between 84.04˚ and 99.07˚ with most of the bond angles between 84˚ and 93˚ – indicating an approximate octahedral structure around the Au (III) atom. Convergence of Au (I) DFT calculations were notably more stable when comparing to convergence of Au (III) calculations. Both N, O and S, O substituted complexes with Au (III) converged to skewed structures with a higher degree of irregularity. The $Au(Sacac)_3$ (f) complex converged with one of the ligand groups folded toward another, forming a "U" shape on the one side (lower two branches of f) in Figure 9.

Molecular orbitals and stability

The precise form of molecular orbitals can often be difficult to calculate as it employs differential equations. An alternate method – with reasonable accuracy and simplicity – is to use combinations of the underlying atomic orbitals and linear weighting coefficients (People and Beveridge 1970). The highest occupied molecular orbital (HOMO) and lowest unoccupied molecular orbital (LUMO) – and especially the HOMO-LUMO energy gap – are important metrics for assessing the stability of molecules formed. The HOMO is a site from where electrons are most likely to be donated, the LUMO is a site from where newly acquired electrons are likely to go. The energy level gap, referred to as the HOMO-LUMO gap, is a particular problem for some DFT larger DFT systems as there is an apparent "vanishing" of the HOMO-LUMO gap that leads to poor self-consistent field convergence for B3LYP and PBE functionals (Lever *et al.* 2013). This is not of concern in this study as the large systems mentioned by Lever *et al.* (2013) are for 1000 – 3000 atoms. However, it does highlight an important point that small HOMO-LUMO gaps – not necessarily due to an unknown convergence error but rather naturally small gaps – can give rise to troublesome convergences that were experienced in this work for the larger molecules studied.

The HOMO and LUMO for Au(acac), Au(Sacac) and Au(Nacac) are presented in Figure 10, Figure 11 and Figure 12 respectively. The HOMO and LUMO for

$[Au(acac)_2]^+$, $Au(acac)_3$, $Au(Sacac)_3$, $Au(Nacac)_3$ are presented in Figures 13-16 and the HOMO-LUMO energy gaps are displayed in Table 1.

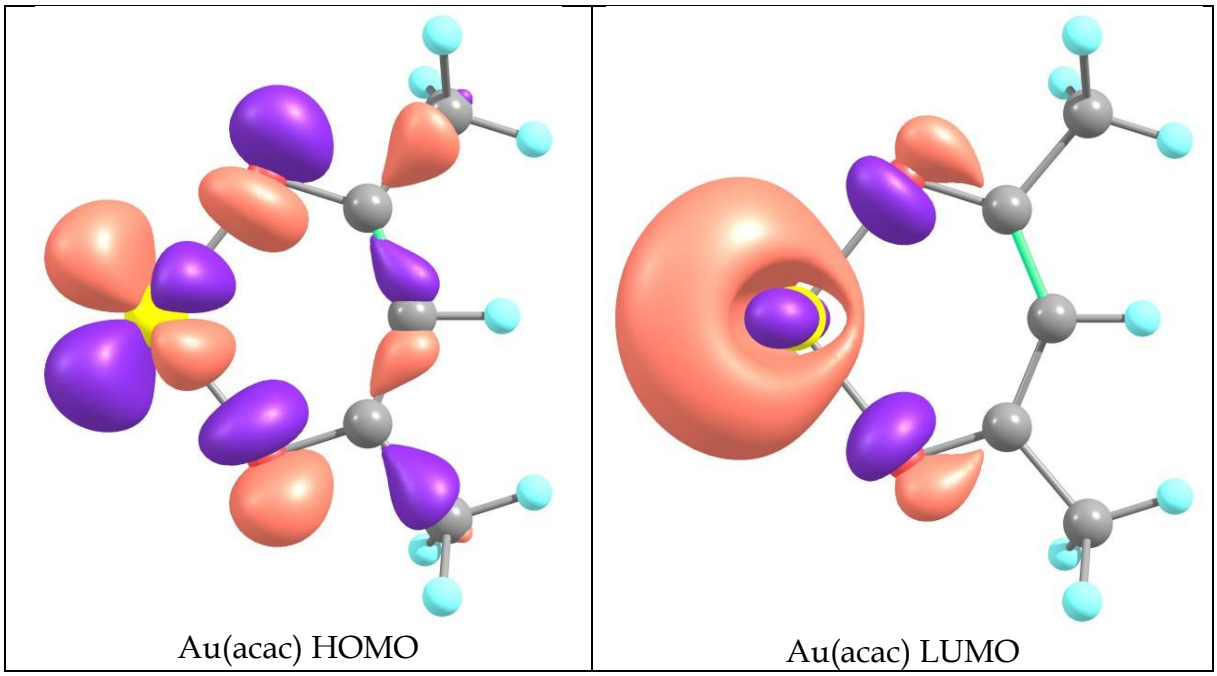

Figure 10: Molecular Orbital drawing of HOMO and LUMO of Au(acac) displayed with with 0.05 eÅ-3 contour, atomic structure is the same as in Figure 7 a) Colours: Au (yellow), C (grey), O (red), H (blue).

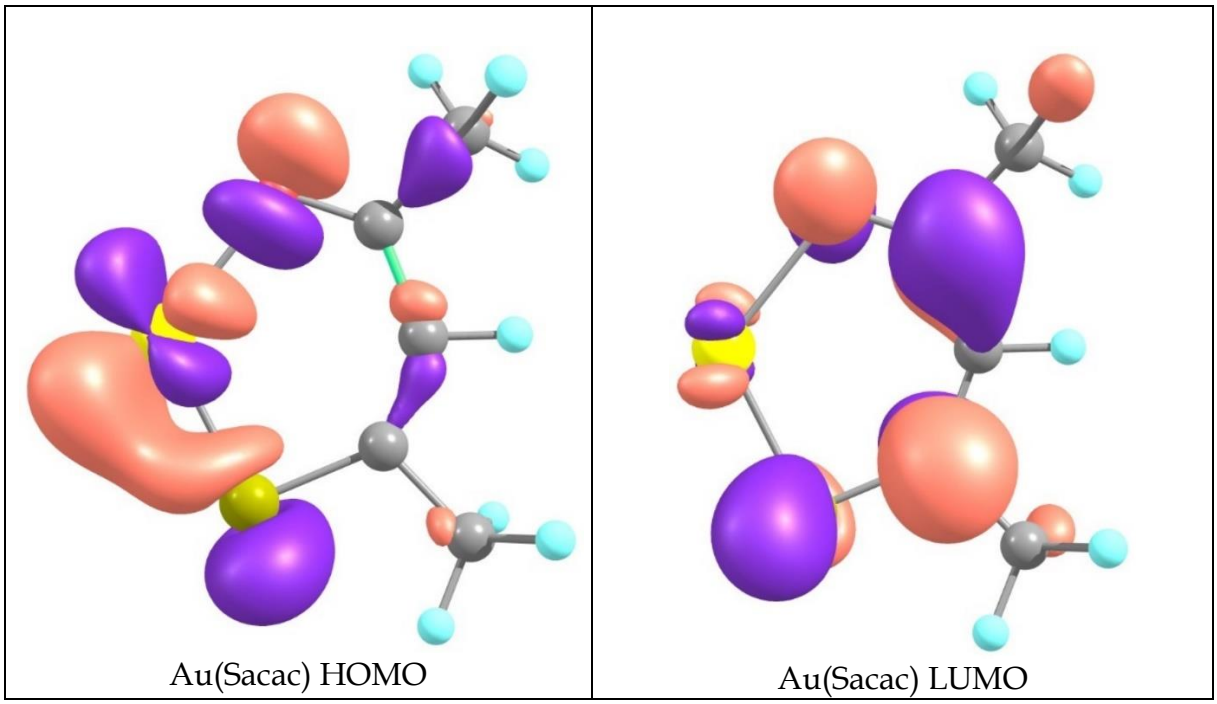

Figure 11: Molecular Orbital drawing of HOMO and LUMO of Au(Sacac) displayed with with 0.05 eÅ-3 contour, atomic structure is the same as in Figure 7 b) Colours: Au (yellow), C (grey), O (red), S (dark yellow), H (blue).

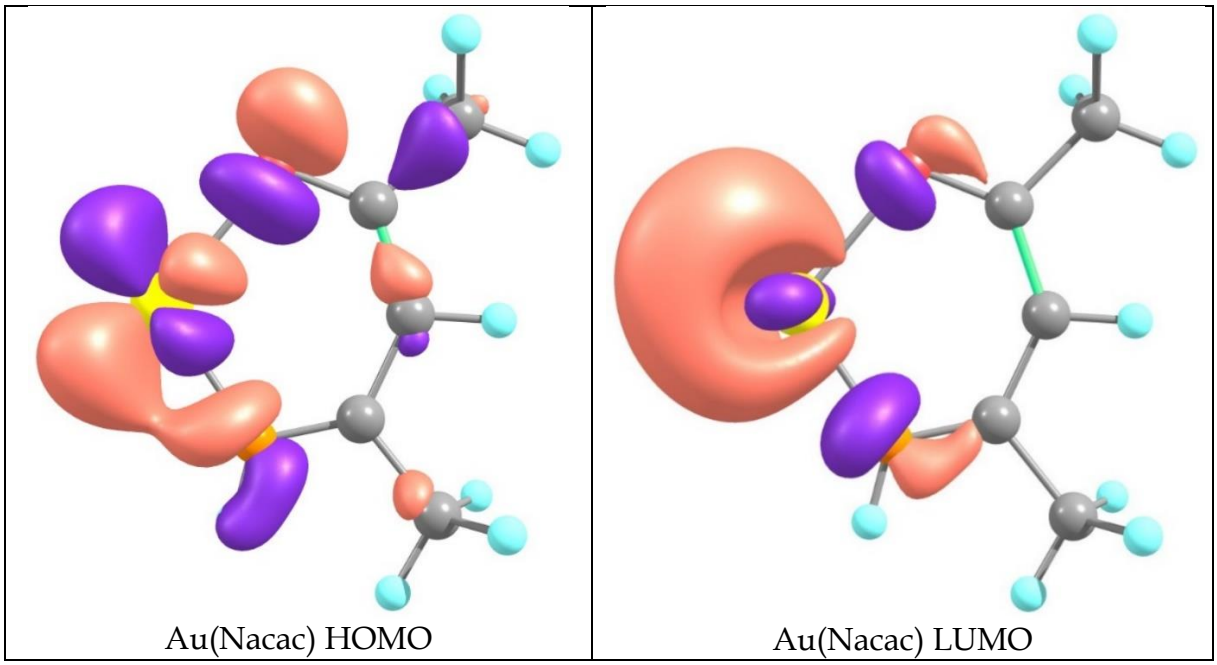

Figure 12: Molecular Orbital drawing of HOMO and LUMO of Au(Nacac) displayed with 0.05 eÅ-3 contour, atomic structure is the same as in Figure 7 c) Colours: Au (yellow), C (grey), O (red), N (orange), H (blue).

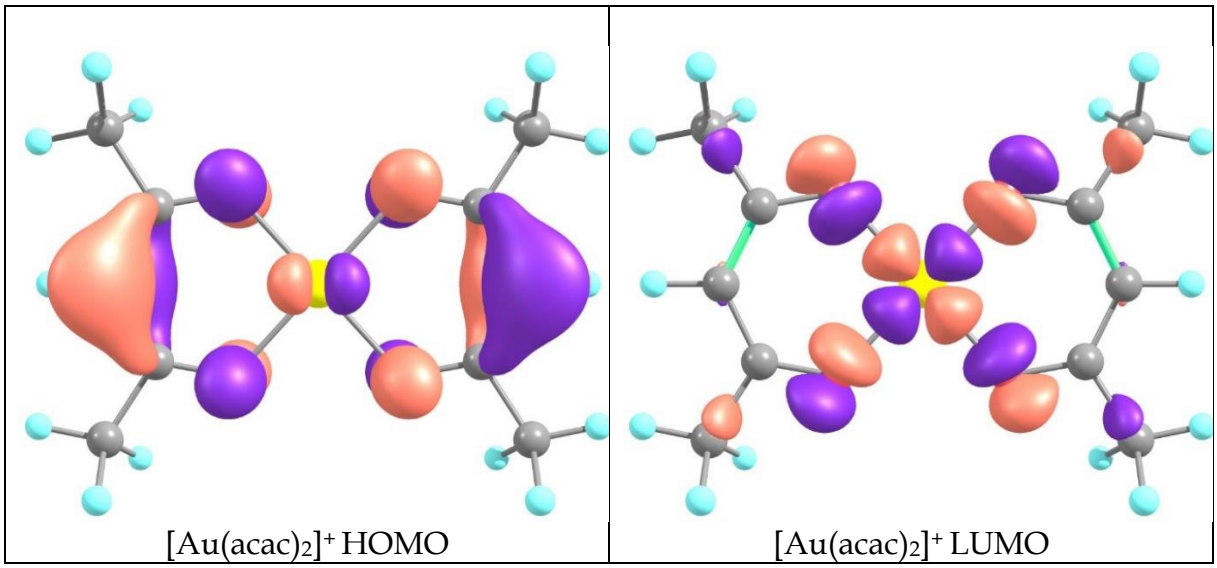

Figure 13: Molecular Orbital drawing of HOMO and LUMO of $[Au(acac)_2]^+$ displayed with 0.05 eÅ-3 contour, atomic structure is the same as in Figure 8 d) Colours: Au (yellow), C (grey), O (red), H (blue).

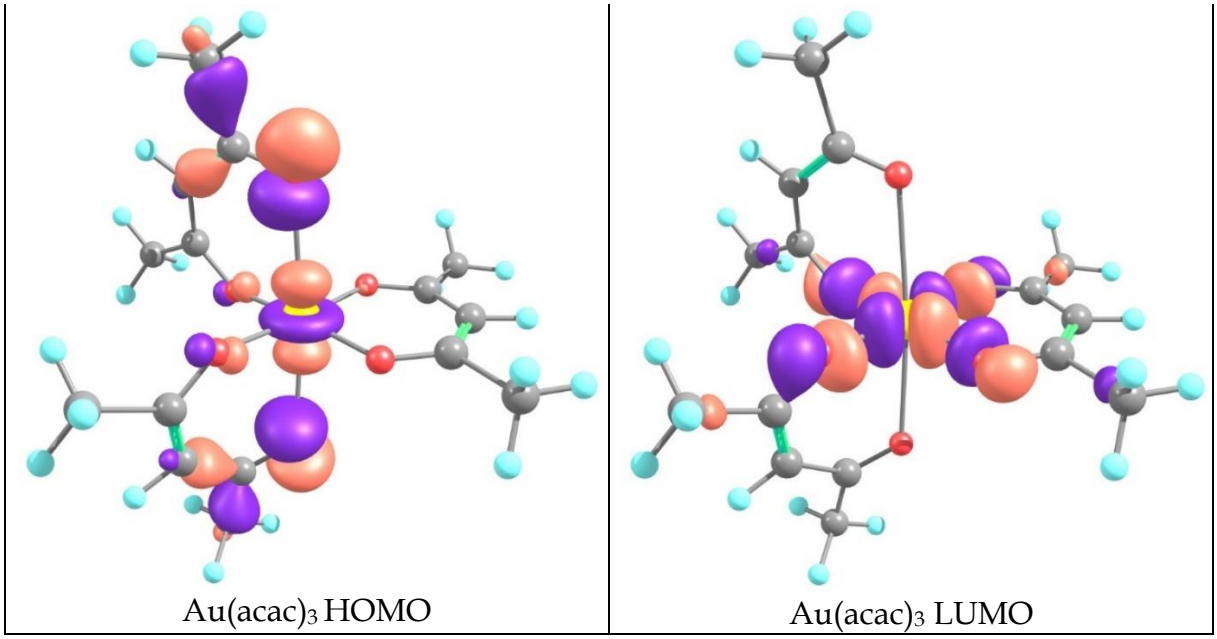

Figure 14: Molecular Orbital drawing of HOMO and LUMO of $Au(acac)_3$ displayed with 0.05 eÅ-3 contour, atomic structure is the same as in Figure 8 e) Colours: Au (yellow), C (grey), O (red), H (blue).

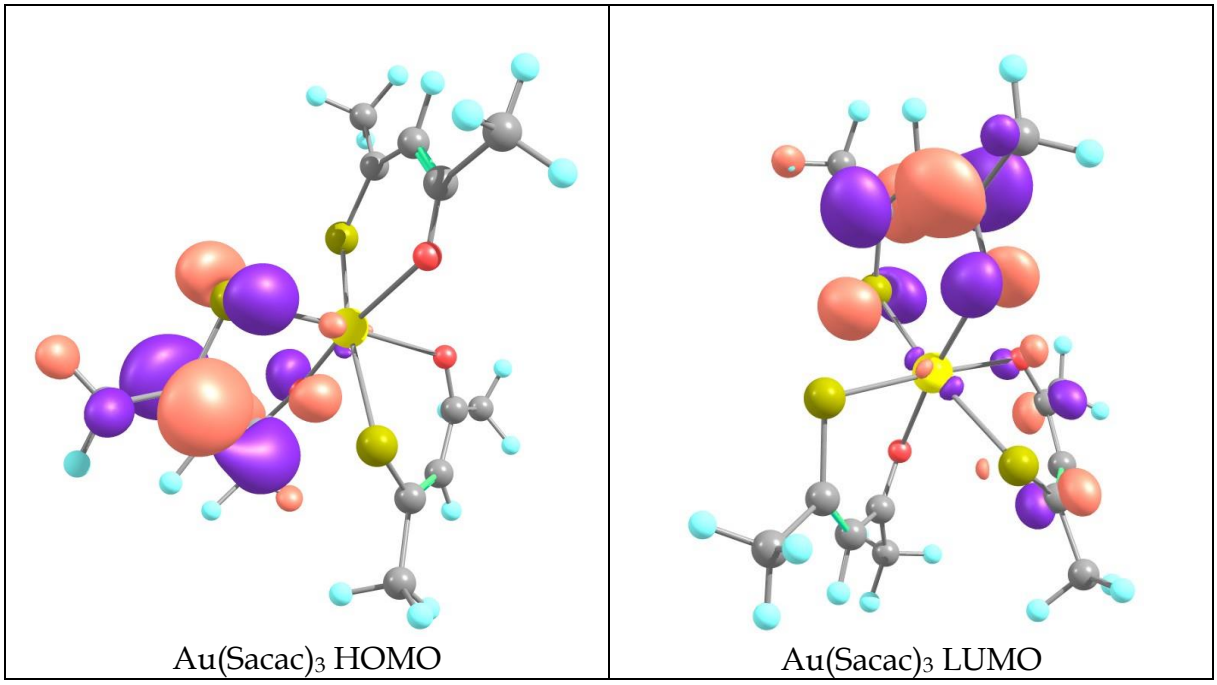

Figure 15: Molecular Orbital drawing of HOMO and LUMO of $Au(Sacac)_3$ displayed with 0.05 eÅ-3 contour, atomic structure is the same as in Figure 8 f) Colours: Au (yellow), C (grey), O (red), S (dark yellow), H (blue).

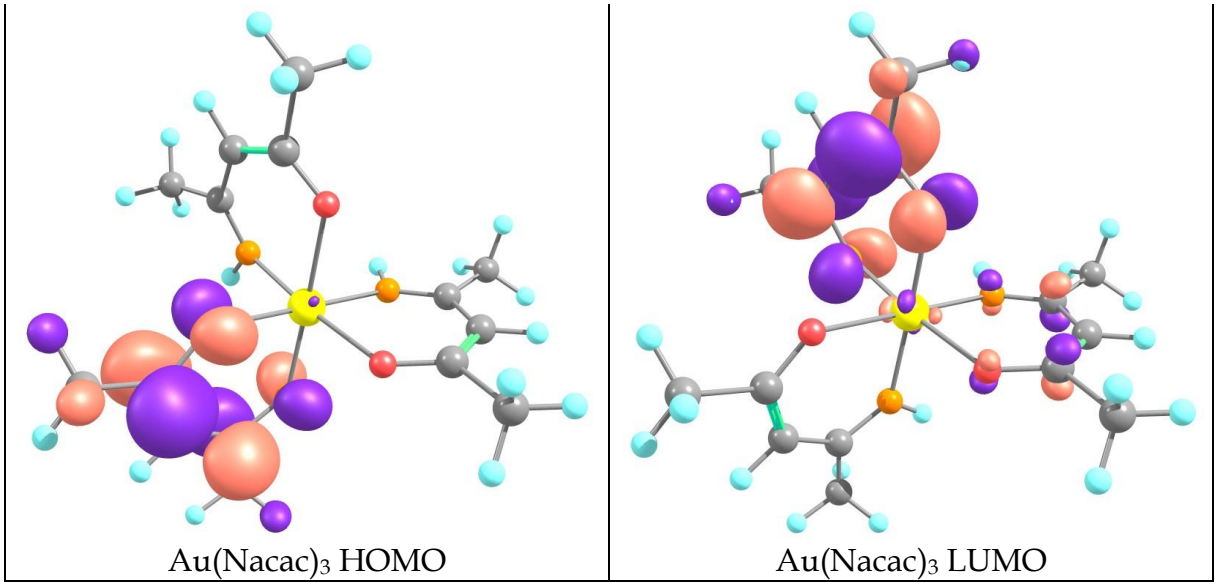

Figure 16 Molecular Orbital drawing of HOMO and LUMO of $Au(Nacac)_3$ displayed with 0.05 eÅ-3 contour, atomic structure is the same as in Figure 8 g) Colours: Au (yellow), C (grey), O (red), N (orange), H (blue).

Table 1: HOMO-LUMO gap and energy levels for Au (I) and Au (III) diketonate-style complexes

Oxidation State	Complex	HOMO (eV)	LUMO (eV)	HOMO-LUMO gap (eV)
Au (I)	Au(acac)	−4.911	−3.581	1.330
	Au(Sacac)	−5.124	−2.825	2.299
	Au(Nacac)	−4.714	−2.919	1.795
Au (III)	$[Au(acac)_2]^+$	−9.800	−7.761	2.039
	$Au(acac)_3$	−4.636	−3.643	0.993
	$Au(Sacac)_3$	−2.968	−2.596	0.372
	$Au(Nacac)_3$	−2.193	−1.614	0.579

The first series of Au (I) complexes indicate that both a sulphur and nitrogen substitution of one of the oxygens in acetylacetone improves stability – indicated by the HOMO-LUMO energy gap – with sulphur substitution seemingly adding the most stability. This would suggest a possible advantage to using S/N substituted β-diketone ligands for gold extraction if the gold is oxidized to +1 oxidation state during gas phase extraction. Empirical confirmation would prove useful further work if the cost of ligand does not change substantially with substitution.
When looking at the Au (III) series of complexes, it is suggested that $[Au(acac)_2]^+$ would be more stable than $Au(acac)_3$ – having a significantly larger HOMO-LUMO gap – once formed and could be a more likely complex produced during previous extractions. The HOMO-LUMO gap of $Au(Sacac)_3$ and $Au(Nacac)_3$ was very small comparatively. When considering the difficulty experienced in SCF convergence, the indications are that these complexes are unlikely to form in a gas phase extraction. Based on the energy gap alone, it is not recommended to pursue N/S substituted ligands if the expected oxidation state is Au (III).

Theoretical chemical reactions

A select group of theoretical chemical reactions between Au, O_2, and acetylacetone are evaluated in this section. Only reactions with acetylacetone ligand are considered due to ligand availability for empirical comparison. Both Au (I) and Au (III) are also considered.

The focus is to compare the ΔG of reaction to assess the spontaneity of each potential reaction. The HOMO-LUMO energy gap is useful in determining the stability of compounds once formed but does not say much for its likelihood to form. When considering what substance one is likely to find at the end of a real-world gold extraction, both likelihood of formation and stability are important to consider.

$$4Au + O_2 + 4acacH = 4Au(acac) + 2H_2O \qquad \Delta G_{rxn} = -326.95\ kj/mol;\ \Delta H_{rxn} = -403.91\ kj/mol$$

(*Equation 1*)

$$4Au + 3O_2 + 8acacH = 4[Au(acac)_2]^+ + 4[OH]^- + 2H_2O \qquad \Delta G_{rxn} = 1427.87\ kj/mol;\ \Delta H_{rxn} = 1205.41\ kj/mol$$

(*Equation 2*)

$$4Au + 3O_2 + 12acacH = 4Au(acac)_3 + 6H_2O \qquad \Delta G_{rxn} = -824.94\ kj/mol;\ \Delta H_{rxn} = -1175.11\ kj/mol$$

(*Equation 3*)

Theoretically, Equation 1 is spontaneous and is the favourable complex to form under standard conditions. This is also due to the lower energy required to oxidize Au to Au (I) rather than Au (III); and the negative ΔG_{rxn} indicates that the reaction is spontaneous under standard conditions.

Both reactions involving Au (III) complexes present an interesting result: the formation of $[Au(acac)_2]^+$ appears extremely difficult (with ΔG_{rxn} = 1427.87 kj/mol) when compared to that of $Au(acac)_3$, yet $[Au(acac)_2]^+$ has higher a stability than $Au(acac)_3$. A possible explanation is that a high activation energy barrier exists when oxidizing gold to form $[Au(acac)_2]^+$. Once this barrier is overcome, it requires a similarly high energy to reverse the reaction – giving the complex increased stability.

The indication that the ion $[Au(acac)_2]^+$ is the most likely product to form, suggests that gas-phase extraction may not be favourable for this system as ions cannot exist in gas phase at the low temperatures required for acetylacetone vaporisation. Formation of $Au(acac)_3$ may be more likely in gas-phase; however, a lower stability would make it potentially difficult to detect as either reversal or decomposition is likely to occur before a sample can be analysed.

Attempted synthesis of Au (III) acetylacetonate complex

Current knowledge of gas phase gold extraction in the group has yet to determine the exact oxidation state of gold that forms during a reaction between gold, acetylacetone, and air (Ali 2021). To verify the validity of the DFT calculations, and figure out which complex may form during extraction, an attempt at synthesizing gold acetylacetonate followed the DFT calculations as a basis of empirical comparison. Before moving to extraction at elevated temperatures, synthesis was attempted at lab conditions to have a closer comparison to the standard conditions that the DFT calculations utilize (H^{o} = 298 ^{o}K) (Frisch *et al.* 2019).

Perhaps the most useful feature of DFT to this study, is the ability to predict infrared spectra of each complex calculated. It enables one to measure an infrared spectrum of an experimental sample and compare the results to a predicted spectrum – a match or high degree of similarity indicating the compounds could be one and the same.

A well-established method for synthesizing β-diketonato complexes with many different transition metals was used in an attempt to synthesize either $[Au(acac)_2]^+$ or $Au(acac)_3$. This work will only consider Au (III) complexes due to reagent availability. Gold (III) chloride (99 % CAS No.: 13453-07-1) was obtained from Sigma Aldrich, methanol (100 % CAS No.: 67-56-1) was obtained from ACE Chemicals, acetylacetone (99 % Reagent Plus® CAS No.: 123-54-6) and ammonium hydroxide (ACS reagent 28.0-30.0 NH_3 basis CAS No.: 1336-21-6) were obtained from Sigma Aldrich.

The process used for synthesis is as follows:

1. Dissolve 0.5 g gold (III) chloride salt in 2 ml methanol and agitate until fully mixed.
2. Add 0.4 ml acetylacetone and agitate for 2-3 minutes.
3. Add 1 drop ammonium hydroxide and agitate to allow crystals to form.

A chloride salt of gold was used to remove the obstacle of oxidizing gold with oxygen – a theory that will be tested later in this dissertation. Figure 17 shows the change in colour of the gold solution when acetylacetone is added, indicating a

potential reaction taking place. The addition of ammonium hydroxide is to allow the acetylacetonate crystals to form. After addition of ammonium hydroxide, a precipitation was observed. The solid was analysed with both FTIR and single crystal X-Ray Diffraction (XRD).

$AuCl_3$ dissolved in methanol

$AuCl_3$, methanol and acetylacetone

Figure 17: Images of gold (III) acetylacetonate synthesis attempt from $AuCl_3$ salt

Analysis and comparison of synthesis products and DFT-calculated spectra

Firstly, the predicted IR spectra of $[Au(acac)_2]^+$ and $Au(acac)_3$ are presented in Figure 18. Graphs are displayed using ChemCraft with Gaussian band broadening enabled. The following, Figure 19, shows the FTIR scan of the synthesis precipitate, and a reference FTIR scan of acetylacetone from the NIST database.

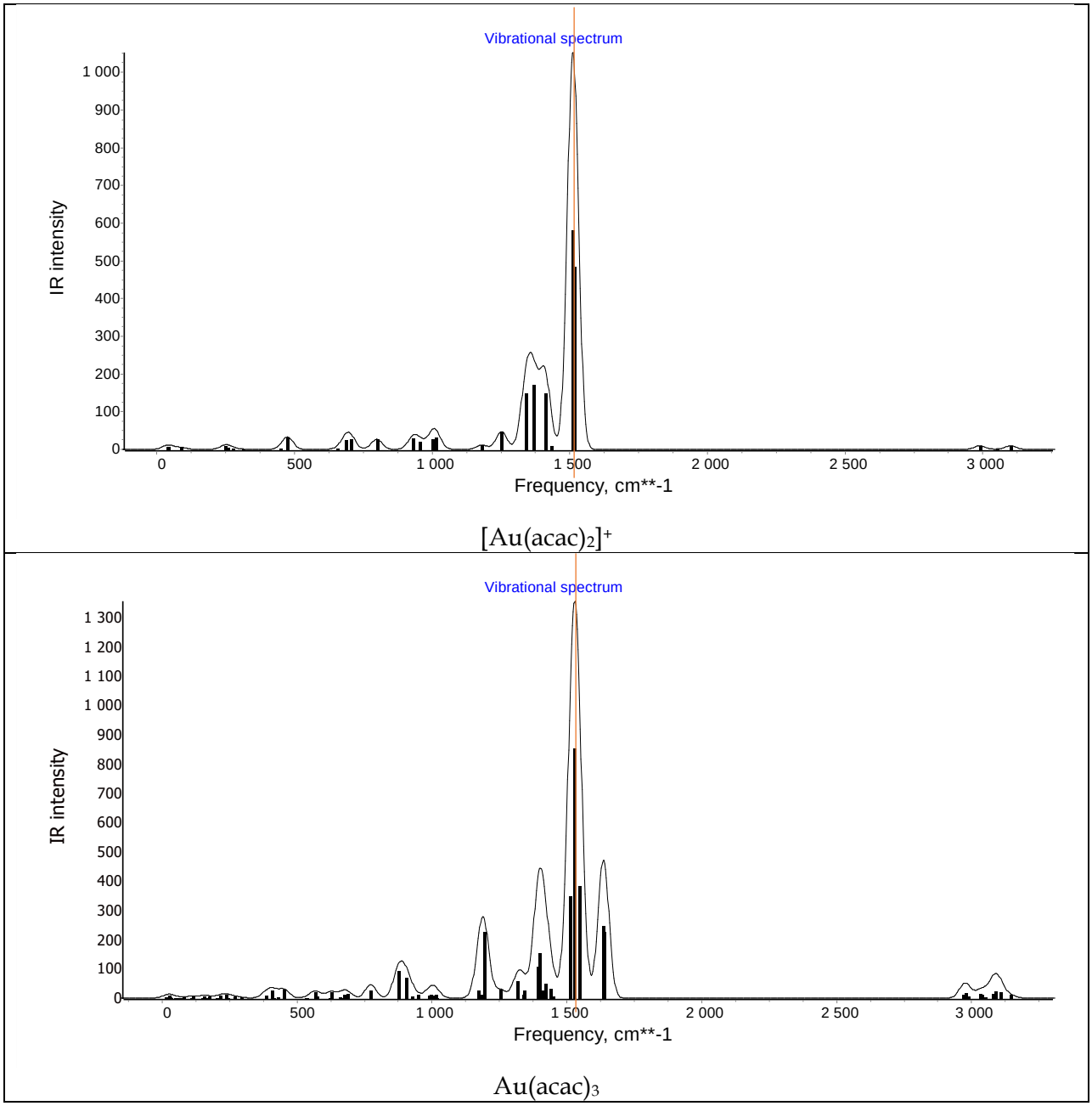

Figure 18: Predicted IR Spectra of $[Au(acac)_2]^+$ and $Au(acac)_3$, calculated in Gaussian16 (Frisch *et al.* 2019)

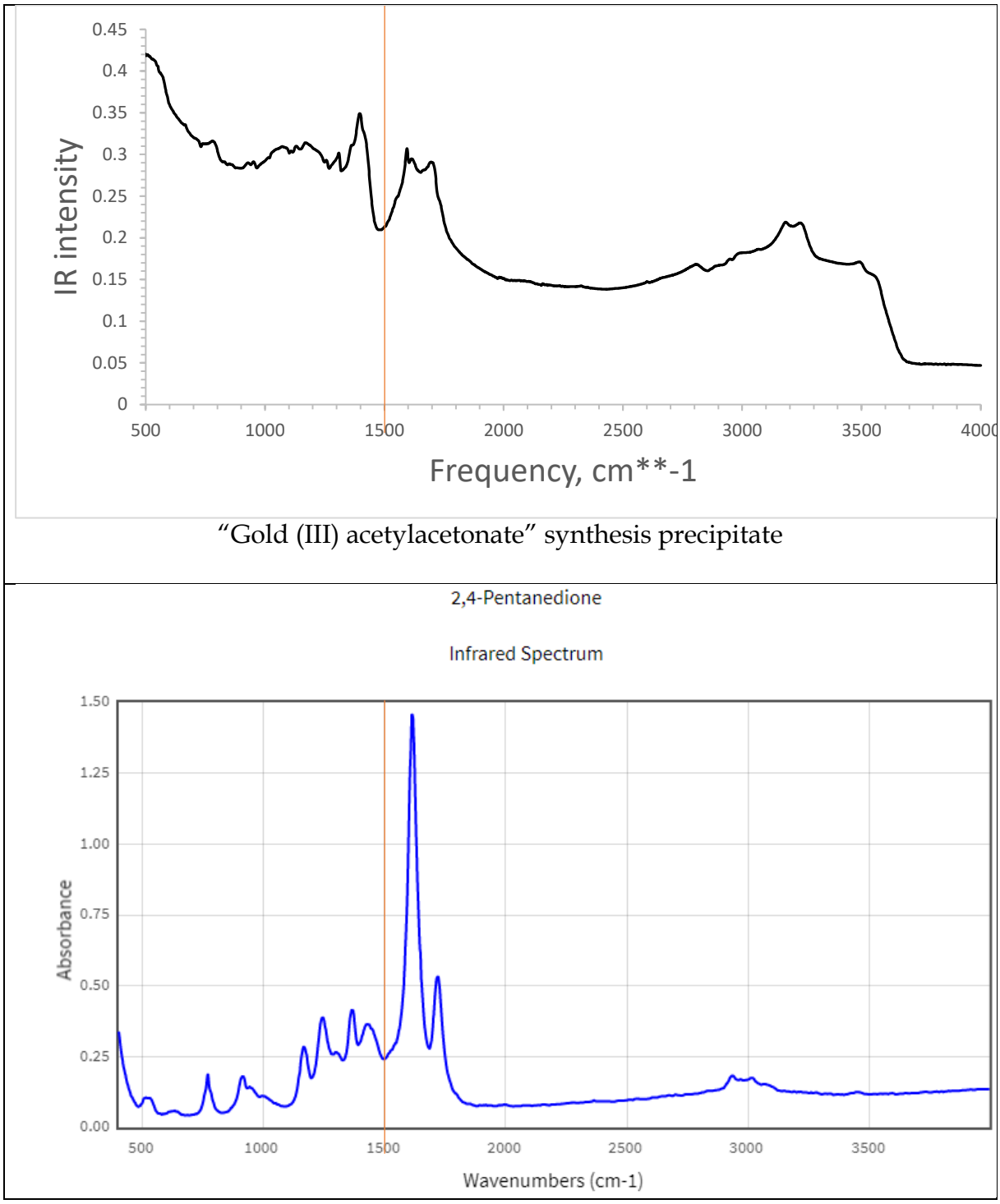

Figure 19: Measured FTIR of "gold (III) acetylacetonate" synthesis precipitate and reference IR spectra for acetylacetone (NIST 2021)

The synthesis precipitate sample measured in Figure 19 was an oily grey/yellow solid. Both predicted IR spectra for $[Au(acac)_2]^+$ and $Au(acac)_3$ have the dominant peak at 1500 cm^{-1} with smaller peaks around 1200-1400 cm^{-1} and a small double peak at about 3000 cm^{-1}. The spectrum of $Au(acac)_3$ has an additional peak at

approximately 1650 cm^{-1}. The measured spectrum shows little similarity with the predicted ones; where the predicted spectra are dominant (at 1500 cm^{-1}), the measured spectra has a trough. The dominant peak for the measured precipitate spectrum occurs at approximately 1400 cm^{-1}, and a small double peak is visible at around 3200 cm^{-1}.

A reference spectrum of acetylacetone from the NIST database is provided for comparison as the oily substance that coated the precipitate is suspected to be unreacted acetylacetone. The measured precipitate and acetylacetone spectra both have a trough at 1500 cm^{-1}, a small double peak at 3000-3200 cm^{-1} and a larger peak followed by a smaller just to the right of the 1500 cm^{-1} trough. This would suggest the presence of unreacted acetylacetone – an unsurprising result as it is one of the reagents.

FTIR analysis of the synthesis precipitate appears to indicate that there was little to no gold (III) acetylacetonate formed. Single crystal XRD was used as a secondary analysis to validate the results of the FTIR. Single crystal XRD drawing is presented in Figure 20, it shows that the gold complexed with the available chlorine (from the $AuCl_3$ originally used) to form a gold chloride-ammonium salt, $[AuCl_4]^-$ $[NH_4]^+$, acetylacetone was not part of the matrix at all.

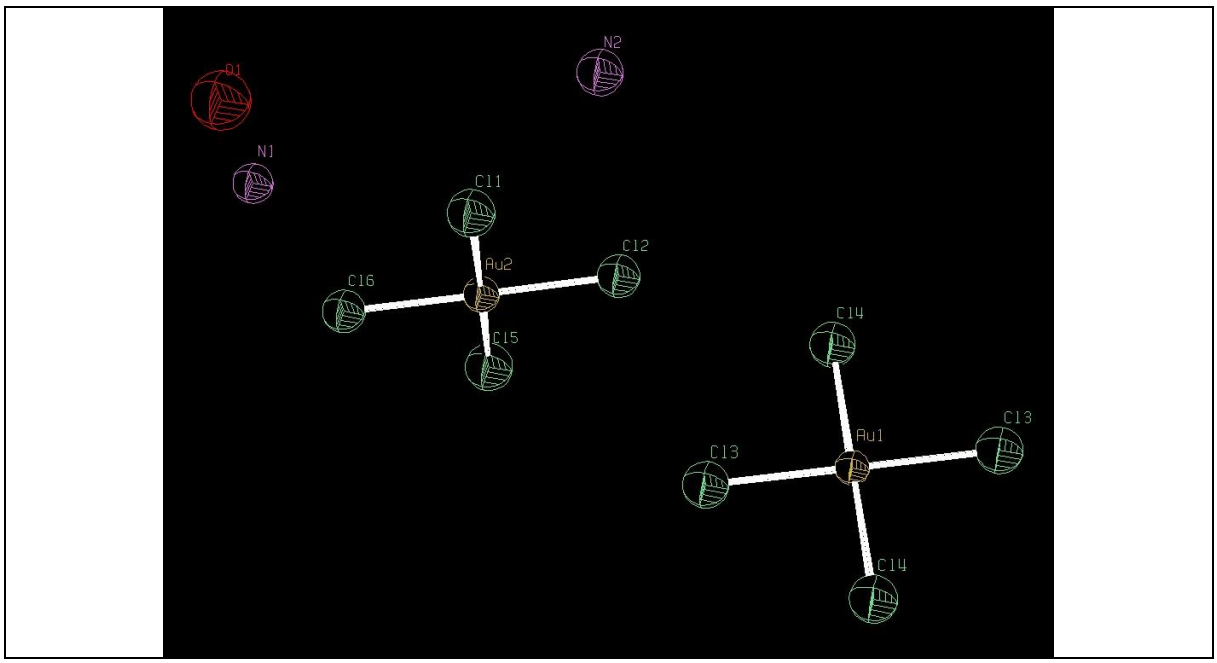

Figure 20: Drawing of Single Crystal X-Ray Diffraction of ammonium gold (III) chloride precipitated during attempted synthesis of gold (III) acetylacetonate (Muller 2021)

While the synthesis method used is suitable for many metal acetylacetonates, it does not appear to work at all for Au (III) salts. The same method was used on Fe (III) to produce $Fe(acac)_3$ successfully with good conversion (verified by mass spectroscopy). Since gold is a far more stable metal than iron, it was thought that the presence of other species such as chloride ions and methanol would inhibit formation of an acetylacetonate complex. To give gold and acetylacetone the best chance of forming a complex, a simplified approach would be required – one where the only reagents in the system are those that would be expected to participate in the complex. This was the basis of thinking that was used when proceeding with the following chapters in this dissertation.

CHAPTER FOUR
Pure gold extraction with acetylacetone —A fundamental approach

Review of previous gold extraction dissertations

Several studies in the last 15 years have focussed on utilising gas-phase acetylacetone to extract different valuable metals (Potgieter *et al.* 2006, Van Dyk *et al.* 2010, Shemi *et al.* 2012, Tshofu 2014, Olehile 2017, Machiba 2020, Ali 2021). The list of studies discussed in this dissertation is not exhaustive; it is likely that more will follow. In this Chapter I focus on two studies—namely those of Machiba (2020) and Ali (2021)—that cover gold extraction.

Many of the studies investigating gas-phase extraction with acetylacetone in the School of Chemical and Metallurgical Engineering at Wits used the same or a similar experimental apparatus. Machiba (2020) and Ali (2021) used the apparatus that Olehile (2017) built (see Figure 21). Its roots go back to the original acetylacetone work undertaken by Potgieter *et al.* (2006). In the setup presented by Olehile (2017), a peristaltic pump feeds acetylacetone through a preheating coil into a plenum flask, in which the ligand is boiled. The vapour passes up through the bed of fine particles, some of it complexing with gold and metals in other minerals *as expected*. The organo-metallic complex is carried along with unreacted acetylacetone up through the bed and into a condenser, where the excess ligand and metal complexes are collected in a cold trap of ethanol. Ali (2021) introduced air into his system. It served as a carrier and a source of oxygen needed for the reaction with gold. The condensate in the cold trap was withdraw at intervals (½ h to 1 h) and analysed with AAS to determine the concentration of the metal of interest.

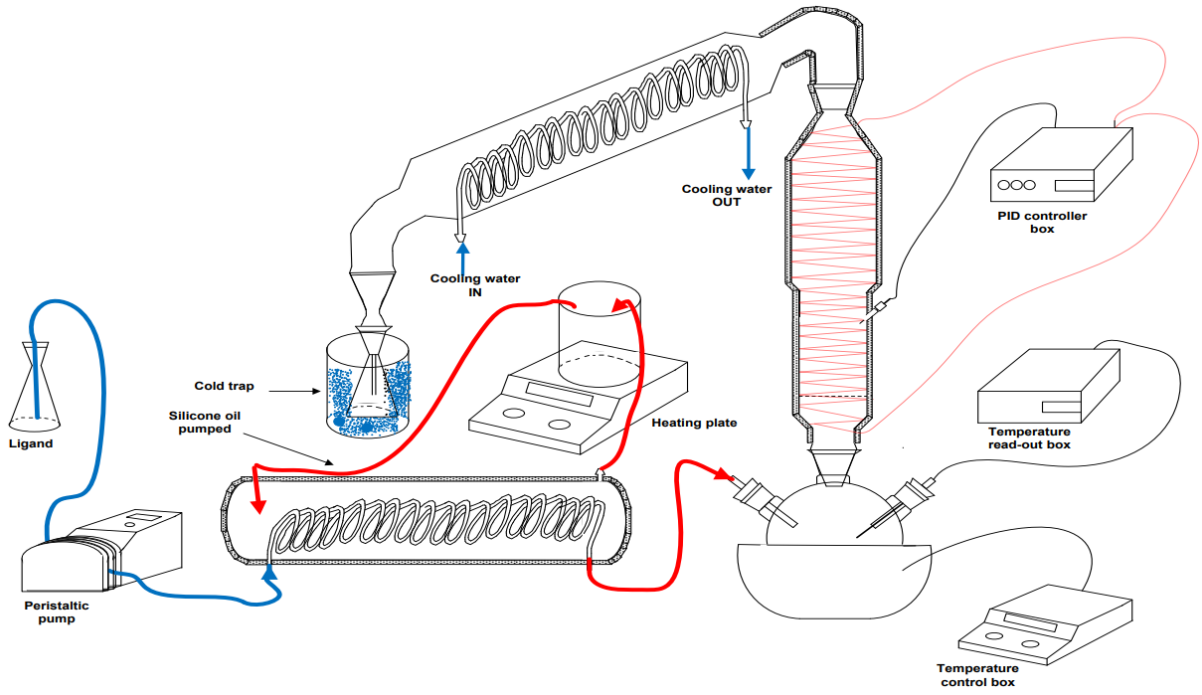

Figure 21: Gas phase extraction apparatus used in previous studies at Wits (Olehile 2017, Machiba 2020, Ali 2021)

Both studies reported similar trends of gold extraction from refractory gold ore, obtained from the DRDGold Ergo plant. The general trend reported within a 240min extraction window, was a slight increase in gold extraction with increasing temperature in the range of 190 ℃ to 250 ℃. Both studies also reported an increase in total gold extraction with an increase in extraction time and a flattening-off of extraction curve after 180min. Higher extractions were reported for lower bed masses – indicating that this extraction method favours low-grade gold sources. Ali (2021) reported a maximum gold extraction of 49.71 % after 4 hours at 250 ℃ with a ligand flowrate of 3 ml/min and a bed mass of 20 g. Machiba (2020) reported a maximum extraction of 78.74 % after 4 hours at 250 °C with a ligand flowrate of 6 ml/min and a bed mass of 50 g.

Using AAS to measure gold concentration in condensate has the benefit of very low detection limits – at levels in the region of 0.015 mg/L. The detection limit is dependent on the noise intensity of each instrument (Cao *et al.* 2009). However, detection with AAS does not provide any information to the goals of this work – understanding what happens when gold is extracted and what possible reactions occur.

Extraction apparatus and design methodology

Following the failure to synthesize a gold acetylacetonate complex from a gold chloride salt, where Au(III)Cl was merely converted into $AuCl_4NH_4$, a further simplification of the reacting material was required. It became clear that bonding gold ions with acetylacetone were easily out competed by chloride ions. This information itself is an interesting discovery as one would expect chloride ions to preferentially react, however, this does not appear to be the case with Fe. Many other metals such as V, Pb, Cr and other lanthide metals are reported to behave similarly to Fe (Potgieter *et al.* 2006). As mentioned earlier, a sample of $Fe(acac)_3$ was synthesized from iron(III) chloride. It would seem there is something unique about gold ions that allow chloride ions to out compete acetylacetone.

With such problems in competitive reactivity in mind, the need for further simplification is clear. If it is reported that gold can be extracted by acetylacetone in gas phase (Machiba 2020, Ali 2021), then the simplest system to investigate this extraction further would be one with only gold, acetylacetone and a carrier gas. Ali (2021) discussed the need for an oxidant and hence, compressed air containing oxygen was used as a carrier gas.

The primary goal of this work is to understand the reactions between gold and acetylacetone when gas-phase extraction occurs. One could think of the objective of this research to be synthesis of gold acetylacetonate, synthesis of a sufficient quantity for analysis of the complex. To assist in possibly observing what happens in gas-phase extraction of gold with acetylacetone, materials were used in far higher quantities than Ali (2021) and Machiba (2020).

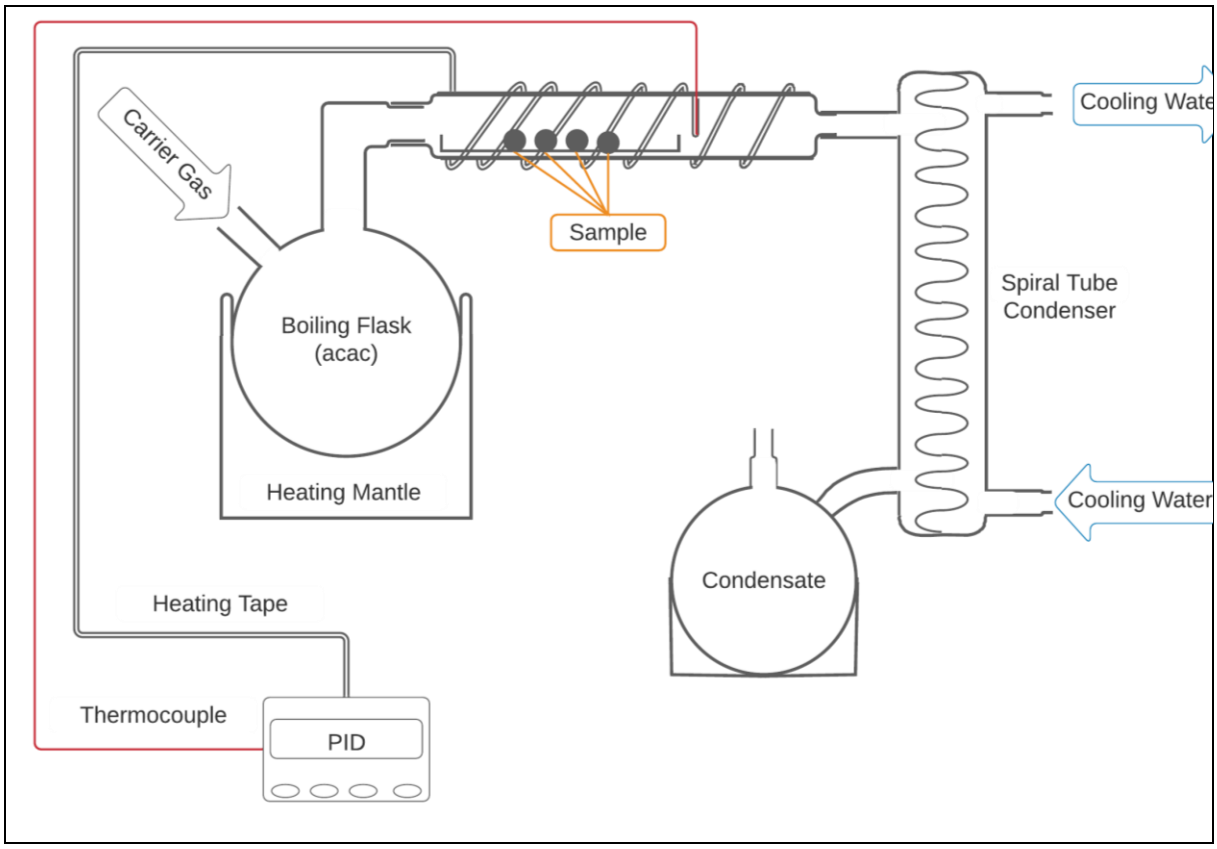

Figure 22: Schematic diagram of experimental setup used for gas-phase extractions with acetylacetone

The simplified apparatus presented in Figure 22 was designed to eliminate as many variables as possible, while still maintaining the same conditions within the reaction zone as previous works. The conditions within the reactor still provide the elevated temperatures and expose a sample to flowing acetylacetone vapours. Use of large quantities of reagent also allows for the simple validation of previous understanding of extraction with a critical test.

The critical test for gold extraction is to answer a simple yes/no question: can acetylacetone extract gold in a gas-phase reaction. With large quantities of material, measurement of any extraction is much easier than measuring the difference in gold when already present at ppm levels. Measuring the exact quantity of gold present in cyanide tailings is practically very difficult, whereas the measurement of a gold nugget can be achieved on a scale. Extracted gold can also be measured in the condensate to provide a full mass balance on the gold – an aspect that challenged previous works. Further, individual pieces of gold (in this method) were inspected

before and after extraction for any change in surface characteristics that might give further insight into the reaction that took place.

Extraction attempts were performed with the following procedure (in reference to Figure 22):

1. Samples were weighed three times and average mass was used. The sample was weighed into a glass trough (used for added ease in moving and weighing sample) and placed into the reactor.
2. The boiling flask was filled with 200-300 ml of acetylacetone, and all glass joints sealed with high vacuum grease to prevent vapour leaks.
3. The heating tape was set to temperatures between 180 °C and 220 °C and controlled with a PID control unit. After thermocouple had reached setpoint temperature, a further 10 minutes wait was used to allow for thermal equilibrium within the reactor.
4. The cooling water circuit was turned on, followed by the carrier gas.
5. The heating mantle was switched on and left on for the duration of the boil of acetylacetone until all the ligand had evaporated.
6. Once all liquid in the boiling flask had evaporated, the heating mantle was switched off and the carrier gas allowed to flow through the system for a further 7 minutes.
7. Accumulated condensate (mostly unreacted acetylacetone) was transferred back into the boiling flask and the heating mantle switched on again. The reactor setpoint remained constant throughout the recycle process.
8. Steps 8 and 9 were repeated until the desired extraction time was reached. The start and end point of the time for each experiment was taken as the times when the carrier gas was switched on and off. This was done because acetylacetone has a high vapour pressure and some of it would be carried into the heated reactor and react before the boiling flask was brought to boil.
9. To shut down, all heating apparatus was turned off, the carrier gas flow was halted after 5 minutes, and the reactor was left to cool sufficiently before the sample trough was removed.

10. The sample was weighed as soon as possible after the end of the extraction experiment and samples of the boiling flask residue and acetylacetone condensate were taken for later analysis.

Three different samples derived from the same batch of pure gold (>99.99 %) beads were used for gold extractions. The first, a sample of gold filings with a mass of 998.8 mg, was exposed to a 200 ml charge of acetylacetone over a period of 33 minutes. The reactor was set to 170 °C. No recycle was used for this run. This resulted in an approximate ligand flowrate of 6.1 ml/min.

The second sample was a 1709.2 mg sample consisting of two gold beads, approximately 9 mm diameter with irregular shape, that were exposed to a charge of 100 ml acetylacetone that was recycled three times during the total extraction time of 68 minutes. The reactor was set to 200 °C for this experiment. Minimal loss of acetylacetone was observed between each recycle. This resulted in an approximate ligand flowrate of 5.9 ml/min.

The third gold sample was 1316.4 mg, consisting of three beads with an approximate diameter of 6 mm. The sample was exposed to a charge of 200 ml acetylacetone that was recycled five times over a period of 182 minutes. The reactor was set to 190 °C. This resulted in an approximate ligand flowrate of 6.6 ml/min.

The combination of extraction conditions used cover a wide range of possible extraction conditions. The purpose of this is to cover both long and short extraction times. Filings were used in one experiment to assess if there is any measurable effect of surface area on extraction. Exposure time was also varied to see if the extraction time changed the extraction products significantly.

Carrier gas flow was measured with a FP 1/4-25-G-5/81 tube with SS-14 float. The carrier gas flowrate was approximately 0.6 L/min for all extraction attempts.

The large gold beads were favoured due to the ability to target specific pieces. Each gold bead was observed under an optical microscope to look for any change in the surface character that would indicate a chemical reaction. The surface of the gold was also analysed with Raman Spectroscopy. Liquid samples of the boiling flask residue and condensate were analysed for metal content with Inductively coupled plasma

mass spectrometry (ICP-MS) at the University of Johannesburg, all ICP-MS testing was conducted by Petrus Philippus Pieterse.

It is important to note that sampling was only conducted at the end of each run, rather than continuously in 30min intervals, as done in previous work. The primary reason for this difference is to reduce analytical uncertainty as a single measurement – of a potentially higher concentration – would carry less uncertainty than the addition of multiple, lower concentration, measurements. This simplification prevents the additive uncertainty of each measurement taken and was also done because this work is not concerned with a specific fraction of gold extracted within smaller time intervals, most significant to a kinetic study.

Initial observations and indications

A summary of the experimental conditions for the pure gold samples is presented in Table 2. Over the range of temperatures considered, and the different exposures of gold to acetylacetone, there did not appear to be any visual or measurable signs of an interaction between pure gold and acetylacetone. There was no measurable mass change in the gold sample for both single-pass, and recycled acetylacetone configurations. Minor fluctuations are reported up to 0.3 mg, however, it should be noted that this was the last digit displayed on the mass meter that was used – some level of variance is expected.

Table 2: Summary of experimental conditions and mass changes of gold samples

Sample	**Temperature of reactor**	**Approximate ligand flowrate**	**Exposure time**	**Initial sample mass**	**Mass difference after extraction**	
	(°C)	*(ml/min)*	*(min)*	*(mg)*	*(mg)*	*(%)*
1	170	6.1	33	998.8	+ 0.2	+ 0.020
2	200	5.9	68	1709.2	- 0.3	- 0.018
3	190	6.6	182	1316.4	+ 0.3	+ 0.023

The gold pieces were inspected under an optical microscope to look for any changes in surface texture, pitting, colour change – any indication of a reaction. No such changes were observed on any of the pieces in the three samples used in this work. Additionally, no visible change in colour of the acetylacetone condensate was

observed. The acetylacetone evaporated and condensed back to a liquid indistinguishable from the original.

The indications from the information available at this point were that if there is gold extraction was taking place, it was on a very minor scale that could perhaps be difficult to detect visually or by mass difference. Further investigation with more sensitive techniques was required to verify the suspected findings from simple observation.

Insights gained from further analysis on ICP-MS

After the first extraction attempt conducted on gold filings, it became clear that production of large quantities of gold acetylacetonate would be difficult – if possible at all – with gas-phase conditions. This prompted the subsequent sampling of condensate for later analysis on ICP-MS. Liquid samples taken from both the boiling flask residue and condensate were analysed for the presence of Au, Fe, Cr and Ni with ICP-MS. The metal contents of selected liquid samples from the attempted extraction of gold beads with acetylacetone are presented in Table 3:.

Table 3: ICP-MS results reporting the concentration of Au, Fe, Ni, Cr in the liquid samples of the attempted extraction of gold with acetylacetone.

Metal	**Sample 2 metal content** *(mg/L)*		**Sample 3 metal content** *(mg/L)*
	Residue	**Condensate**	**Condensate**
Gold	0.006	0.001	0.002
Iron	39.441	8.978	10.151
Nickel	0.478	0.367	0.294
Chromium	0.677	0.154	0.151

The metal concentrations found on ICP-MS give critical insight toward explaining what occurred during the extractions. There appears to be a small amount more of each metal present in the residue when compared to the condensate across all metals. This suggests that the re-boiling of the condensate acts as a concentrating step towards all metals considered in this study – most critically, gold. However, the issue of separation is more complex than simple evaporation. The iron, chromium and nickel levels were all higher in the residue when compared to the condensate. If any

of these metals would be present along with gold – and this is practically guaranteed when extracting from gold tailings – then they too would concentrate into an evaporate-residue.

It is extremely important to note at this point, the numbers presented in Table 3 may appear to show evidence of gold extraction – this is most likely not the case. One may find it tempting to explain the gold levels as extraction, the condensate presents the "single pass" extraction concentration, and the residue presents the accumulation of the gold extracted from each pass and subsequent recycle.

Firstly, the accumulation of "extracted" gold is addressed. It is a skewing of data that is due to the size of each sample. Each condensate sample was a 50 ml sample taken from the 100-200 ml of acetylacetone in the condensate flask. The residue sample was taken by redissolving the solid residue in the boiling flask. The residue was dissolved in approximately 15 ml of acetylacetone. The original volume of acetylacetone within the boiling flask was around an order of magnitude higher (100-200 ml). It is suspected that the base level of gold found within the acetylacetone was simply concentrated via evaporation.

The Reagent Plus® acetylacetone supplied by Sigma Aldrich is quoted as ≥99 %. There is no mention of what the approximately 1 % impurities might contain. It is clear from the ICP-MS data that at least one of those impurities is iron – hypothesised to be present as a remnant of Sigma Aldrich's production process. A residual gold concentration of 1-2 parts-per-billion (ppb) is possible.

The concentrations of gold measured in this work are near the limit of detection of gold via ICP-MS (Allabashi *et al.* 2008). Other results supplied by Mr Pieterse (ICP-MS technician) quote gold content as <1 ppb. This would indicate the detection limit of the specific instrument used in this work (for gold) to be in the region of 1 ppb. The possibility of noise readouts cannot be definitively ruled out in this case.

Decomposition of acetylacetone

From the onset of the first extraction, there appeared to be an unknown residue forming in the boiling flask that was not present in the condensate flask. Initial suspicion was that there was a contaminant leaking into the apparatus, possibly from

the high vacuum grease used to seal the glass joints. The residue was a light-yellow colour when present in low quantities and a dark maroon colour when concentrated – eventually turning black when isolated into solid form. Four images are presented in Figure 23 that show the development of the residue. Residue was particularly noticeable on longer experimental runs where the acetylacetone was recycled.

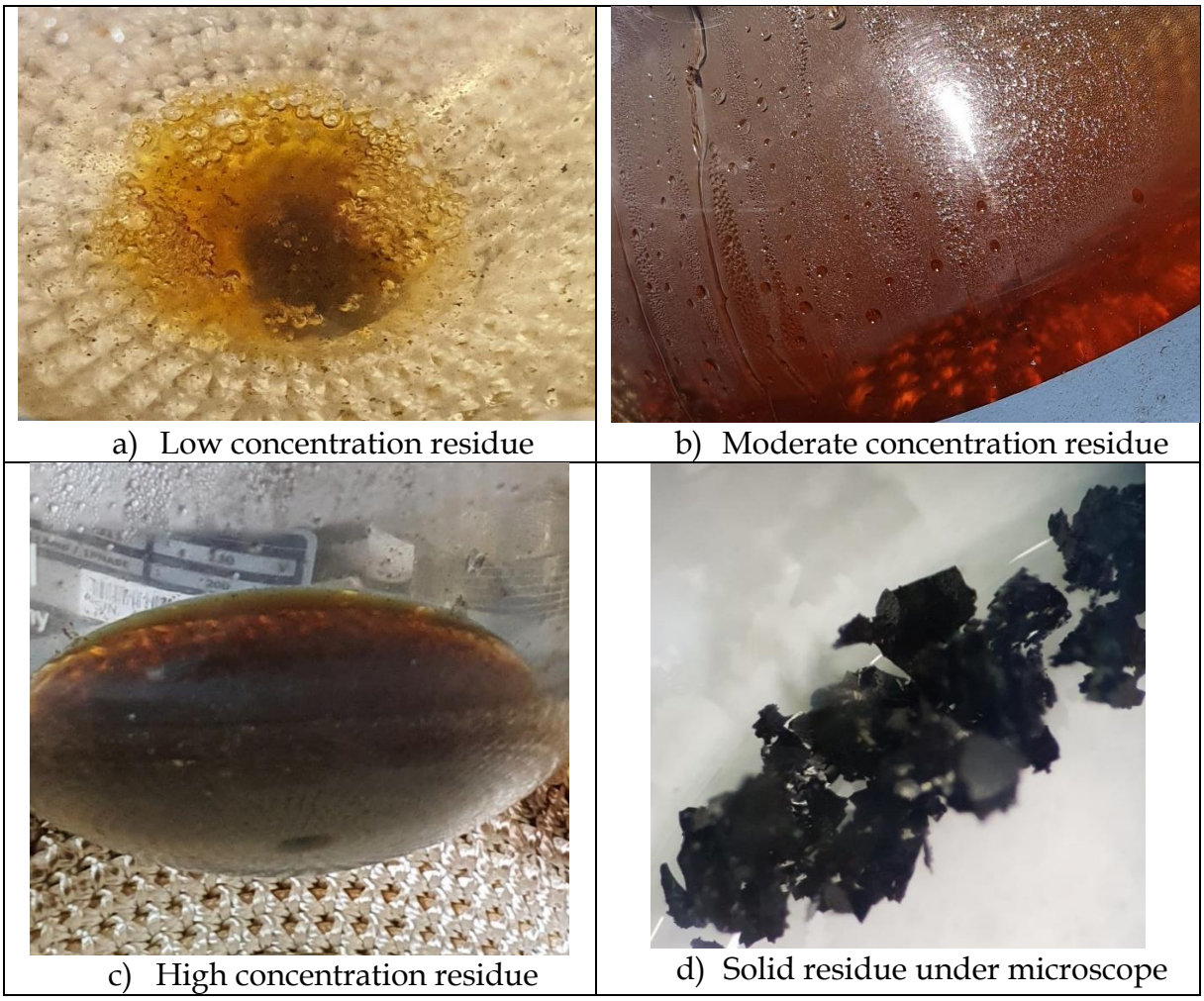

a) Low concentration residue

b) Moderate concentration residue

c) High concentration residue

d) Solid residue under microscope

Figure 23: Photographs of residue forming in boiling flask at a) low concentration b) moderate concentration c) high concentration and d) solid form under optical microscope. All liquid samples are presumed to be dissolved in acetylacetone – the only other substance present.

The second thought was that through recycling, an unknown metal/ligand complex was accumulating in the boiling flask, a complex that may not be noticeable in quantities produced in a single pass of acetylacetone. To rule out this theory, the same apparatus was used for a "blank run" where no sample was placed in the reactor. The only substance in the system was acetylacetone and air that formed the function of a carrier gas. A temperature of 190 °C was used for the reactor

temperature. The residue was produced in both cases where compressed air, and later nitrogen, were used as a carrier gas. This suggests that oxygen is not participating in the formation of the residue.

The same substance was also found after operating the apparatus with only acetylacetone present. The phenomenon was highly repeatable and was observed in every extraction attempt performed on the apparatus for this work. It is also important to mention at this point that a similar substance was also observed by one of my colleagues, Marc Henderson (2022), that was investigating supercritical CO_2 extraction with acetylacetone. The system operated in the region of 80 ˚C to 105 °C for periods of 8 hours.

This was a strong indication that the substance is most likely a decomposition product of acetylacetone. However, decomposition of acetylacetone is not fully understood. While there is much focus on the decomposition of metal-acetylacetonate complexes, for applications such as thin film chemical vapour deposition, not much literature could be found covering the thermal decomposition of acetylacetone itself.

Choudhury and Lin (1990) reported that the primary pyrolysis products of acetylacetone are Acetone, H_2O, and CO. The first decomposition product is acetone, which would decompose itself due to the high temperatures of 847-1387 ^oC considered in this study. Other literature was found covering electron beam induced decomposition (Warneke *et al.* 2015) and biodegradation (Zhou *et al.* 2020). However, the thermally driven decomposition products discussed by Choudhury and Lin (1990) are more relevant to this work as only heat is responsible for decomposition in this case.

The safety data sheet for acetylacetone that was supplied by Sigma Aldrich (version 6.7 accessed 30 Dec 2021) states a boiling point of 140 ˚C. Strangely, the entry for decomposition temperature states: “Distillable in an undecomposed state at normal pressure.” This appeared to be the case from the observations in this work; the acetylacetone that condensed appeared to be indistinguishable from its original form. However, the same cannot be said for the material that was within the boiling flask. During the formation of the residue, a thermocouple was placed into the heating

mantle and a temperature of 165-167 °C was recorded – significantly above the boiling point of acetylacetone.

An attempt to analyse the solid residue was made after liquid analysis on ICP-MS indicated minimal metal presence (see Table 3 residue sample). Since the substance appeared crystalline under microscope, single-crystal X-ray diffraction (XRD) was attempted. However, no diffraction occurred; the substance was amorphous. The gold samples were also analysed using Raman Spectroscopy. The analysis confirmed that the gold remained unchanged. The analysis also discovered loose carbon adhering to the surface of the gold – likely a result of the decomposition of acetylacetone.

The presence of free carbon indicates that the decomposition observed was – to some extent – a complete decomposition, even though only a small amount of acetylacetone was decomposing. This would suggest a good chance that the residue sample (when also considering the shiny/black outward appearance) could be a form of graphene. It is possible that the heat transfer within the acetylacetone is poor, leading to a layer around the edges of the boiling flask becoming superheated as heat accumulates rather than transferring to the bulk medium to drive boiling. The thin superheated layer would be the origin of the decomposition. This is mostly speculation, further empirical investigation into the exact composition of the residue would make a great addition to literature as an exact decomposition temperature, and products, is unknown.

Thermodynamic study of acetylacetone decomposition

Acetylacetone decomposition was modelled in ASPEN PLUS V10 to investigate the stability of acetylacetone in extended temperature range from an equilibrium point of view. The carbon detected in analysis of the gold samples suggests that decomposition may have occurred in an oxygen-starved environment. An equilibrium study of decomposition will provide additional information about the suitability of acetylacetone as a ligand in gas-phase extraction at temperatures above 250 °C and will also be used as a comparison to empirical evidence.

The decomposition was modelled using the "RGibbs" unit in ASPEN PLUS V10 with the GRAYSON property method that was suggested by the Aspen methods assistant. The property method is described as suitable for hydrocarbon systems at low pressures and relatively low temperatures with hydrogen. Since hydrogen is a possible decomposition product in hydrocarbons, this method was deemed suitable as this study is focussed on trend. The decomposition products considered in this study include carbon (graphene), carbon monoxide, carbon dioxide, hydrogen, water, and methane.

Acetylacetone was modelled with a basis of 1 kmol/hr total feed flowrate and oxygen was added incrementally from 0 mol% to 50 mol% to simulate different acetylacetone concentrations in the carrier gas. A pressure of 1 atm was used throughout all simulations. The software package was also used to convert the 6 ml/min liquid flowrate of acetylacetone to a gas flowrate of approximately 2.1 L/min for comparison.

Decomposition of a 1 kmol/hr stream of pure acetylacetone was modelled and the flowrate of decomposition products are given in Figure 24 for temperatures from 140-500 °C. The equilibrium reaction products show that very small quantities of C, CO, CH_4 and acetone should be produced. The lack of significant decomposition (below 0.2% of total acetylacetone) up to 500 °C suggests that acetylacetone is very stable in inert atmospheres at increased temperatures beyond 250 °C that was the limitation of previous studies involving gas-phase extraction with acetylacetone.

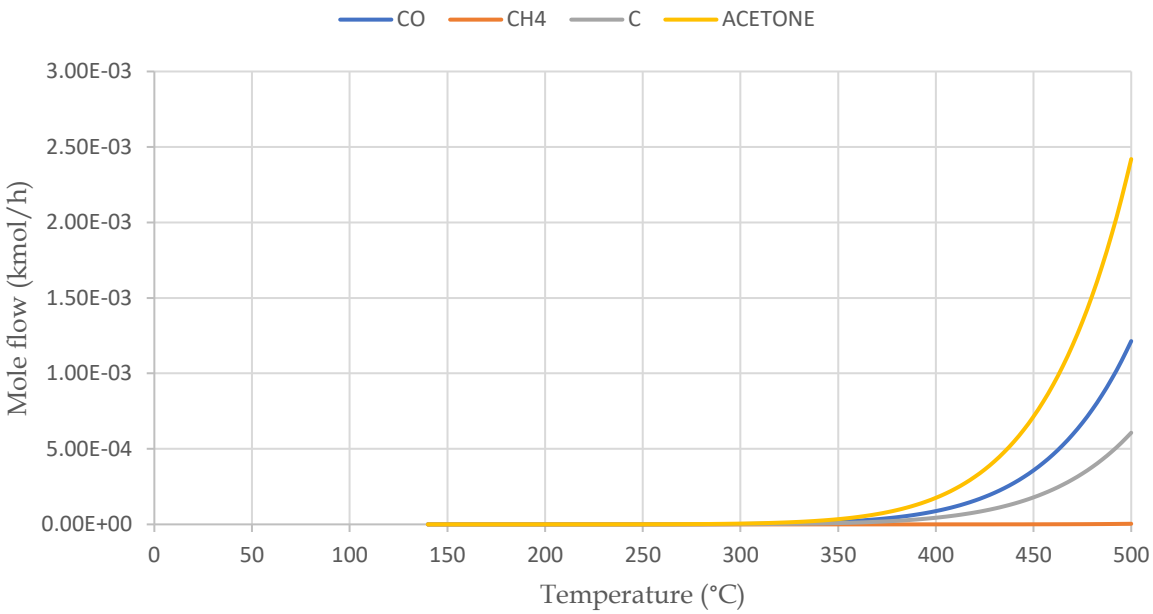

Figure 24: Flowrates of equilibrium decomposition products of acetylacetone in inert atmosphere

The effect of introducing oxygen into the system was evaluated next. Experiments in this work were all carried out at temperatures between 170 °C and 220 °C (following chapter). Different oxygen fractions were evaluated at the extremes of the ranges used for experiments to provide a sense of the significance of oxygen to the system for future investigations.

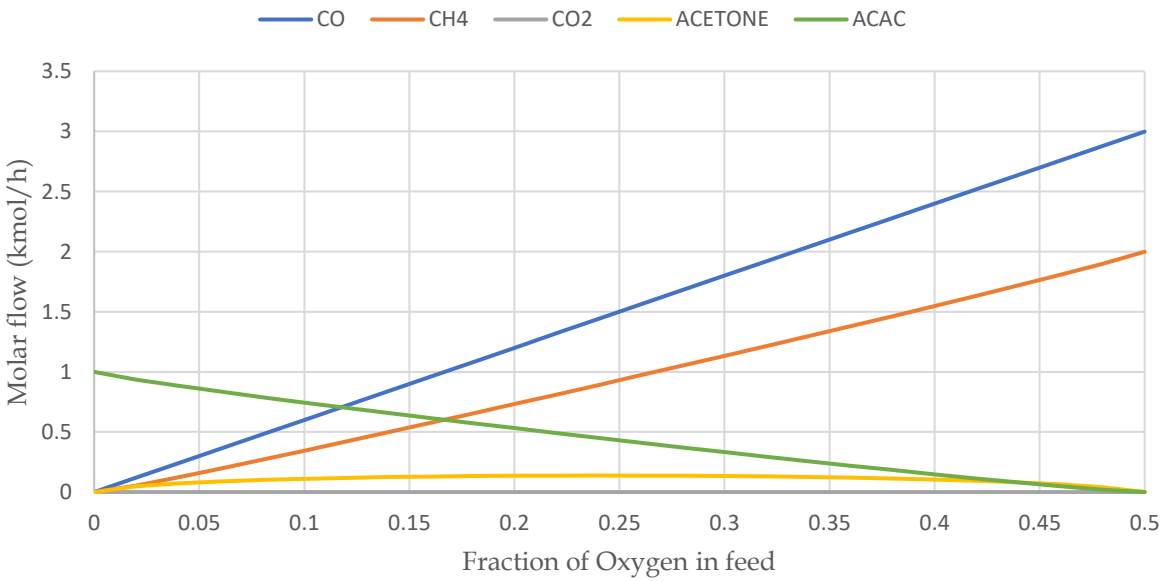

Figure 25: Flowrates of equilibrium decomposition products for acetylacetone with varying oxygen molar fractions at 170 °C

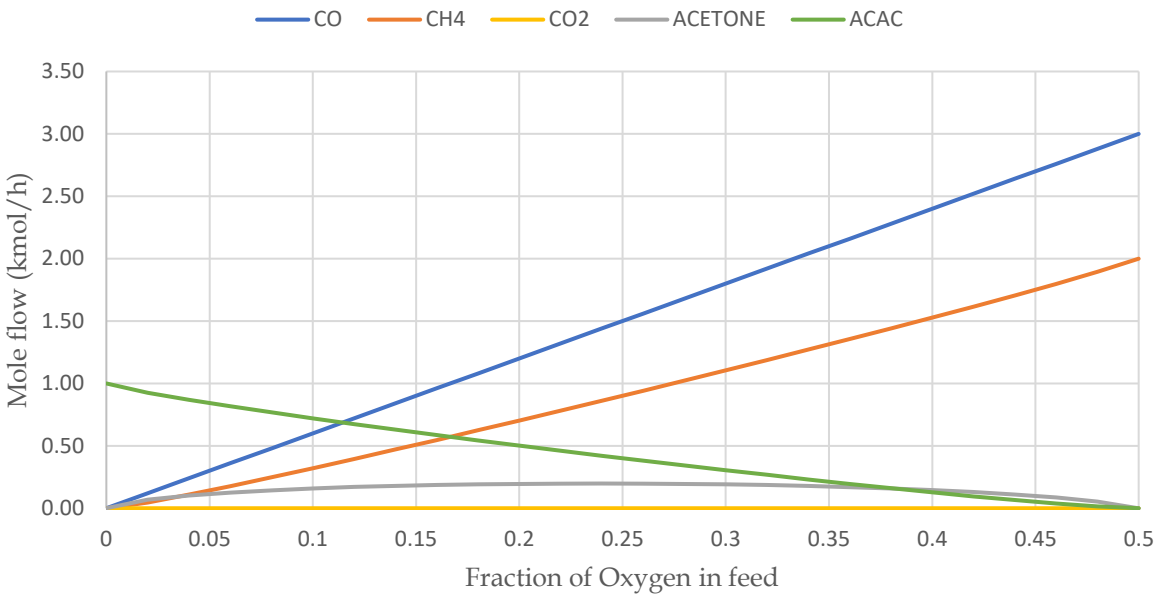

Figure 26: Flowrates of equilibrium decomposition products for acetylacetone with varying oxygen molar fractions at 220 °C

There was no significant difference in equilibrium concentrations between 170 °C and 220 °C. At both extremes there is a reduction in mole flow of acetylacetone in the exit stream until the oxygen fraction reached 0.5 where there was no acetylacetone left in the exit – indicating a complete decomposition at equilibrium. The decomposition products were dominantly CO and CH_4 with a small amount of acetone being produced and peaking at an oxygen fraction of 0.25 in the feed. The simulation results are consistent with the findings by Choudhury and Lin (1990), most of any acetone produced is likely to decompose itself on the path to equilibrium.

The steady decline in acetylacetone reporting in the exit stream as the oxygen fraction increases suggests that decomposition is highly sensitive to oxygen when considering equilibrium. To offer a comparison to experimental data collected in this work, the flowrates of carrier gas and acetylacetone vapours were calculated. An approximate acetylacetone evaporation rate of 10 ml/min of liquid acetylacetone was recorded during extraction attempts. This figure was converted to an approximate vapour flowrate of 3.5 L/min in Aspen Plus using the same settings as the decomposition simulations. The carrier gas flowrate was approximately 0.6 L/min. Using these values, the fraction of acetylacetone in the gas passing over the gold

sample was approximately 78 mol% and the oxygen fraction was approximately 5 mol% and the balance was inert nitrogen.

The input and output streams of the simulation replicating the experimental conditions used in gold extraction attempts are presented in Table 4.

Table 4: Molar flow of simulated equilibrium decomposition of acetylacetone at 170 °C and 1 atm

Compound	**Feed** *(kmol/h)*	**Feed** *(%)*	**Equilibrium outlet** *(kmol/h)*	**Equilibrium outlet** *(%)*
Acetylacetone	0.78	78.0	0.65	48.1
Carbon	0.00	0.0	0.00	0.0
Carbon monoxide	0.00	0.0	0.30	22.2
Acetone	0.00	0.0	0.07	5.2
Methane	0.00	0.0	0.16	11.9
Nitrogen	0.17	17.0	0.17	12.6
Oxygen	0.05	5.0	0.00	0
Total	1.00	100	1.35	100

Simulation of the experimental conditions used for gold extraction showed that with 5 mol% oxygen, there is significant potential for decomposition. At equilibrium, approximately 17% of the acetylacetone was predicted to decompose into carbon monoxide, methane, and acetone.

Observation of the apparatus during experiments did not present any signs that the distillate contained acetone, there was no obvious change in smell either. However, most of the decomposition products were predicted to be gasses and the exit gas composition was not considered in this study. There was a small loss of acetylacetone between each recycle that might be attributable to acetylacetone decomposition to gasses. The small loss of acetylacetone indicates that the decomposition of acetylacetone is limited by slow decomposition kinetics. It may be possible that the kinetics are sufficiently slow that decomposition at raised temperatures is mostly negligible.

Detection of carbon in experiments is proof that some level of decomposition occurred. It is recommended that future acetylacetone extraction work consider the composition of exit gas. Investigation into the kinetics of acetylacetone

decomposition is also advised to determine the extent to which decomposition could affect gas-phase acetylacetone extractions.

How this work changes previous understanding

When considering that no indications of extraction were observed on a large piece of gold by either mass difference or to the naked eye, this alone starts to question the previous understanding that gold extraction can be achieved in the region of 30 % - 70 % (Machiba 2020, Ali 2021). One would expect to observe a change on the surface of the gold pieces at the least.

Results from ICP-MS confirm the observation that there is practically no gold extraction taking place. If the gold measured within the samples is not trace gold that was present in the acetylacetone, some small amount of gold extraction might have taken place. However, the scale of the extraction would be far smaller than previously thought. Previous work used AAS, with a theoretical detection limit in the region of 0.015 mg/L (Cao *et al.* 2009). This work used ICP-MS, with a theoretical detection limit of around 0.00015 mg/L (Allabashi *et al.* 2008). ICP-MS is more suitable for trace gold detection due to the higher flame temperatures used (plasma flame), that ionize more gold particles. If one considers the measurement of trace levels of gold, ICP-MS would provide more reliable measurements as the amount of gold present is more likely to be above detection limits.

If one concedes that the entire gold content measured in both condensate and residue were resultant from extraction, the outcome to the objective of this work does not change. This section set out originally to synthesize a large sample of gold acetylacetonate that could be used for further analysis to understand more about the compound and the reactions at play. It was not possible to synthesize gold acetylacetonate by utilizing the same conditions where complexation was thought to occur. This may be due to the lack of OH^- ions in the system. Kundu *et al.* (2005) reported that the presence of OH^- ions in a liquid-phase synthesis between gold and acetylacetone improved stability by aiding chelation. However, the study notes rapid decomposition at room temperature – it is unlikely to form at elevated temperatures required for gas-phase even if OH^- ions were present.

This finding indicates that gas-phase extraction of gold with acetylacetone would not be possible at a level acceptable for a commercial extraction process in the current form. This finding is reinforced with the indications that acetylacetone will also decompose during such a process – equilibrium limitations allowing for significant decomposition with oxygen – leading to an increase in process complexity and cost that could be exacerbated by increasing extraction times in search of higher recovery. One should recall at this point, the underlying goal of researching this topic: to find a suitable replacement to cyanide-based extraction techniques. In this regard, acetylacetone falls short in delivering a comparable level of extraction and is not likely to be a viable alternative if used in gas-phase extractions within the conditions studied in this work.

The stark difference in results between this work and that of Ali (2021) and Machiba (2020), prompted a more critical investigation into what could be the underlying cause of such a difference. This investigation started by considering the origins of gas-phase extraction with acetylacetone. The work of Ali (2021) and Machiba (2020) both report similar trends in extractions that are also found in many earlier works involving iron, vanadium, aluminium, lead and chromium. It is suspected that whatever lies behind the difference in results between this work and that of Ali (2021) and Machiba (2020), will also be the case for the other works involving similar methodology on other metals. For this reason, an investigation into the extraction of iron follows this chapter (Chapter 5). Thereafter, a comprehensive investigation and discussion to address the differences uncovered by this work and the implications of all results will be reported in Chapter 6.

CHAPTER FIVE
Iron extraction from pyrite and hematite —Reviewing perceptions with critical tests

With a stark difference in experimental results of gold extraction runs, further investigation into the broader topic of acetylacetone extractions was necessary. This chapter aims to explore and replicate the findings of previous work done by the research group over the last 15 years.

Fe (III) extraction and complexation with acetylacetone

The reaction between iron and acetylacetone is well studied. Non-polar solvents have been found to increase the extraction of iron with acetylacetone. Katsuta *et al*. (1992) added 3,5-dichlorophenol (DCP) to acetylacetone to extract more iron (III) from a radioactive ^{59}Fe isotope. The extraction formed $Fe(acac)_3$ coordination, a complex that has been studied by others (see Von Hoene *et al.* 1958, Potgieter *et al.* 2006, Van Dyk *et al.* 2010). Katsuta *et al.* (1992) prepared $Fe(acac)_3$ by mixing acac, DCP and ^{59}Fe together and shaking at 25 °C. Without DCP acetylacetone alone extracted a maximum of 40% Fe (III). Extraction improved when DCP was added to the mixture. DCP on its own did not extract any Fe (III), a result suggesting that the association of $Fe(acac)_3$ with DCP by hydrogen bonding is the cause of the increased $Fe(acac)_3$ solubility – allowing increased extraction (Katsuta *et al* 1992).

Acetylacetone is also capable of extracting iron from soil. Bascomb and Thanigasalam (1978) reported that aqueous acetylacetone (0.68 M) is capable of extracting about 30 % Fe from soil in a "usual period" of 7 days. During this time, 40 % of the lepidocrocite, 7 % of the geothite and 1 % of the akageneite dissolved in the solution. The authors do not mention specific conditions; however, ambient conditions are likely to have been used.

Bascomb and Thanigasalam's (1978) extraction of Fe from its oxide form in soil was demonstrated to be too slow for effective implementation into commercial extraction processes. This is also discussed by Van Dyk *et al.* (2010), further adding that economic yields require long residence times and additional steps to obtain pure metals. Potgieter *et al.* (2006) investigated extraction of Fe_2O_3 at elevated temperatures of up to 200 °C in gas phase. Maximum extraction of iron using acetylacetone was reported in their study after 45 min at 180 °C. Longer or hotter extractions saw no change in iron extraction. They also reported that decreasing reaction time led to a decrease in extraction of iron—a high correlation to a first-order reaction. This high correlation to a first-order reaction is something I recall in Chapter 6.

Work done by Van Dyk *et al.* (2010) and later by Tshofu (2014) report that extraction values of iron using acetylacetone are significantly lower when using naturally occurring hematite than synthetic iron (III) oxide. Van Dyk *et al.* (2010) claimed a maximum iron extraction of 87 %—higher than the 75 % iron extraction reported by Potgieter *at al.* (2006). The increase in extraction was achieved by lowering the Fe_2O_3 from 3 % to 1 % (the balance silica), increasing temperature from 180 °C to 250 °C, lowering the acetylacetone flow rate from 3 mL/min to 1 mL/min, and increasing the extraction time from 45 min to 6 h.

Whilst the higher extraction reported by Van Dyk *et al.* (2010) may valuable when considering low-grade ores, the extraction conditions used by Potgieter *et al.* (2006) claim a greater mass of iron extraction within greatly reduced extraction times. This is important to note when considering extraction from natural ore bodies as the concentration of iron oxides will vary and optimal extraction from an operational perspective could be refined using this information.

Tshofu (2014) investigated iron extraction from both synthetic Fe_2O_3 (99 %) and natural iron ore fines that contained 6−7 % impurities. Extraction at 250 °C using an acetylacetone flowrate of 6 mL/min for 6 hours yielded a 32 % iron extraction from synthetic Fe_2O_3 and a 1.55 % iron extraction from natural iron ore fines. The primary impurities in the natural iron ore fines were SiO_2 (5.00 %) and Al_2O_3 (1.30 %). SiO_2 does not react with acetylacetone (Shemi *et al.* 2012). The decrease in extraction is

unlikely to result from side reactions with impurities but rather, some of the decrease in extraction could be attributed to competition for available reactive surface area on each particle.

A different study, using a similar setup but focussed on aluminium, investigated the extraction of Al from coal fly ash (CFA). Shemi *et al.* (2012) reported similar trends in extractions from synthetic and natural material using acetylacetone. They used a fluidized-bed reactor charged with a 50 g sample of CFA or synthetic CFA (31 % Al_2O_3 and 69 % silica). The reactor was heated to reaction temperature with acetylacetone flowing through the bed—the same procedure followed by Van Dyk *et al*. (2010). They reported a maximum Al extraction of 46.7 % from synthetic CFA and 17.9 % from natural CFA. The best extraction conditions for both natural and synthetic CFA were reported to be 250 ^{o}C with a flow rate of 6 mL/min acetylacetone into the evaporator.

They attributed the difference in extraction using acetylacetone to a difference in phase composition between CFA and synthetic CFA. "The Al_2O_3 in CFA exists in crystalline mullite form and non-crystalline amorphous form" (Shemi, et al., 2012). Al_2O_3 in synthetic CFA only exists as non-crystalline amorphous form. The crystalline structure of natural CFA appears to kinetically unfavourable for metal extraction using acetylacetone when compared to synthetic CFA as the metal atoms are less accessible.

Purpose of investigating iron extraction in this work

There are two primary objectives in this chapter. Ali (2021) discovered indications that acetylacetone was reacting with pyrite in the tailings, breaking it down and possibly opening an avenue for gold liberation. The first part of this chapter looks more deeply into the reaction between pyrite and gas-phase acetylacetone.

The second part of the chapter revisits gas-phase extraction of iron from hematite, but in the same simplified extraction setup detailed in Chapter 4. A critical test of the reaction with hematite will verify if extraction does occur, bring to light factors such as carrier-gas composition, and to assess the repeatability of previous work.

The current view is that iron extraction using acetylacetone is much easier to achieve than gold. Extractions are high. Previous studies present the following (or similar) reaction when explaining the extraction of iron (Pogieter *et al.* 2006, Van Dyk *et al.* 2010, Mariba 2010):

$$Fe_2O_3 + 6H(acac) = 2Fe(acac)_3 + 3H_2O \qquad \text{(Equation 4)}$$

The focus will be on identifying if the complex $Fe(acac)_3$ does indeed form. This was suggested but not confirmed analytically.

Experimental methodology

Similarly to the attempts at gold extraction, large quantities of each sample and acetylacetone ligand were used to give the best chance of detecting any possible reactions that might occur. The exact procedure used is detailed in Chapter 4. The insights gained from the experiments involving gold were applied to this section. The samples were weighed before and after exposure to acetylacetone. With extraction expected to be low, boiling flask residue and condensate samples were analysed for iron content on ICP-MS. The samples were also inspected under optical microscope to look for any changes in surface characteristic. The samples were also analysed with Raman Spectroscopy with the intention of identifying compounds that may form and deposit on the surface.

Following the result suggesting gold extraction occurs at near negligible scale from pure gold, one main difference was noted between this work and that of Ali (2021): gold tailings versus pure gold. At this point in the work, it was theorized that the pyrite – often in company with gold – might have an interaction that could be the cause of such a difference in results. If pyrite reacts with acetylacetone, there could be an intermediate that forms because of the reaction between the two that might give rise to gold extraction. Such a theory warranted investigation as the reaction pathways of gas-phase acetylacetone extractions are completely unknown.

For this round of extractions, conditions were selected to give a fair test to the previous conditions that reported good, measurable, extraction. Temperatures approximately in the middle of the range of previous works were used. A summary of the conditions investigated is provided in Table 5. The pyrite pieces were selected

pieces that appeared to be near-pure pyrite. The gold beads used were from the same batch of 99.99 % gold beads as in Chapter 4. The hematite samples used were verified to be of high-purity by Raman spectroscopy (discussed later in this chapter).

Table 5: Summary of extraction conditions used in this section and sample description of iron sources.

Sample No.	**Description of Sample**	**Temperature** *(°C)*	**Approximate ligand flowrate** *(ml/min)*	**Exposure time** *(min)*
1	Pyrite only	190	10	146
2	Pyrite and gold beads	190	10	145
3	Hematite (air)	220	10	211
4	Hematite (nitrogen)	220	10	200

All samples were weighed before and after exposure to acetylacetone. Thereafter, a Raman Spectrum scan was taken on at least five random points to identify material present on the surface that might have indicated a reaction or reaction products. Iron extraction from hematite (Fe_2O_3) was studied by both Potgieter *et al.* (2006) and Van Dyk *et al.* (2010) in similar conditions. Further samples were taken for analysis on ICP-MS for direct comparison of concentration measurements and extraction mass from the Fe_2O_3.

The previous work used nitrogen carrier gas, for this reason, the setup was changed to use nitrogen instead of compressed air. This change allowed the fairest possible comparison between results as all works have utilized inert carrier gas to expose acetylacetone vapour to a sample of Fe_2O_3 at a temperature of 220 °C for over three hours. An extraction was also attempted with compressed air as a carrier gas to offer a crude insight into the effect – if any – of the presence of oxygen. This element has not been considered in previous work and could provide valuable information about the nature of the chemical reactions. Using compressed air as a carrier gas would be more cost effective than nitrogen in a commercial process if it is feasible to use.

Observations from iron extraction attempts

The differences in mass measured for each sample are presented in Table 6. Once again, there was very little mass difference measured after exposure to acetylacetone.

All mass differences were comfortably within 1 % of the starting mass. This indicates that any interaction that might occur, was to a very small extent – nearly negligible.

Table 6: Summary of experimental conditions and mass changes of pyrite and hematite samples. Au is short for gold beads, Py is short for Pyrite.

Sample	**Temperature of reactor** *(°C)*	**Approximate ligand flowrate** *(ml/min)*	**Exposure time** *(min)*	**Initial sample mass** *(mg)*	**Mass difference after extraction**	
					(mg)	*(%)*
1	190	10	146	953.6	+ 0.4	+ 0. 412
2	190	10	145	1 419.3 (Py) 1 316.5 (Au)	- 0.9 + 0.0	- 0.063 + 0.000
3	220	10	211	15 200.4	+ 4.6	+ 0.030
4	220	10	200	23 358.4	- 6.7	- 0.029

However, mass difference alone does not describe the full picture. It was clear that the presence of gold with pyrite had no measurable impact. It could be considered an inert material to this process. More interestingly, the pyrite exhibited a noticeable colour change within the first 30 minutes when inside the reactor. The pyrite pieces became coated in a colourful mixture of a blue, purple, and black substance that appeared to be adsorbed to the surface. Images of the layer are presented in Figure 27, Figure 28, and high magnification images later in Figures 29-38.

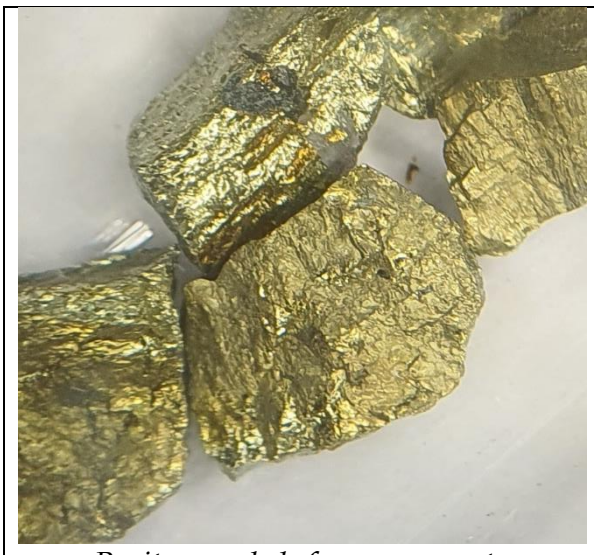

Pyrite sample before exposure to acetylacetone

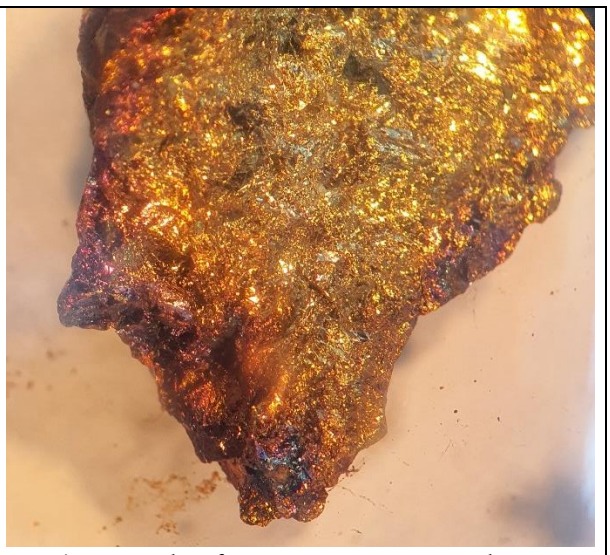

Pyrite sample after exposure to acetylacetone

Figure 27: Images of pyrite sample pre-exposure to acetylacetone (left) and low surface covering (right).

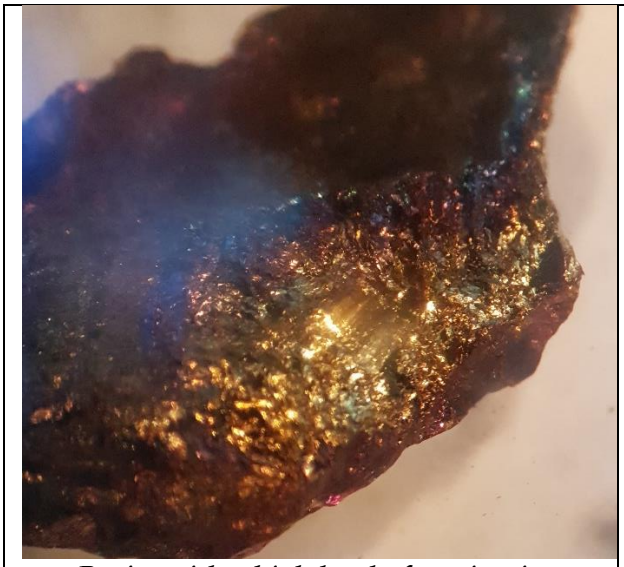

Pyrite with a high level of coating in unknown substance

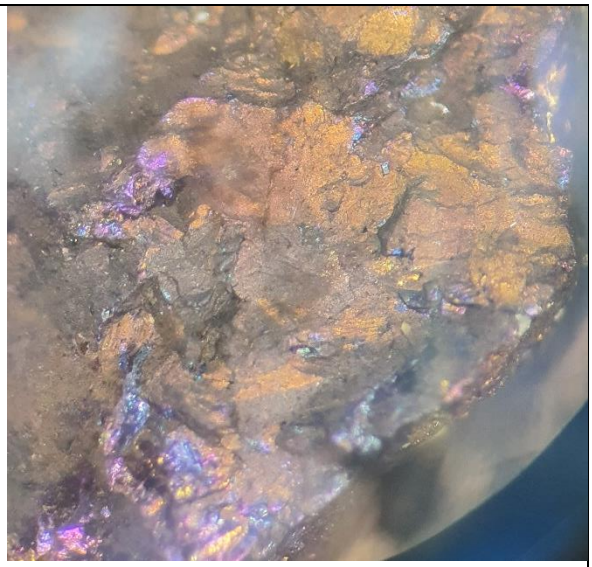

Pyrite with total coating in unknown substance

Figure 28: Images of pyrite with high surface covering (left) and full surface covering (right).

The observable reaction with pyrite pieces and acetylacetone confirms the finding by Ali (2021) that there is some form of reaction with pyrite. The primary product of this reaction was suspected to be $Fe(acac)_3$. The formation of this layer was formed relatively quickly, thereafter nothing appeared to happen for the remainder of the extraction. With this observation, it is theorized that the layer forms as a reaction between the pyrite surface and either the acetylacetone, or one of its decomposition products. The layer that forms becomes a passivating layer that inhibits further reaction. Upon further investigation, the layer immediately below the dark outer layer was found unreacted.

In both hematite extraction attempts, the hematite sample appeared to remain inert. There was no observable change in colour or surface characteristics. This was supported by the negligible change in mass that presented itself more as a variance in scale readings. The variances measured in all samples is most likely attributed to a variance in moisture of the sample, resulting from acetylacetone absorption. However, mass variance due to a minor chemical reaction cannot be ruled out.

In each of the extraction attempts, the same dark residue (displayed in Figure 23) formed. The condensate also remained completely clear to the human eye, with

exception of Sample 4. The condensate of sample 4 (nitrogen carrier gas) was light yellow. At the time the yellow colour was thought to be attributable to iron content within the liquid from extraction. To confirm this, the surface of the samples was analysed with Raman Spectroscopy and the liquid samples were analysed on ICP-MS.

One criticism of the method used in this work that was addressed is the exposure time to acetylacetone. While Potgieter *et al.* (2006) did report a rapid reaction between Fe_2O_3 and acetylacetone, there was still some suspicion that reaction kinetics might be causing the apparent inert character of hematite. To address this, a single piece of hematite (approximately 1 cm diameter) was left submerged in liquid acetylacetone for 10 days. While the test was conducted under atmospheric conditions, the long exposure time should provide sufficient time for a reaction to occur. Bascomb and Thanigasalam (1978) reported liquid-phase extraction of iron from Fe_2O_3 within three days, stabilization of solubility was found after 10 days. The results of the liquid-phase exposure are also given in the hematite section of Raman Spectroscopy and in ICP-MS.

Insights from Raman Spectroscopy

While it is theorized that the outer layer forming on the pyrite might be $Fe(acac)_3$, this theory required further testing for confirmation. Raman spectroscopy was used to test for the presence of $Fe(acac)_3$, and other materials, on the surface. It is an excellent analytical technique for sampling single point surface characteristics. Samples of both pyrite and hematite were analysed and sampled on at least 5 random points to account for any point-to-point variations in surface composition.

1. Pyrite

High magnification images of the pyrite surfaces from Sample 1 (Table 5) that were analysed with Raman spectroscopy are presented in Figures 29-38. The images in Figures 29-38 are high magnification images of randomly selected points used for each spectrum sampled from Sample 1 (Table 5). The images also provide a good close-up of the blue/purple substance on the surface of the pyrite. Through all the images, there are what appear to be black spots or pieces on the surface. Some of

these areas are a result of a small cavity on the surface. However, others were tested and were found to exhibit a signature for carbon. All figures are captioned according to the key on the spectra combinations in Figure 39 and Figure 40. In each image, there is a small red line in the bottom right. This line indicates a scale distance of 2 µm. The centre of each image (0, 0) is the point where the laser was targeted for each scan.

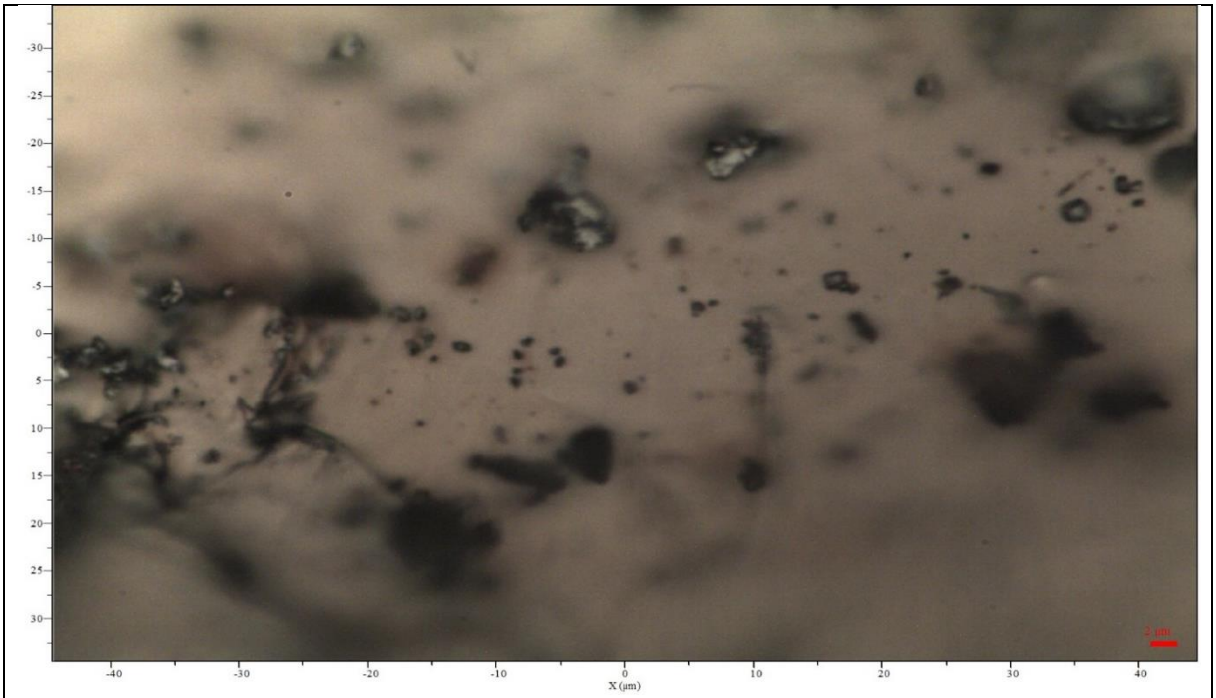

Figure 29: "Pyrite only – a". High magnification image of pyrite sample surface. The red line indicates 2 µm distance.

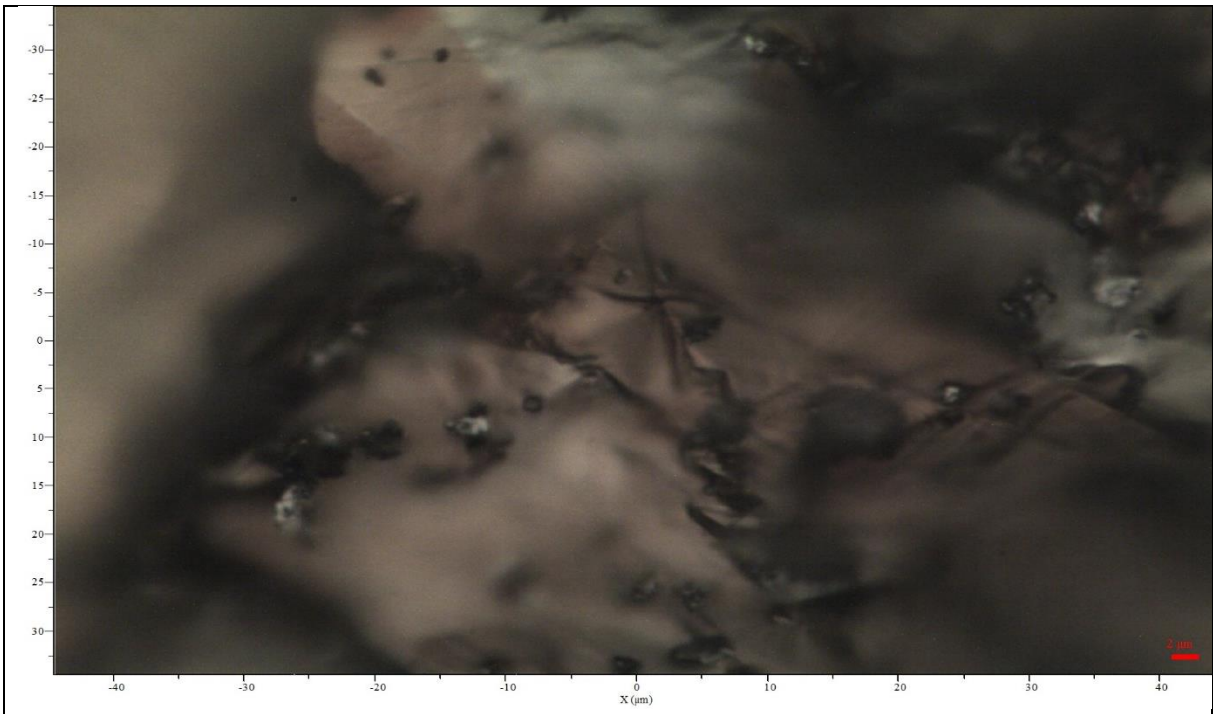

Figure 30: "Pyrite only – b". High magnification image of pyrite sample surface. The red line indicates 2 µm distance.

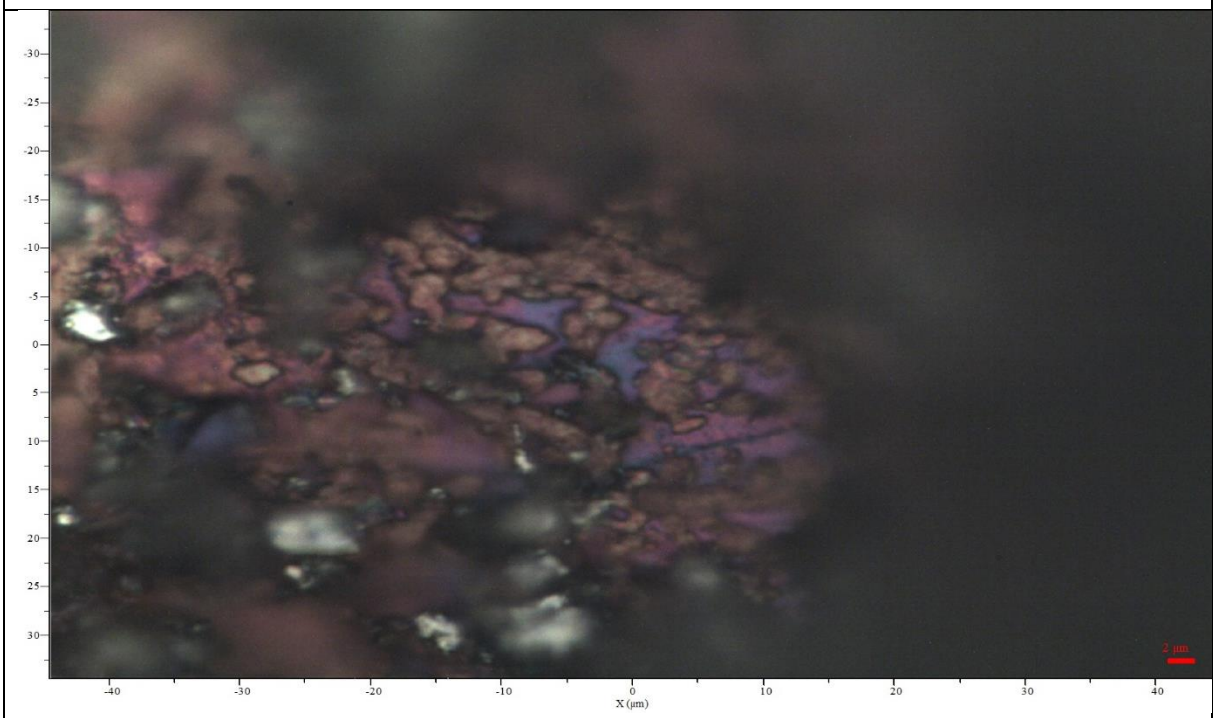

Figure 31: "Pyrite only – c". High magnification image of pyrite sample surface. The red line indicates 2 µm distance.

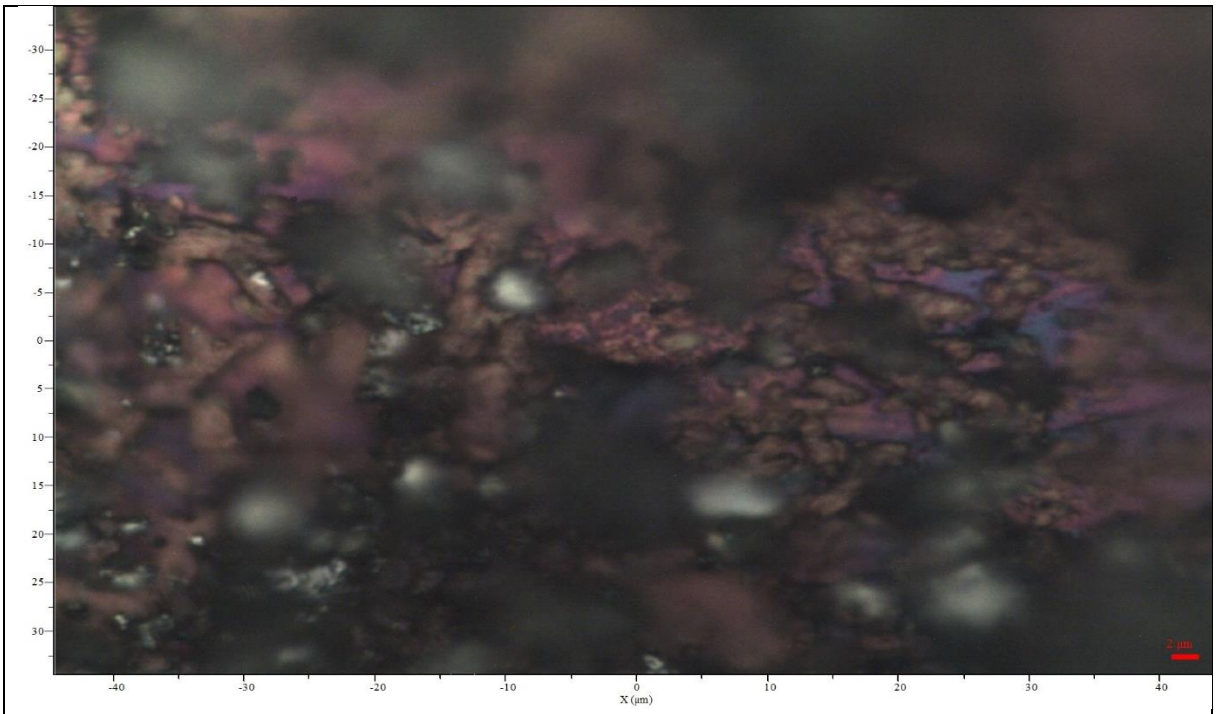

Figure 32: "Pyrite only – d". High magnification image of pyrite sample surface. The red line indicates 2 µm distance.

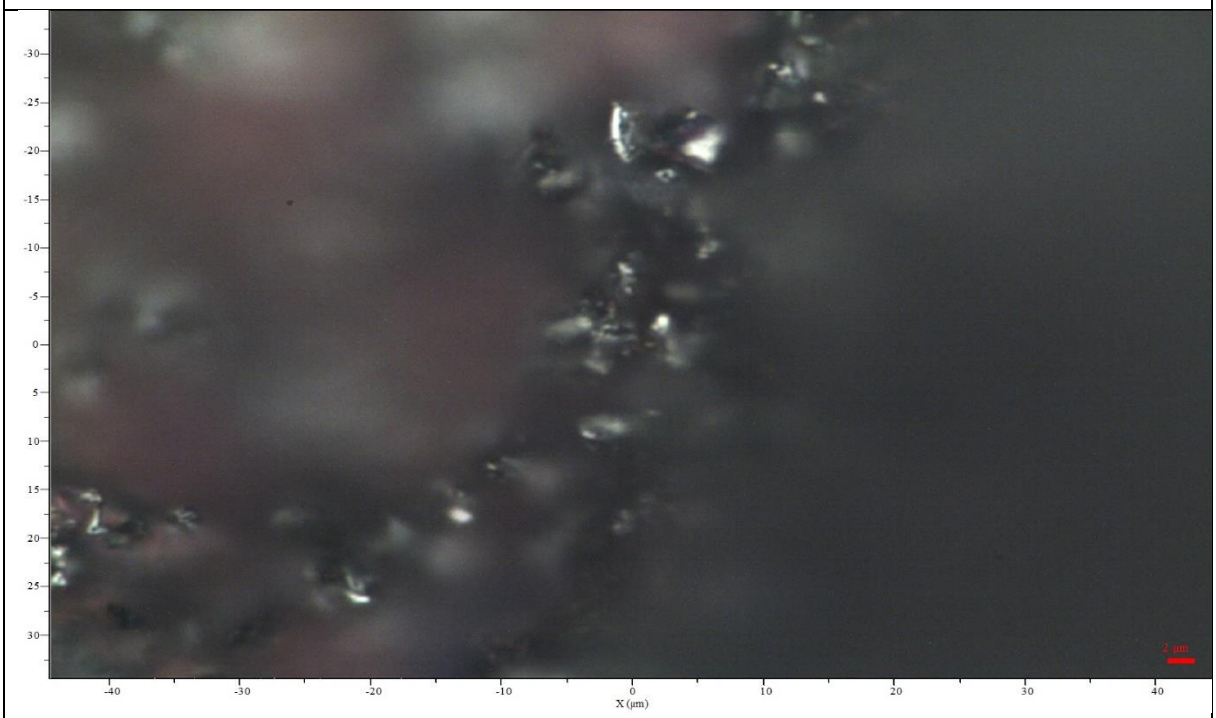

Figure 33: "Pyrite only – e". High magnification image of pyrite sample surface. The red line indicates 2 µm distance.

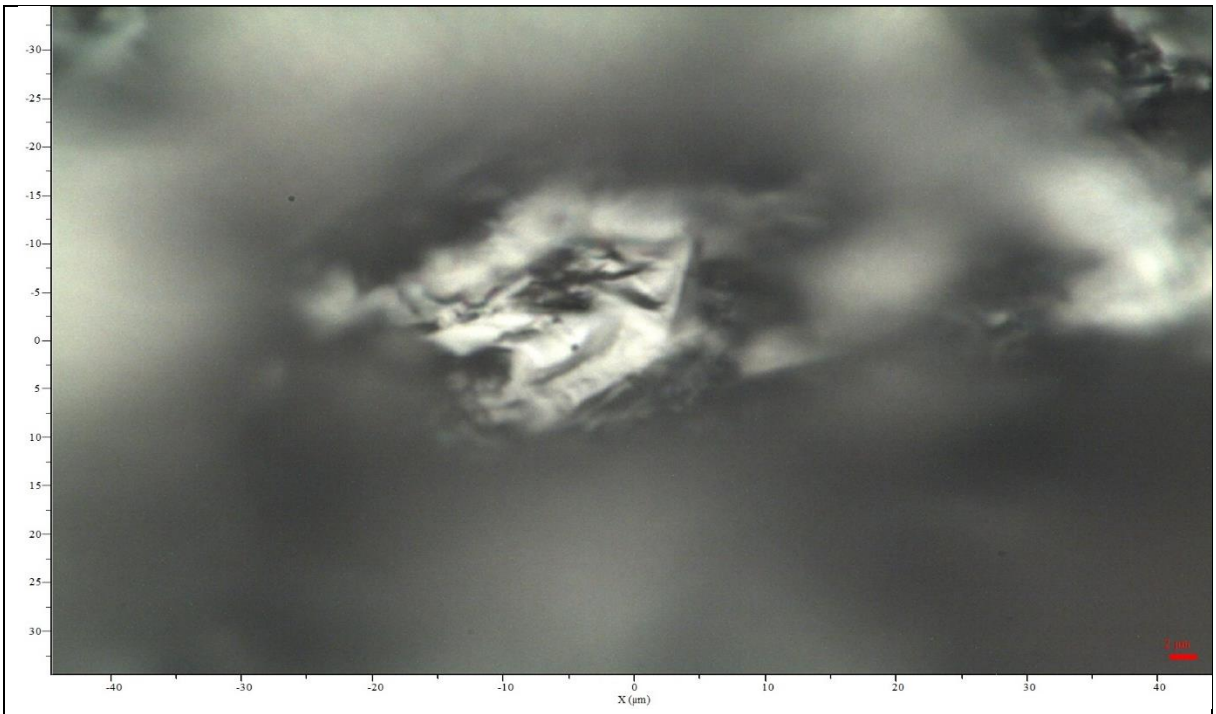

Figure 34: "Pyrite only silvery edge". High magnification image of pyrite sample surface. The red line indicates 2 µm distance.

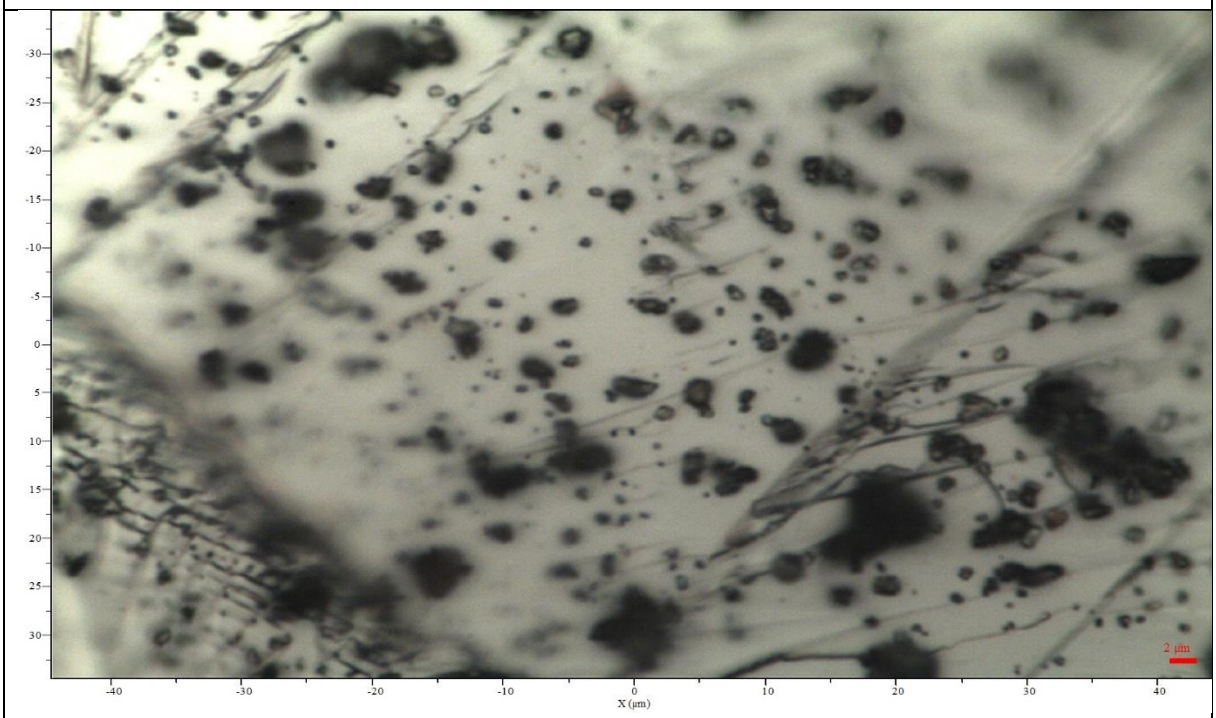

Figure 35: "Pyrite only silvery edge – b". High magnification image of pyrite sample surface. The red line indicates 2 µm distance.

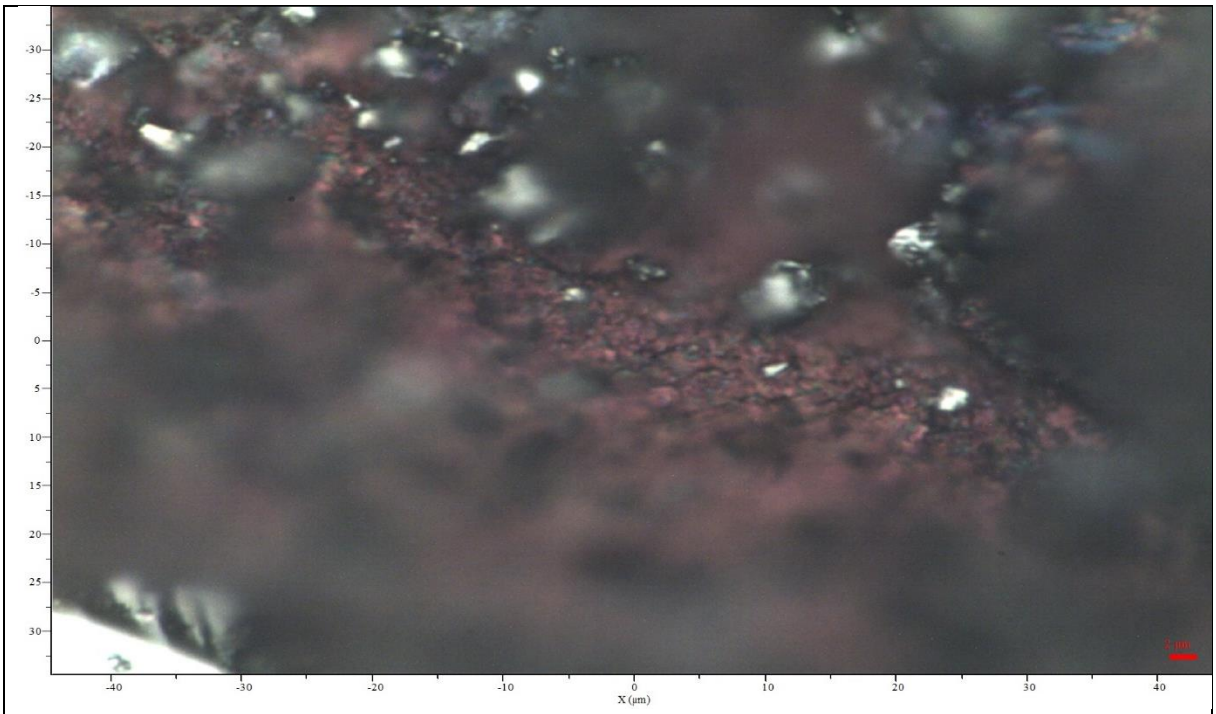

Figure 36: "Pyrite only silvery edge – c". High magnification image of pyrite sample surface. The red line indicates 2 µm distance.

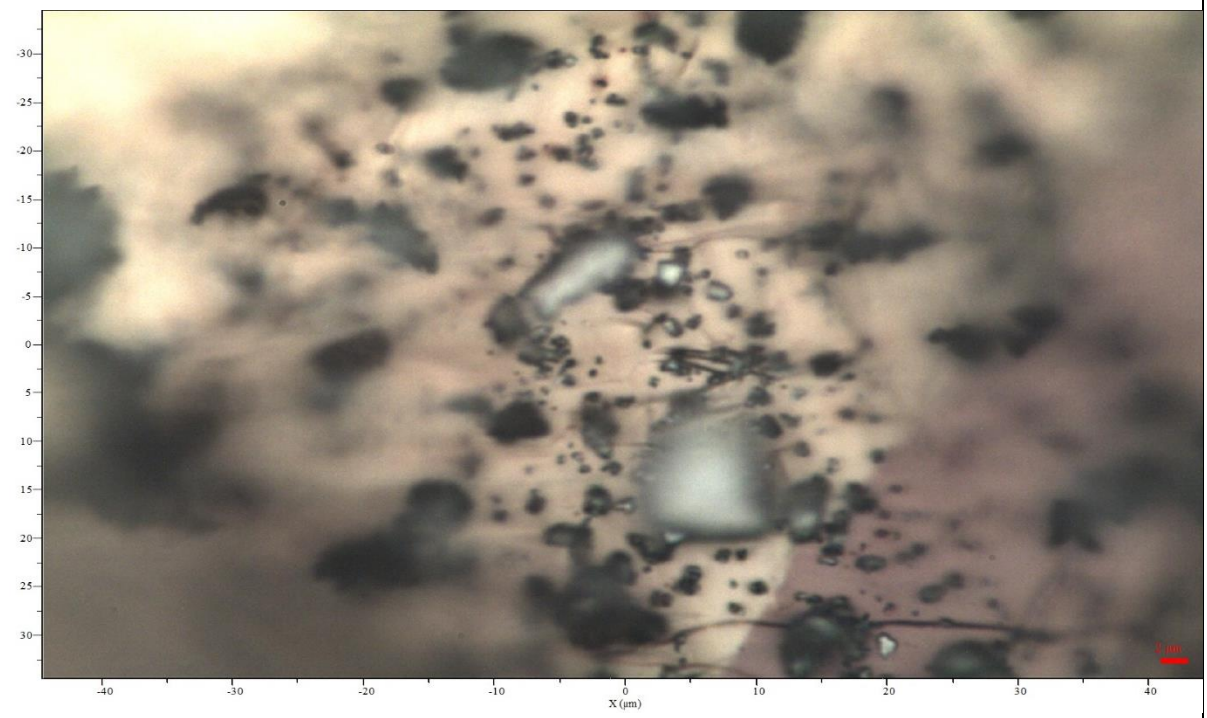

Figure 37: "Pyrite only small chip yellow – a". High magnification image of pyrite sample surface. The red line indicates 2 µm distance.

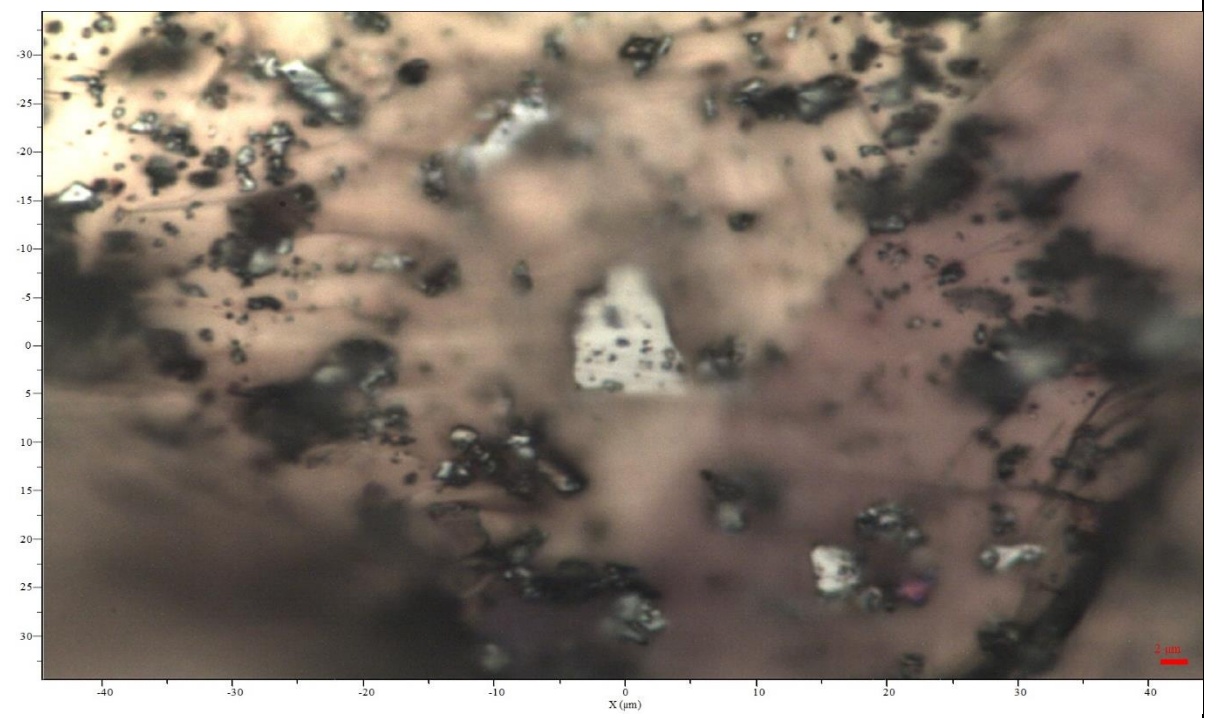

Figure 38: "Pyrite only small chip yellow – b". High magnification image of pyrite sample surface. The red line indicates 2 µm distance.

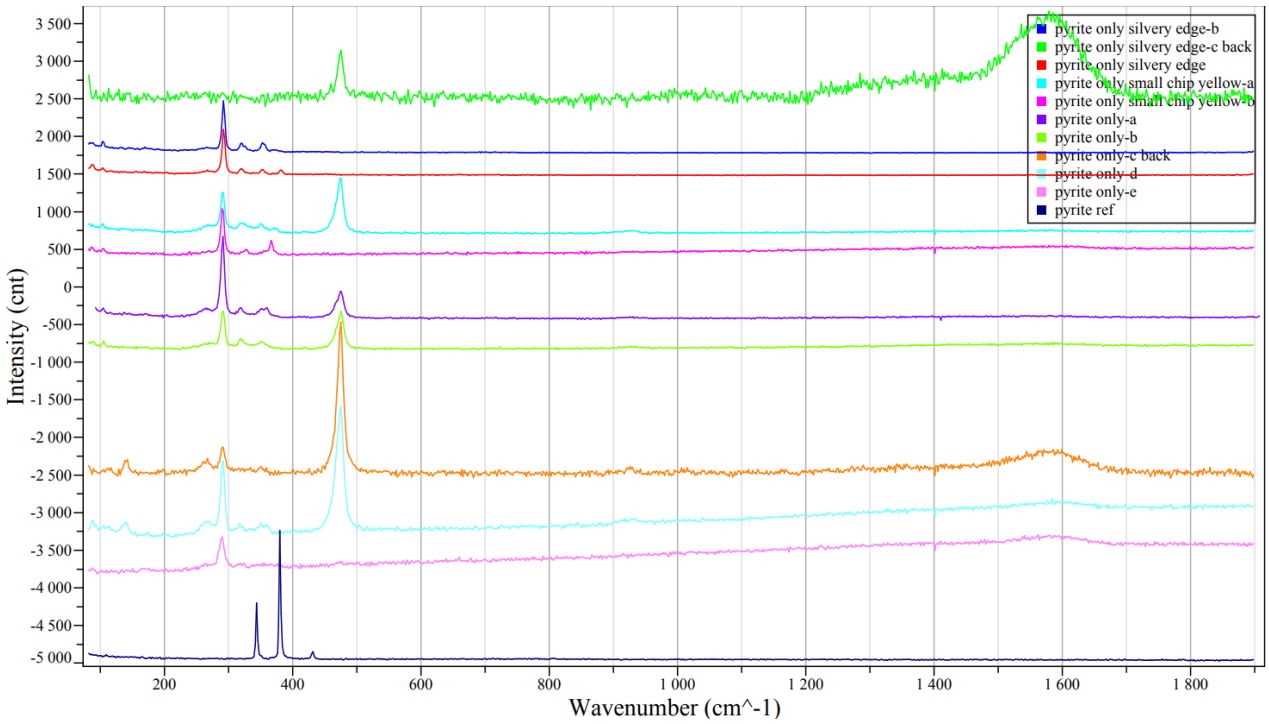

Figure 39: Combined Raman Spectra Intensities for pyrite samples with a pyrite reference. Naming convention matches images presented in Figures 29-38. Intensities are not to scale.

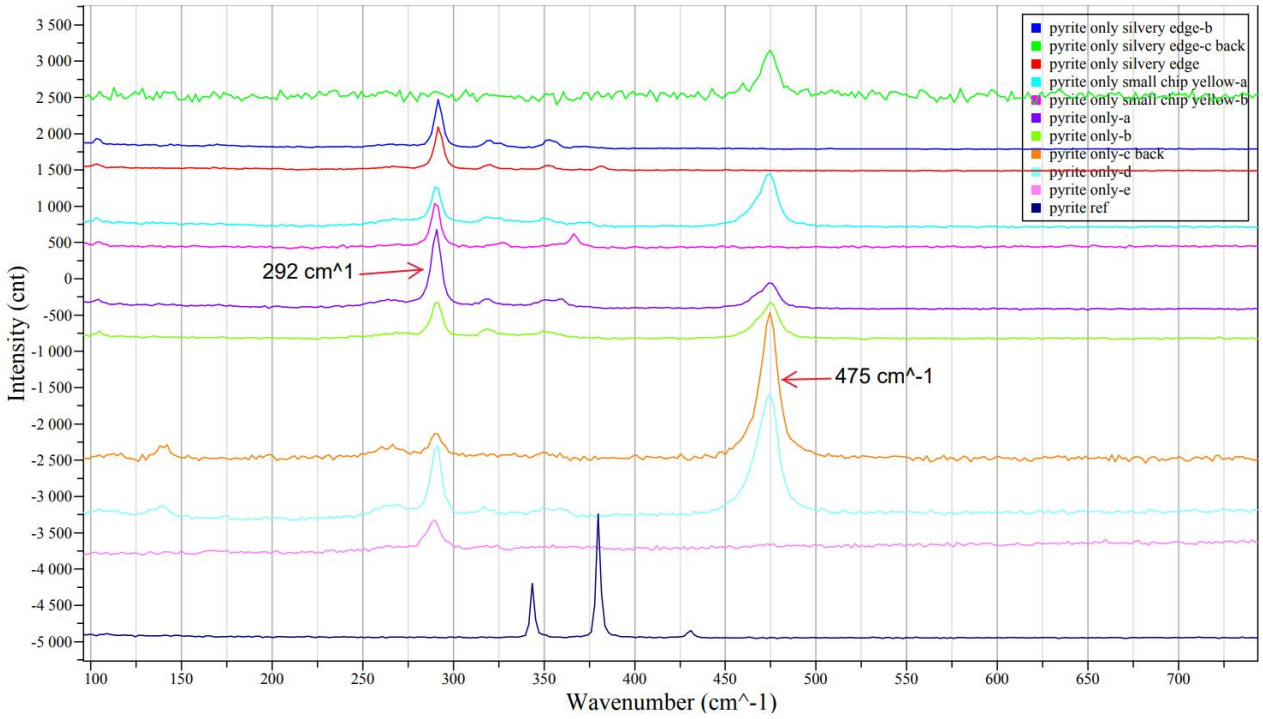

Figure 40: Zoomed Combined Raman Spectra Intensities for pyrite samples with a pyrite reference. Naming convention matches images presented in Figures 29-38. Intensities are not to scale.

There appear to be two major peaks that form on areas covered with the substance that formed on the surface of the pyrite pieces. The first, at wavelength of 292 cm^{-1} and the second, at a wavelength of 475 cm^{-1}. Neither of these peaks are common to the reference pyrite sample that is given at the bottom of both combined spectra graphs. Both peaks presented themselves at different intensities depending on the specific area under the laser. The peaks at 292 cm^{-1} appear to be attributable to the darker areas and the peaks at 475 cm^{-1} appear to be from the brighter purple/magenta-coloured areas.

The substance forming on the surface of the pyrite pieces was thought to be $Fe(acac)_3$. Fortunately, this compound is readily available and has reference Raman spectra such as the one given below in Figure 41 (John Wiley and Sons Inc. Spectrabase 2022).

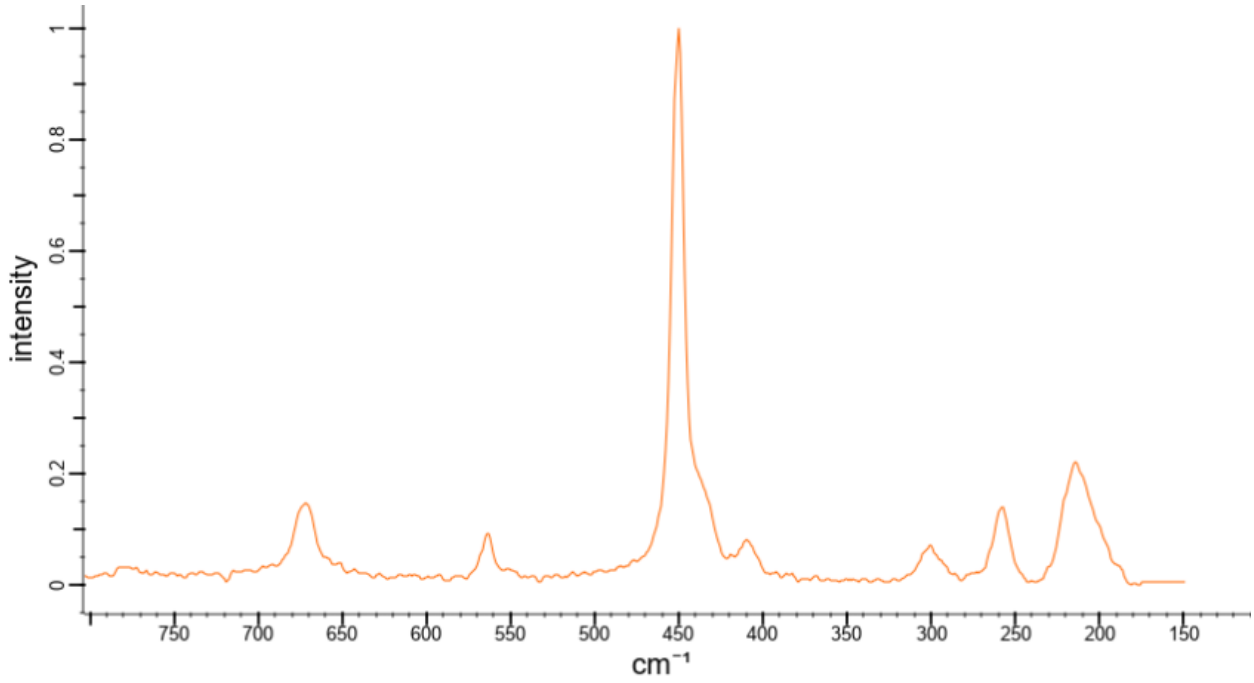

Figure 41: Reference FT-Raman spectrum of $Fe(acac)_3$ (John Wiley and Sons Inc. Spectrabase 2022

There does not appear to be a match between the reference spectrum and those measured in this work. The reference has a dominant peak at 450 cm^{-1} and a peak close to 300 cm^{-1}. However, the peaks at approximately 210, 260, 563, and 675 cm^{-1} are all absent from the spectra taken from the pyrite pieces from this work. This confirms that the substance observed to be forming on the pyrite pieces is not $Fe(acac)_3$.

Since a pyrite reference spectrum is also given, it is clear to see that there is no match between the pyrite reference and the measured spectra. The substance forming is likely something completely different. No match to any expected substance could be determined within the scope of this work. Instead, a high probability match for chalcopyrite ($CuFeS_2$) was found, unsurprising when considering that the pyrite source was natural where a mixture of pyrite derivatives is likely to occur together. The substance that was observed on the surface was not tested for iron content. The possibility remains that the coating does not contain iron at all. Further investigation in future work is recommended.

2. Hematite

High magnification images of hematite (Samples 3 and 4 in Table 6) after exposure to acetylacetone are presented in Figures 42-49. A Raman Spectrum of the liquid-phase extraction of hematite is also included with the gas-phase spectra in Figure 50.

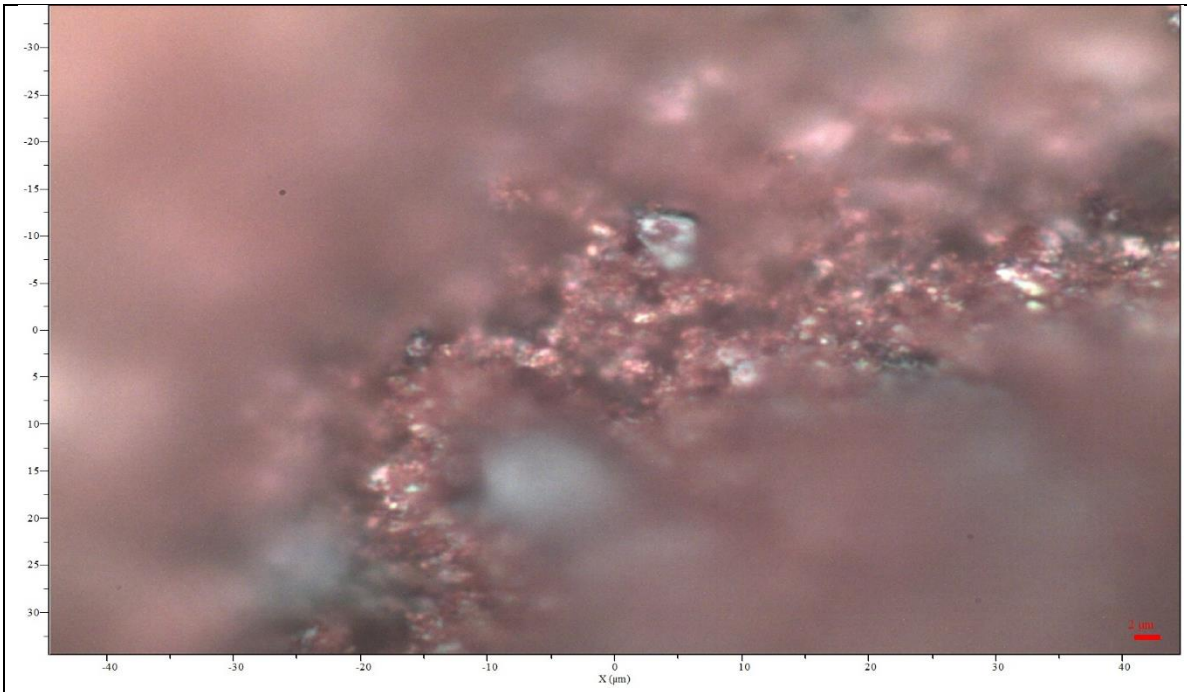

Figure 42: "Hematite – b". High magnification image of hematite sample surface. The red line indicates 2 µm distance.

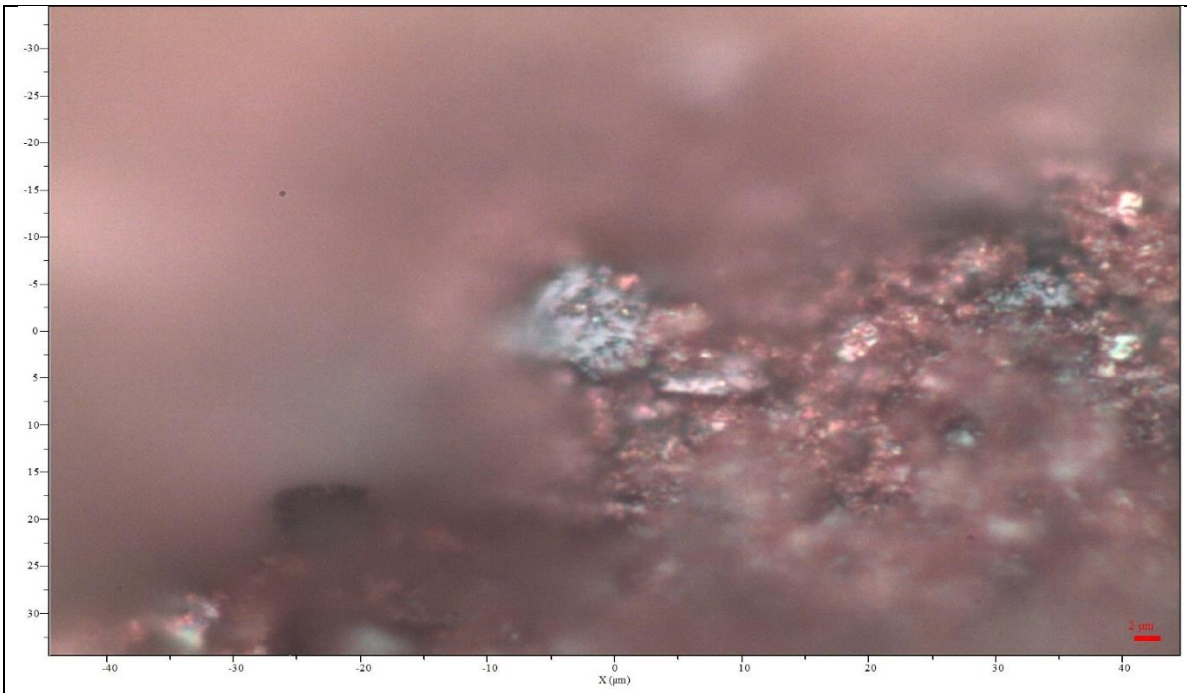

Figure 43: "Hematite – c". High magnification image of hematite sample surface. The red line indicates 2 µm distance.

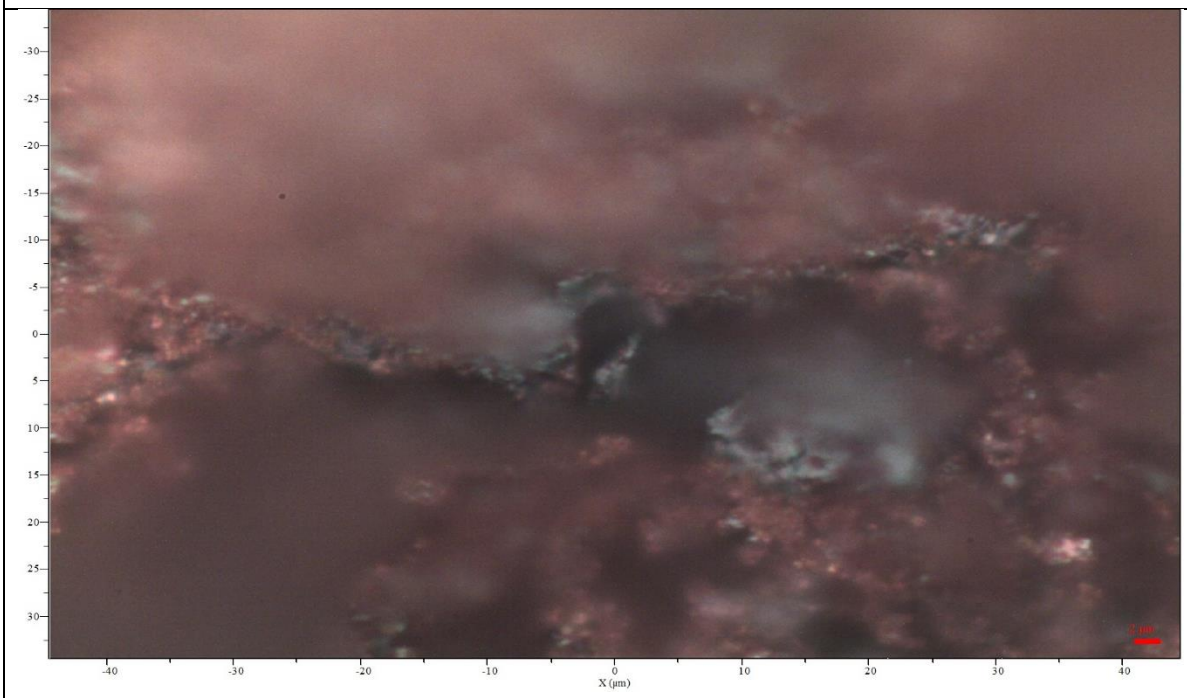

Figure 44: "Hematite – d". High magnification image of hematite sample surface. The red line indicates 2 µm distance.

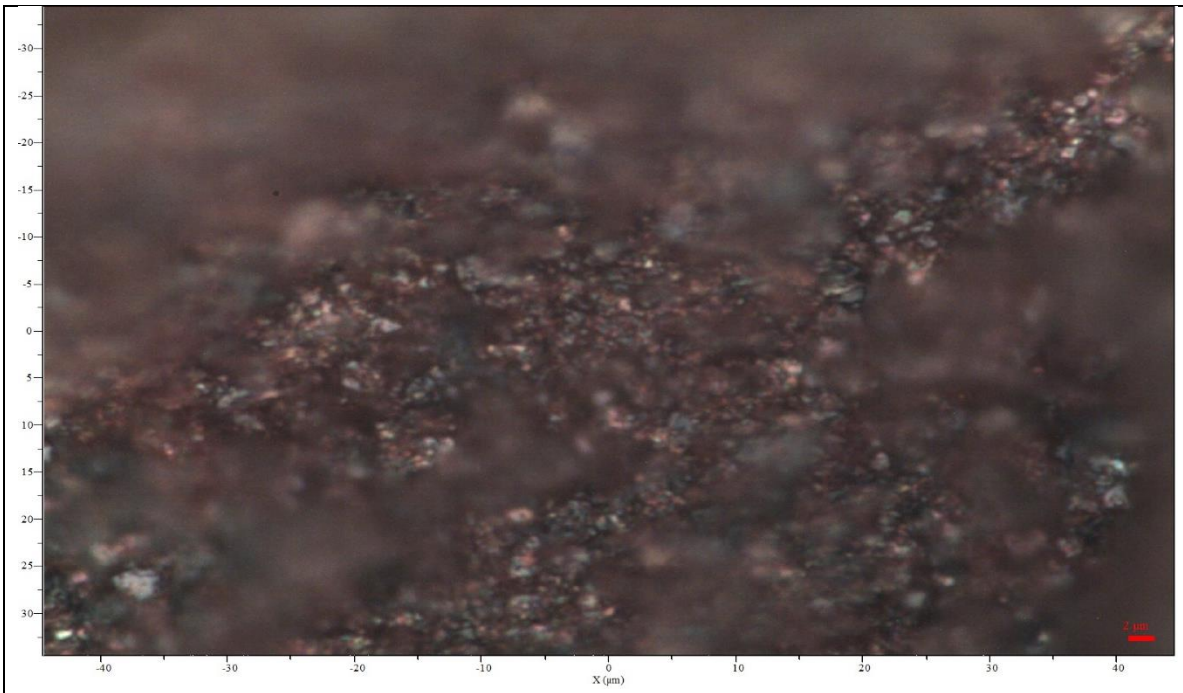

Figure 45: "Hematite in liq 10d – a". High magnification image of hematite sample surface. The red line indicates 2 µm distance.

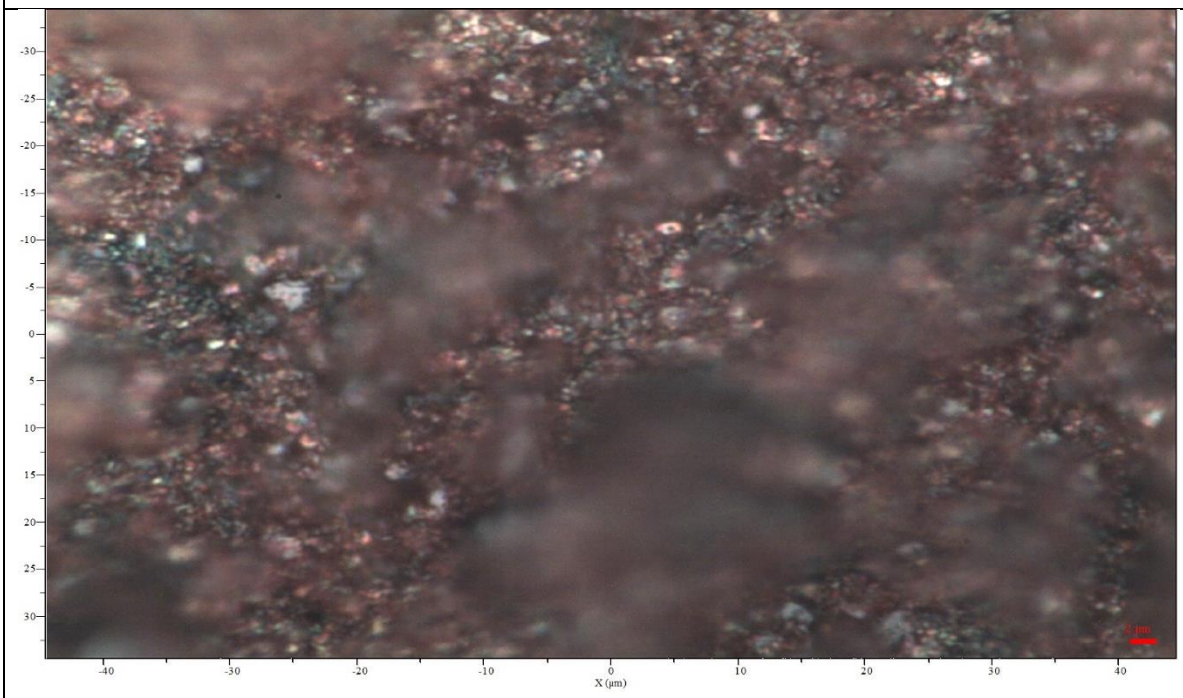

Figure 46: "Hematite in liq 10d – b". High magnification image of hematite sample surface. The red line indicates 2 µm distance.

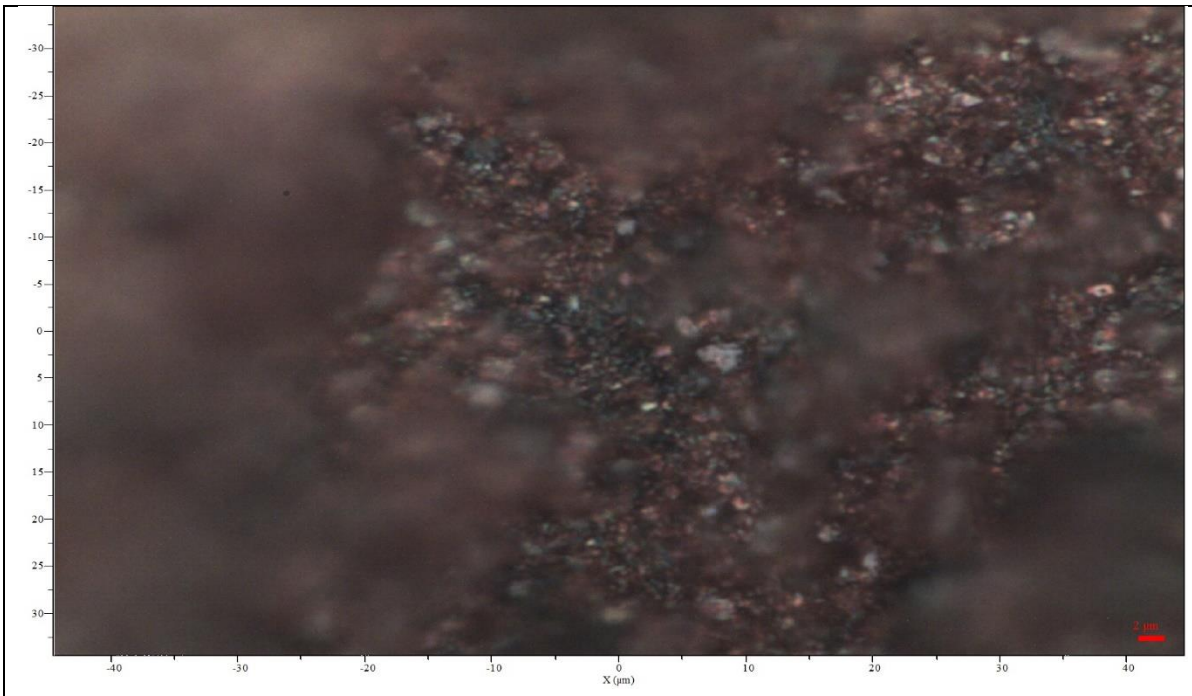

Figure 47: "Hematite in liq 10d – c". High magnification image of hematite sample surface. The red line indicates 2 µm distance.

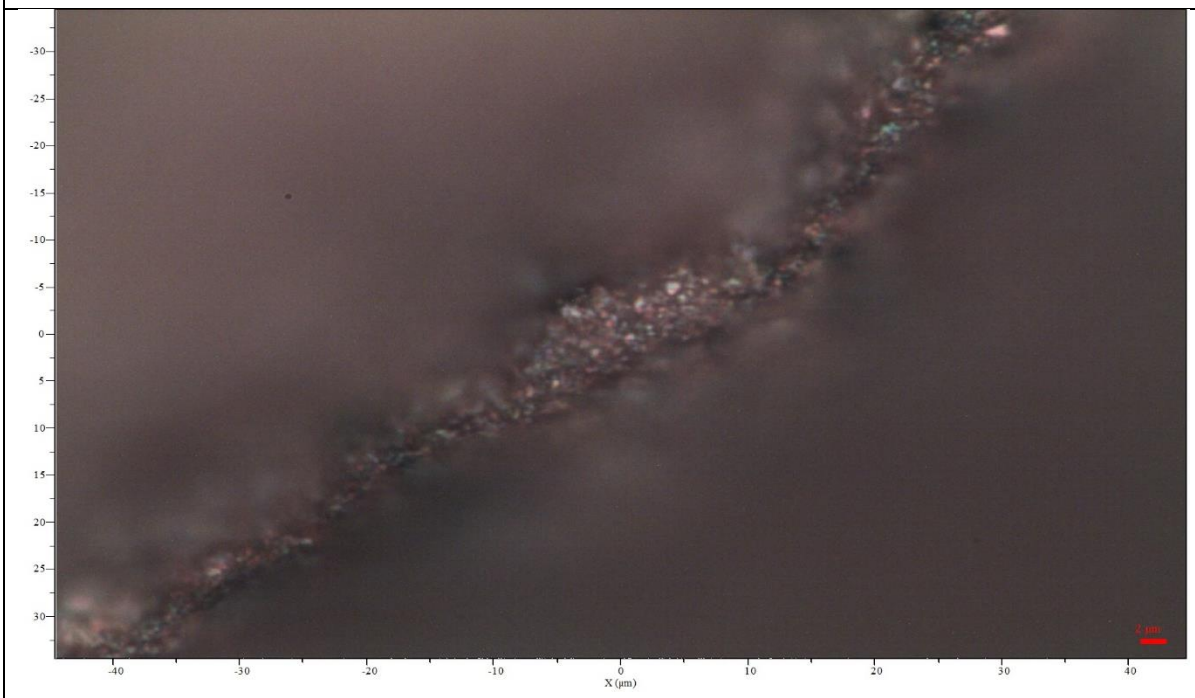

Figure 48: "Hematite in liq 10d – d". High magnification image of hematite sample surface. The red line indicates 2 µm distance.

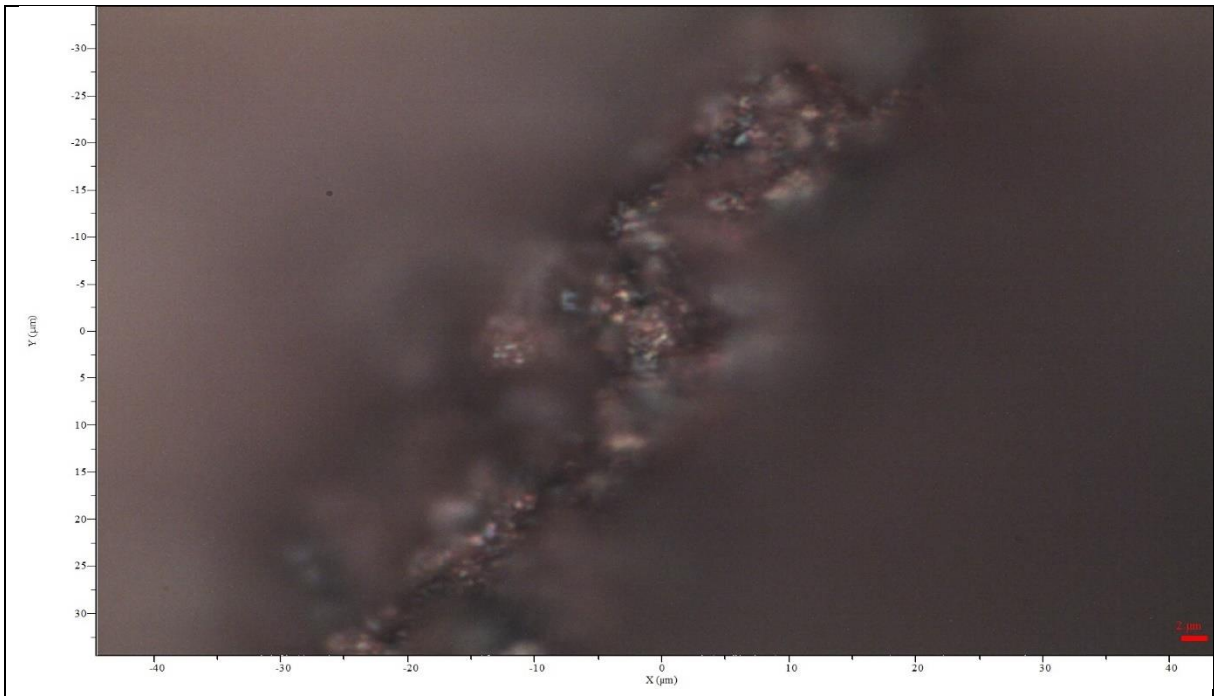

Figure 49: "Hematite in liq 10d – e". High magnification image of hematite sample surface. The red line indicates 2 µm distance.

The most noticeable difference between gas-phase and liquid-phase exposures is the texture to the naked eye. The hematite that was submerged in liquid had a notably smoother surface because the loose powdery particles that adhere to the surface were removed. The sample was washed in acetylacetone before being placed into the test liquid to attempt to remove the possibility of micro-particles suspended within the acetylacetone falsely reporting as extraction on ICP-MS when the liquid was analysed.

The Raman spectra presented in Figure 50 for the hematite samples display textbook peaks for hematite. The reference for hematite is given by the pink line starting at the 0 point on the y-axis. There was no detectable difference between the surface of hematite that was exposed to either gas-phase or liquid-phase acetylacetone. The images also depict areas either black or brick red in colour. The colour difference did not have any impact on the measured Raman spectrum.

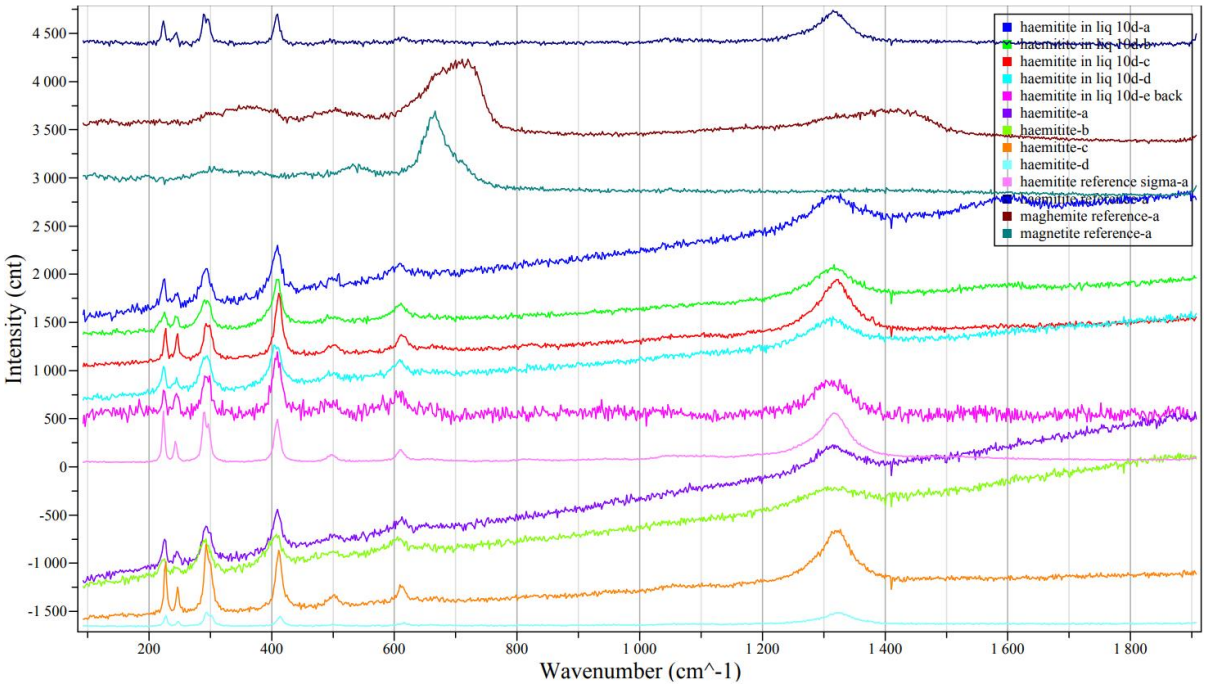

Figure 50: Combined Raman Spectra Intensities for hematite samples with a hematite, maghemite, and magnetite reference. Naming convention matches images presented in figures 42-49. Intensities are not to scale.

The degree of similarity in the Raman spectra for hematite indicates two things: the samples of hematite are of a high purity with little variation, and there is no detectable surface reaction between Fe_2O_3 and acetylacetone. This reinforces the argument hinted earlier – by the negligible mass difference – that there may be no significant reaction between hematite and acetylacetone.

Insights from ICP-MS

One cannot rule out any form of reaction with mass difference and Raman spectra alone. Within this framework, it is possible for small-scale surface extraction to occur in a manner that completely removes Fe_2O_3 from the surface of the hematite – preventing detection by either analysis presented so far. For this reason, the liquids from both the condensate and from the acetylacetone liquid-phase extraction were tested for iron, copper, and gold with ICP-MS. The concentrations for the liquid-phase exposure, hematite condensate and residue in air, and hematite condensate and residue in nitrogen are presented in Table 7 with sample naming following from Table 5 earlier in this chapter.

A control, sampled directly from the same bottle of acetylacetone that was used for all extraction experiments, was also included for a reference to account for base levels of material that would be detected on ICP-MS (especially iron).

Table 7: Analysis using ICP-MS to determine iron, copper, and gold concentrations within acetylacetone exposed to hematite in liquid-phase after 10 days exposure, gas-phase extraction with air carrier gas, gas-phase extraction with nitrogen carrier gas. Numbers reported to 3rd decimal to show accuracy of each measurement, each measurement was sampled once on ICP-MS.

Sample *(from Table 5)*	**Description**	**^{56}Fe** *(mg/L)*	**^{63}Cu** *(µg/L)*	**^{197}Au** *(µg/L)*
Control	Untouched acetylacetone from same bottle used in extractions	33.2	293	<1
3	Hematite (air) condensate	27.9	257	<1
	Hematite (air) residue	30.2	707	<1
4	Hematite (N_2) 1st pass condensate	22.5	145	<1
	Hematite (N_2) 2nd pass condensate	22.4	127	<1
	Hematite (N_2) 3rd pass condensate	21.8	114	<1
	Hematite (N_2) 4th pass condensate	20.9	91.0	<1
	Hematite (N_2) residue	66.8	709	<1
5	Hematite liquid-phase 10 day	24.0	176	<1

Concentrations of iron in the liquid samples of acetylacetone showed unexpected results. There is a substantial difference between the iron concentration of the residues when air and nitrogen were used as a carrier gas. Both Samples 3 and 4 were exposed to acetylacetone at 220 ^{o}C, for 200 and 211 minutes respectively. The only material difference between these results is the difference in carrier gas. However, there is a much smaller difference in the iron concentrations of the condensates. Sample 3 had a slightly higher concentration of 27.947 mg/L compared to the final concentrate of Sample 4 at 20.921 mg/L – inverse to the difference in iron concentration of the residues. The most plausible explanation is that oxygen presence in the carrier gas has an influence on the ability of the iron to be carried within acetylacetone vapour. This does not appear to affect copper as the concentrations of copper in both residues of Samples 3 and 4 are similar.

Looking exclusively at the iron content of the nitrogen carrier gas condensates (Sample 4), the iron content appears to be highest on the first pass and then drops

with each successive pass. Without the control as a reference, this would appear as iron extraction – the extraction starts higher and becomes progressively lower as the source of iron is depleted – in the same general trend that was reported by Potgieter *et al*. (2006), Van Dyk *et al.* (2010), Shemi *et al.* (2012), Tshofu (2014), Olehile (2017), Machiba (2020), and Ali (2021). However, one cannot look at the iron concentration of the acetylacetone condensate without a reference. The control is used as a baseline to give all preceding measurements meaning. In this case, the control had a higher concentration of iron (and copper) than all other condensates – indicating that there is no iron extraction taking place. Rather, there were indications that either iron deposition had occurred or that iron was accumulating in the boiling flask as acetylacetone boiled off. There is no mention of a baseline metal content reading being taken for the acetylacetone in any of the works cited. Many of the works say that the acetylacetone (>99% Reagent Plus®) was used without further purification. The same trend observed with iron, also appeared with copper. This is important because no copper was detected in the Raman spectra of the hematite. It is only an impurity found within the acetylacetone from manufacturing, proving that the trend can likely be replicated without a source of iron anywhere in the sample. This confirms that the hematite is acting as an inert in this system. There is no indication from ICP-MS that any iron extraction took place.

To rule out the issue of extraction times and kinetic limitations, the liquid-phase extraction was included here. Exposing hematite to liquid acetylacetone for 10 days also does not appear to indicate any measurable extraction of iron. The iron content within the acetylacetone was lower than in the control – suggesting a slight iron deposition might have occurred.

Disparity in results between different works

Through investigation of pyrite and hematite in this chapter, it was discovered that extraction does not occur at the level that was previously thought. The evidence suggests that acetylacetone reacts with pyrite on the surface but does not form $Fe(acac)_3$ as theorized – the products formed remain unknown. There was also no

evidence to suggest that gold, when present with pyrite, changes the interaction of gold and acetylacetone. The gold was still measurably inert.

The findings surrounding hematite differ fundamentally from previous work. There is no indication from the results in this chapter that any extraction of iron from hematite occurred. Further, using compressed air or nitrogen as the carrier gas did not appear to affect extraction of iron. It did affect the acetylacetone when nitrogen carrier was used, the acetylacetone changed from a clear liquid to a slightly yellow liquid. This is likely resultant from a change between the acetylacetones "keto" and "enol" form (Aromi *et al.* 2008). It may be of interest for further research to investigate the reversibility of the colour change observed. If the acetylacetone turns light yellow when distilled in nitrogen atmosphere, will it change from light yellow to clear when distilled in air atmosphere?

Some elements of the results in this chapter show how it may be possible to replicate the trends observed in previous works. This suggests that there is likely an underlying natural phenomenon at play that would explain how all the results fit together. In the following chapter, a more detailed investigation into disparity in results between this work and the current understanding of acetylacetone-based extractions will be presented.

CHAPTER SIX

Criticising experimental design and analytical data

The trend observed in previous works — focussed on extracting various metals using acetylacetone — suggests that there is an underlying natural phenomenon giving rise to the trends reported. Such a phenomenon, it was assumed, would have a mechanism — how the acetylacetone acting as a ligand extracted metals — that could be identified in a kinetic study that today is common in some quarters. However, the findings reported in this study do not agree with those previous studies. Why the difference when the conditions used were similar. This chapter explains how it is possible to arrive at two different conclusions while evaluating the same data.

Summary of previous findings

The earliest work that reports the use of a fluidized-bed reactor for acetylacetone-based extraction, is a master's dissertation by Mariba (2010). The setup, used for the first time in this work, was developed from suggestions in Kabemba's (2005) work that is also presented in Potgieter *et al*. (2006).

The original setup is shown in Figure 51. The resemblance to the setup used by Shemi *et al.* (2012), Tshofu (2014), Olehile (2017), Machiba (2020), and Ali (2021) is clear. There has been no change to the setup used though all the gas-phase acetylacetone extraction setups until the introduction of air as a carrier gas by Ali (2021).

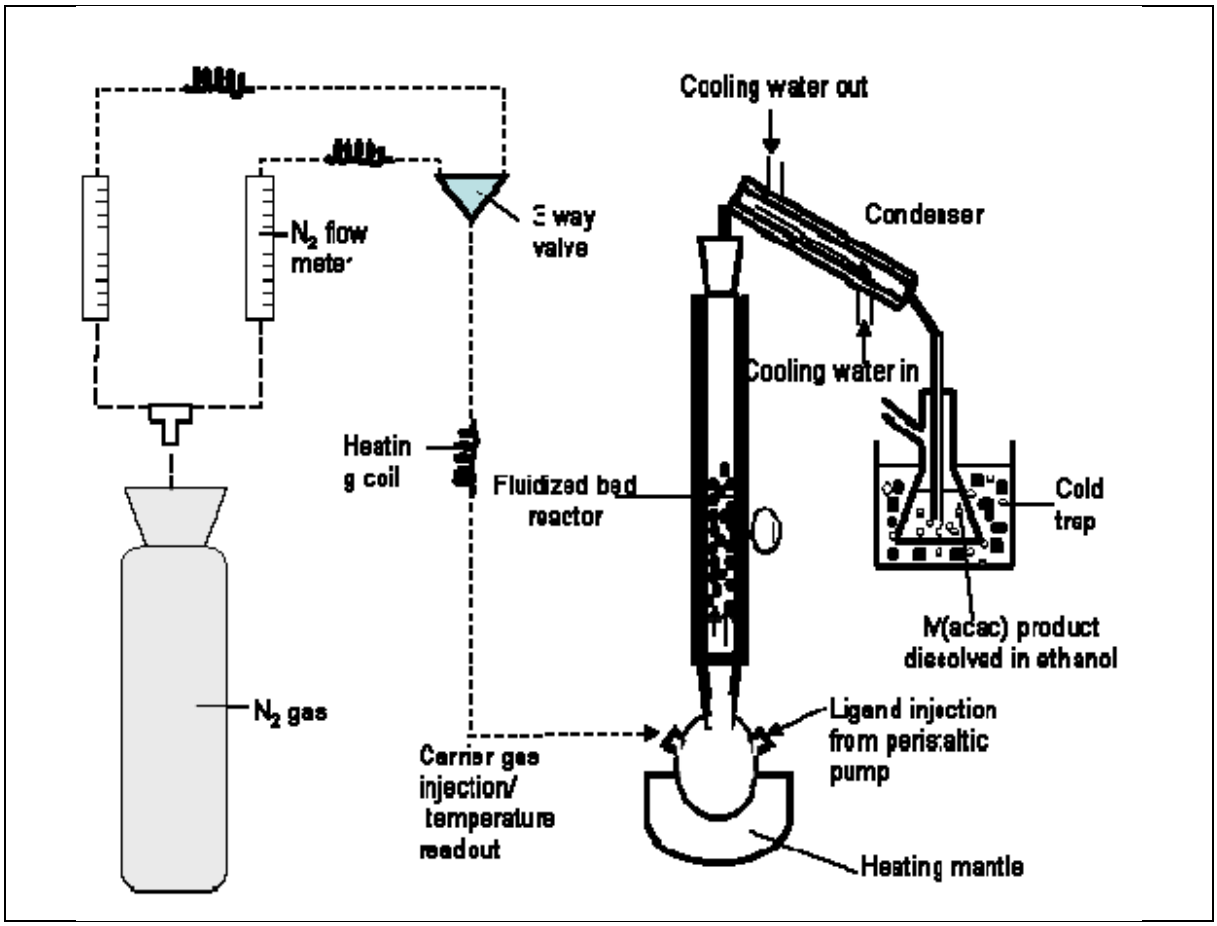

Figure 51: Original gas-phase extraction setup with acetylacetone ligand (Mariba 2010)

The extraction trends reported by all studies using a similar apparatus to Figure 51 are all similar. Figure 52 gives one such example: the extraction increases with time and starts to show diminishing extraction — the rate of extraction decreases — as time moves on. The curves all appear to be flattening off, suggesting that extraction has reached an equilibrium of sorts. Additionally, higher temperatures in the reactor are reported to produce higher extractions.

Similar trends were reported by Potgieter *et al.* (2006) — see Figure 53. Their apparatus differs slightly because the acetylacetone was not fed continuously via peristaltic pump; instead, it was placed in a boiling flask and evaporated with heat and a carrier gas—as in the setup in this study (Chapter 4).

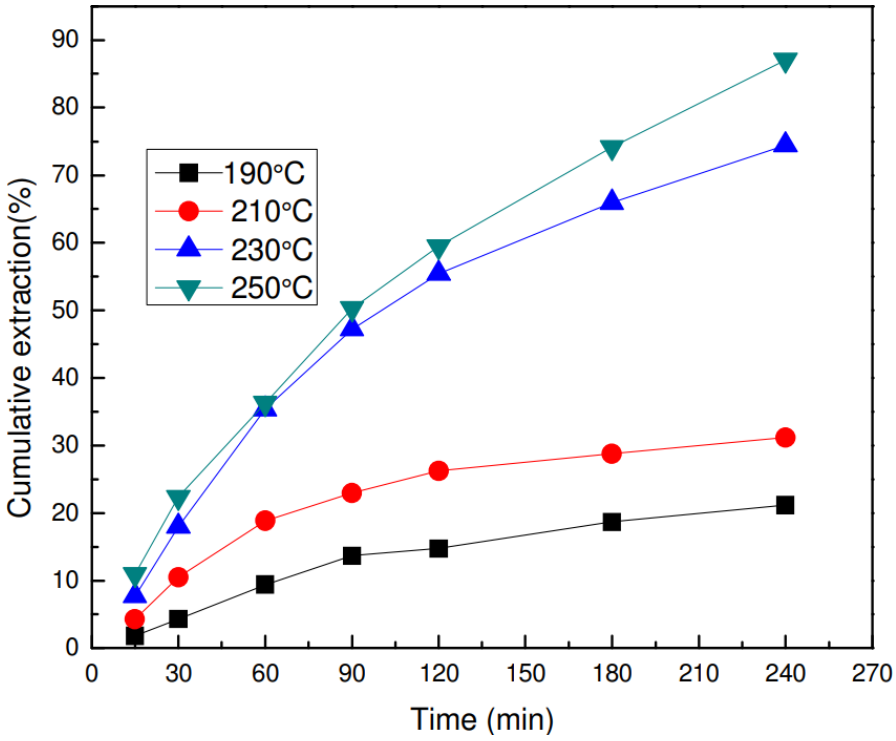

Figure 52: An example of rate curves generated for acetylacetone extraction of a solid mixture containing 1 mass% Fe_2O_3 (Mariba 2010)

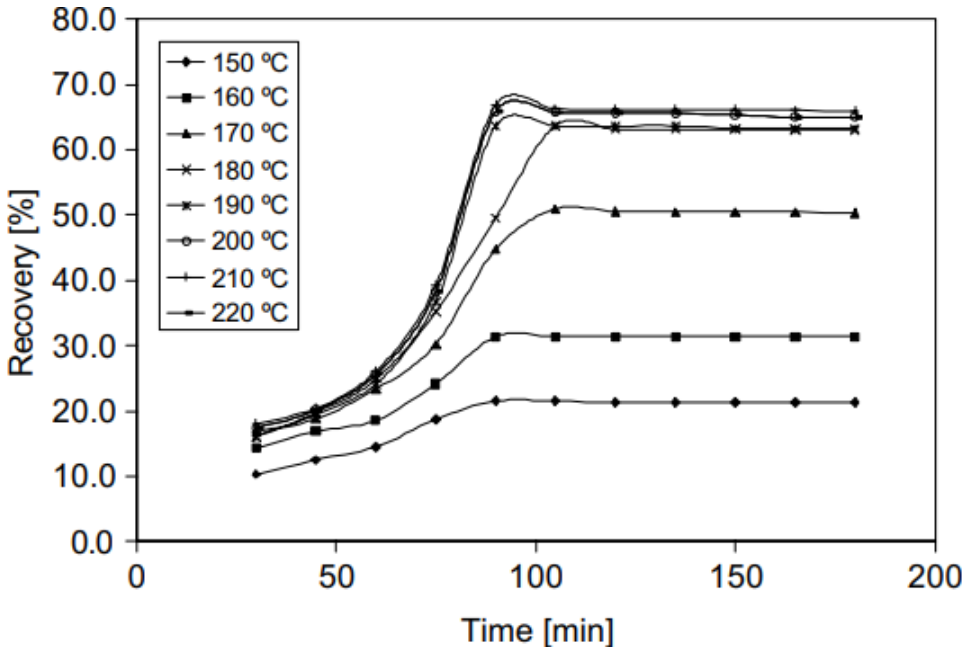

Figure 53: An example of rate curves generated for the extraction of aluminium (Potgieter *et al.* 2006)

The same trend reported with iron has also been reported with lead, chromium, vanadium, aluminium, and, most recently, gold. Examples of the trend for gold — as measured by Machiba (2020) and Ali (2021)—are shown in Figure 54 and Figure 55.

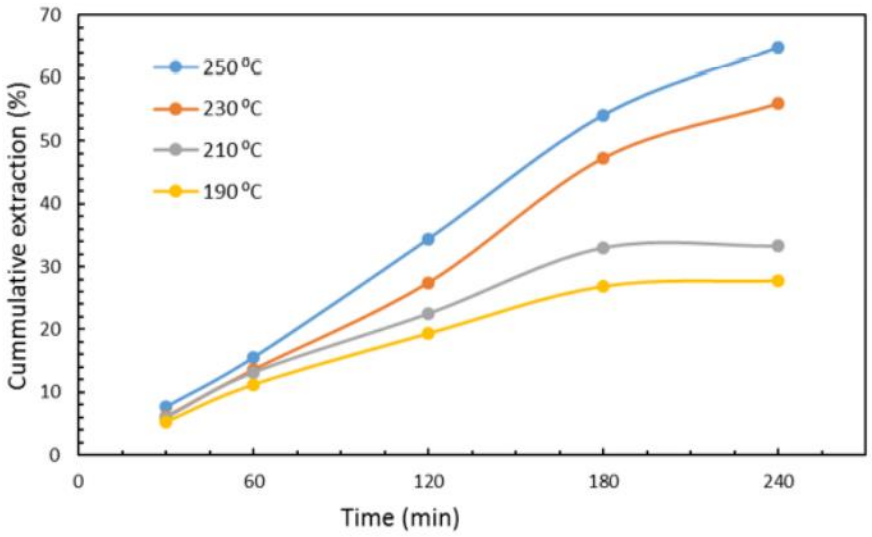

Figure 54: Cumulative gold extraction with acetylacetone at 1 mL/min flow rate and a 50 g bed mass (Machiba 2020)

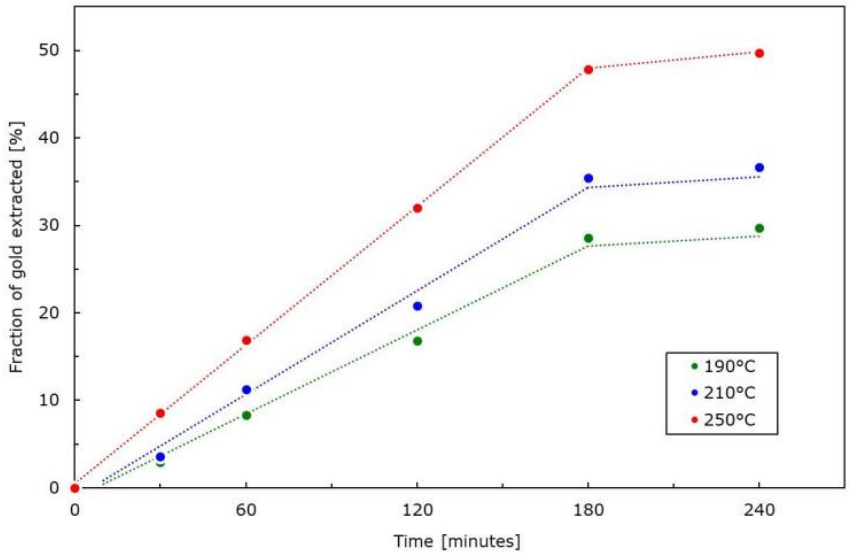

Figure 55: Cumulative gold extraction with acetylacetone at 3 mL/min and a 20 g bed mass (Ali 2021)

Many extracted curves are given here to highlight the high degree of similarity in results across many different metals, giving the impression that acetylacetone is a "one size fits all" ligand for metals extraction, with recoveries of many metals reported in the same range of 40−80 %. High recoveries were reported on the bed

samples that contained the least material of interest. As the metal content within each sample was increased, the reported degree of extraction decreased. This is an important observation to note when explaining how the results could be replicated.

Replicating previous curves from data in this work

The previous work by Van Dyk *et al.* (2010), Shemi *et al.* (2012), Tshofu (2014), Olehile (2017), Machiba (2020), and Ali (2021) all measured extraction in the same way. The acetylacetone condensate was collected in regular time intervals (either 30 or 60 min). Each collected sample then had the metal concentration measured. Both the condensate concentration and volume were measured and translated to give extraction as a percentage from the original sample mass. So, to calculate the mass of metal extracted after 2 hours, the concentration of metal in each condensate sample collected at 30 min, 60 min, 120 min, and 180 min was measured. The concentration was multiplied by the volume of condensate and the masses for each interval was summed to give a mass value for the extraction after 2 hours. This same summation technique (cumulative summation) was used to generate the curves presented in Figures 56 and 57.

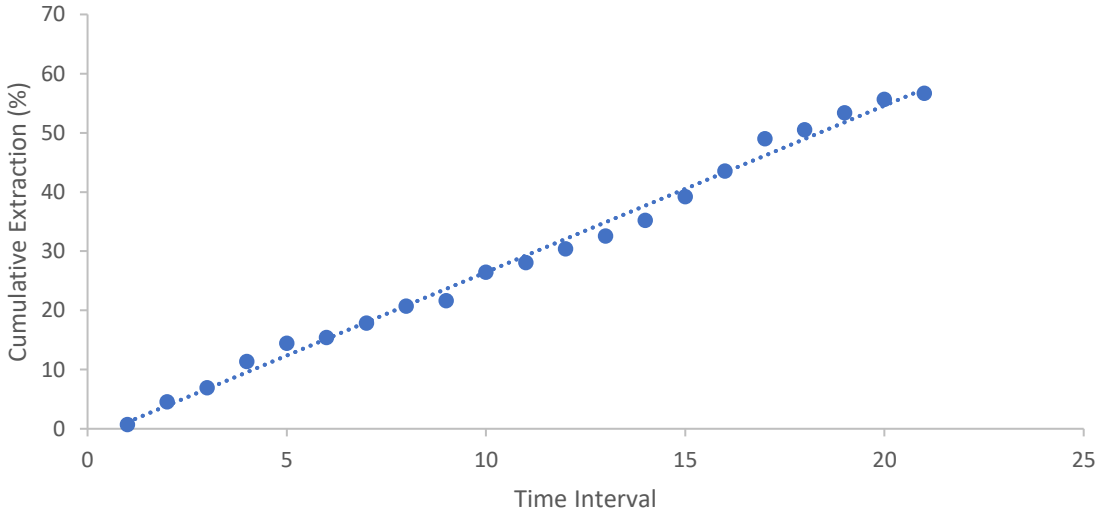

Figure 56: Curve showing similar trend to a first-order reaction, generated with random numbers and cumulative summation

Potgieter *et al.* (2006) noted that acetylacetone extractions of iron "obey[ed] first order reaction kinetics best." The points plotted in Figure 56 would appear to match a first

order trend with good correlation. However, the points in Figure 56 are not measured points from an acetylacetone extraction. The points were generated by a random number generator in MSExcel. The random number serves to replicate the concentration measurement of the condensate. The numbers were then multiplied by another random number, generated with a 0.5 standard deviation and a mean of 5. This value serves to imitate the volume measurement in the system. The points were then multiplied to give a simulated "mass extraction" and summed to give cumulative extraction.

The purpose of using random points is to show that an apparent trend is not necessarily an indication of an underlying natural phenomenon. In this case, the trend is an artefact of the way in which the underlying data were re-worked for the plot. This presents a problem when trying to explain what happens during these experiments as it becomes difficult to separate a potentially natural first-order extraction from the apparent first-order plot that results from data manipulation. The less variance that is present in the samples, the closer the data will appear as first order when cumulative summation is used. In a perfect example with no variance at all, if each measurement is 3 (an arbitrary number), then the line plotted on cumulative summation will be a perfectly straight line (a first order reaction) with the equation $y = 3x$. Conversely, when the underlying data has a high variance, the bias introduced by cumulative summation has a less pronounced influence on the plotted points—eventually reaching a point where a straight line is no longer recognisable. This does not mean that the data points on previous works were measured incorrectly; rather, it is an example of how a trend can sometimes be misleading. It further highlights the importance of reviewing critically not only experimental technique, but also the way in which data are re-worked for reporting. It may introduce a regularity into the data that is easily misinterpreted as the manifestation of a natural phenomenon.

Another aspect of data that is sometimes overlooked is meaningful a comparison. The points in Figure 57 illustrate an apparent trend observed – like many previous studies involving acetylacetone extractions – where there is increasing cumulative extraction over time and diminishing extraction after longer periods.

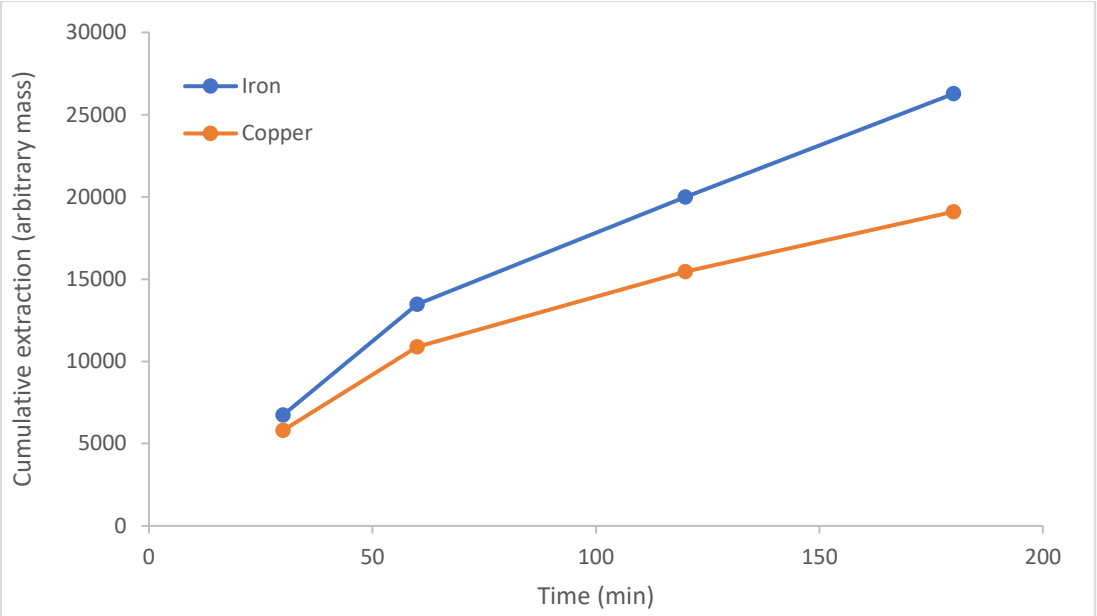

Figure 57: Cumulative mass extraction of iron and copper with data points taken from Table 7 and manipulated to in the same fashion as previous acetylacetone extraction works.

Figure 57 depicts the expected extraction characteristic of both iron and copper — curves drawn from literature. This is expected as the apparatus used were similar and the data were reworked in a similar fashion to prepare the graph. The curves appear to flatten slightly at higher extraction times. The underlying reason for this flattening is that the metal concentration is not that the metal within the sample is depleting (causing reduced extraction rates as extraction continues). Rather, the reason for the flattening is that the concentrations of metals measured in condensates from longer periods were lower. An explanation for why the concentrations might be lower is given in Chapter 5.

Measuring the concentrations of metals in condensate tells only half the story. Without knowing what the concentration started at, it is impossible to attribute the concentration of samples to extraction — this would only be speculation. Any concentration measured could be attributed to impurities within the acetylacetone from manufacturing. At the least, it will cause extraction values to be exaggerated as the base metal content was not subtracted from the measurements.

When the points in Figure 57 are compared to a baseline measurement of the metal content within the acetylacetone used, 33.19 mg/L iron and 293.56 µg/L copper, the

graph loses meaning. All concentrations measured for the points plotted in the graph were lower than the baseline iron and copper content in acetylacetone. This means that the metal concentration in acetylacetone decreased over time — fundamentally altering the discussion. While one can still generate the same trends, when the understanding gained from comparison to a control is added, one can see that no extraction has taken place – the data motivates for deposition instead.

This case study highlights the importance of context. It may not always be suitable to plot curves, it is more beneficial to compare the concentrations to the baseline. This illustrates the need to carefully consider data comparisons that are made. For example, the metal concentrations measured in acetylacetone condensate. This case study further shows how context of measurements can completely change the conclusions drawn from the data.

Temperature dependence explained

With the shape of the curves in previous extraction works accounted for, there is another apparent trend that is reported in the previous works cited. Potgieter *et al*. (2006), Van Dyk *et al.* (2010), Shemi *et al.* (2012), Tshofu (2014), Olehile (2017), Machiba (2020), and Ali (2021) all report an increase in extraction with an increase in temperature. This is an interesting finding when the prospect of acetylacetone degradation is introduced.

Higher reactor temperatures were observed to produce slightly higher evaporation rates in this study and the studies by Tshofu (2014), Machiba (2020) and Ali (2021). It is suspected to be a result of heat conduction between the glassware used. Heat from the reactor was transferred to the neck of the boiling flask, reducing the amount of reflux within the boiling flask. This observation appears common in the experimental data supplied by Tshofu (2014), Machiba (2020) and Ali (2021), where higher condensate volumes were collected on runs with higher reactor temperatures, however, further investigation into such a phenomenon is required to confirm this theory.

Upon further inspection of the experimental data supplied by Tshofu (2014), Machiba (2020) and Ali (2021). It was found that the volume of condensate collected

in each time interval did not match up to the reported acetylacetone flowrate. This suggests that there was accumulation in the boiling flask and that the evaporation rate was neither constant nor linked to the reported ligand flowrate through the reactor. The reactor temperature appeared to have a greater influencer on ligand flowrate through the reactor than the ligand flowrate into the evaporation flask – the variable reported in the previous studies on acetylacetone extraction.

Checks, balances, and critical tests

It is possible to manage unforeseen analytical errors by implementing additional checks and balances. For example, if sampling the condensate for iron concentration indicates an extraction of 60 % of the initial sample. A similar mass change in the bed weight should be present when measured. This process of verification of findings from multiple sources can help detect inconsistencies in results — especially useful when investigating novel techniques. If there is a difference in bed mass but inconsistent with the expected mass difference indicated by condensate concentration, there may be mass loss to entrainment, a leak in the system, or noise in analytical measurements.

Many of the previous studies involving gas-phase acetylacetone used fluidized-bed reactors. However, no full mass balance was reported. The literature is silent on bed masses after extraction and the topic of entrainment entirely. This can become particularly problematic when investigating sources such as hematite, a powdery ore with ultrafine particles that adsorb to the surface of larger particles. It is highly likely that a portion of ultrafine particles were entrained. These entrained particles would be carried off into the condensate as solid particles where they could be carried into analysis by suspension in acetylacetone condensate. This would not only question the reliability of data for "gas-phase" extractions, but also make it impossible to identify a true reaction time as samples can be left for extended periods before being analysed – allowing an undocumented time for entrained particles to interact with acetylacetone in the liquid-phase.

In this study, the mass difference of each sample was used as the primary indicator to assess extraction. This was chosen because it is the simplest, most effective,

variable to indicate mass being removed from the sample. In the case of pyrite, there was an observable reaction. However, the absence of a measurable mass change suggests that extraction from pyrite fails the critical test of extraction.

The design of experimental method should avoid reliance on a single analytical technique such as AAS or ICP-MS. Implementing additional checks and comparisons such as comparing sample mass, using multiple analytical techniques for concentration tests, and running additional control tests will highlight cases where fundamentals may have been overlooked —producing misleading results.

CHAPTER SEVEN
Concluding summary

This study set out to improve fundamental understanding of gas-phase extractions with acetylacetone. The work started with an *ab initio* study of gold complexes using DFT to give insight into potential gold complexes that might form during gas-phase extraction. The DFT study predicted $[Au(acac)_2]^{-1}$ to be the most stable complex based on HOMO-LUMO gaps. However, the results are inconclusive as the complex could not be empirically verified when synthesis was attempted in liquid-phase from $AuCl_3$, and similar gas-phase extraction conditions to previous works. The product $[Au(acac)_2]^{-1}$ is an ion which is not known to form in gaseous mixtures below 250 °C – adding further doubt into the reliability of DFT to predict Au acetylacetonate complexes.

Gas-phase extraction of gold was investigated on a fundamental level with the use of large pure gold pieces, rather than gold tailings. No evidence of extraction was detected by observation, mass difference, or ICP-MS of the condensates and residues. The lack of observable extraction, when considered with the unprecedented mass of gold used, makes it highly unlikely that gold extraction has occurred in previous literature.

Iron extraction from pyrite and hematite was also investigated using large amounts of material. There was an observable reaction between acetylacetone and pyrite at 190 °C. However, the reaction is likely a surface reaction as no iron was detected in the condensate with ICP-MS – indicating that no extraction took place.

This work also investigated hematite extraction with acetylacetone in both nitrogen and compressed air carrier gasses at 220 °C with a ligand flowrate of 10 mL/min. Oxygen presence in the carrier gas did not affect iron extraction. In both cases, samples had negligible mass change, and no observable change in surface

characteristic detectable with Raman Spectroscopy. Iron concentrations measured with ICP-MS revealed that iron levels in all condensates were below the baseline iron concentration within the new acetylacetone used.

The extraction attempts revealed some new information about the system involving acetylacetone. The presence of free carbon on the surface of the samples after extraction, and the formation of a dark residue in the boiling flask with no metal content, both indicate that acetylacetone was decomposing during boiling. A temperature of 165-167 ^{o}C was measured along the outer edge of the boiling flask. This suggests that acetylacetone may decompose at those temperatures. The best explanation offered at this point is that acetylacetone could have sufficiently poor convection that leads to heat build-up and superheating of the outer layer of liquid that causes decomposition.

For the first time, a direct comparison between nitrogen and compressed air carrier gasses has shown that acetylacetone may be influenced by oxygen. Decomposition did not appear to be affected in any way by the change in atmosphere. However, the colour of acetylacetone condensate was affected. The acetylacetone condensate remained clear when compressed air was used and turned yellow when nitrogen was used. This could be explained by a change between the 'enol' and 'keto' forms of acetylacetone as both clear and yellow are used to describe the compound (Aromi *et al.* 2008).

Reaction products of extraction and an investigation into separation of acetylacetonate complexes were not possible as extraction could not be replicated. Further investigation into previous literature revealed a possible explanation of the previous trends found by Potgieter *et al*. (2006), Van Dyk *et al.* (2010), Shemi *et al.* (2012), Tshofu (2014), Olehile (2017), Machiba (2020), and Ali (2021) that is consistent with the results reported in this work.

Comparison between metal content of condensates and the baseline impurities within acetylacetone appears to be overlooked in previous work. This played a part in giving the false impression of extraction when metal content in the condensate was measured. Addition of a linear bias on extraction curves from cumulative summation furthered the impression of extraction. Together, the reported results

appear as a trend that can mislead one into believing there is extraction as random noise does not normally produce trends.

Further complication was added with extraction having an apparent, expected, temperature dependence. This was explained to be resulting from increased condensate capture of the ligand, as a hotter reactor aided acetylacetone evaporation by warming connecting glassware and reducing reflux within the evaporation flask.

The findings in this work have fundamentally altered the understanding of gas-phase acetylacetone extraction from metal sources. It is evident that extraction does not occur on the level previously thought – if at all. The absence of observable extraction in this work questions the technical and economic feasibility of a new gas-phase extraction process around acetylacetone. β-Diketones are an expensive class of compound, it is unlikely that sufficient gold or iron extraction could ever be achieved with gas-phase extraction using acetylacetone in the manner investigated within this work.

Recommendations

From the insights gained in this work, the following recommendations are given for future research:

- Investigate acetylacetone decomposition in more detail. The exact decomposition temperature remains unknown, it may increase over a range of temperatures. Further analysis of decomposition products with techniques better suited for identification of organics is also recommended.
- Investigate the true reason behind the clear/yellow shift in colour of acetylacetone. It was speculated to be oxygen content of the atmosphere in this work, but it is also possible that the hematite sample acted as a catalyst in the colour shift.
- Revisit extraction of metals using acetylacetone with a comparison to the baseline impurity content within acetylacetone. It is also recommended to address entrainment as this element was also lacking in previous literature. Additional cross-checks should be added such as bed mass before and after extraction, use of multiple analysis techniques, and analysis of the carrier gas outlet stream.
- Investigation into using heated liquid-phase acetylacetone for extraction. It is recommended to begin investigation on pyrites as there was indication of a reaction in this work. Use of liquid-phase may enable removal of reaction products from the surface – improving potential for breaking down pyrite and accessing trapped gold.

REFERENCES

Aghamirian, M. M. (1997). *Reactivity of Sulfide minerals and its Effect on Gold Dissolution and Its Electrochemical Behaviour in Cyanide Solution.* Dept of Mining Engineering . Kingston, Ontario, Canada: Queen's Univeristy.

Ali, I. A. (2021). *Gas-phase extraction of gold from tailings: Insights from density functional theory and the empirical.* Faculty of Engineering and the Built Environment. Johannesburg: University of the Witwatersrand.

Allabashi, R., Stach, W., de la Escosura-Muńiz, A., Liste-Calleja, L., & Merkoći, A. (2008). ICP-MS: a powerful technique for quantitative etermination of gold nanoparticles without previous dissolving. *Journal of Nanoparticle Research*. doi:10.1007/s11051-008-9561-2

Alymore, M. G., & Muir, D. M. (2001). Thiosulfate leaching of gold - a review. *Minerals Engineering, 14*(2), 135-174.

Aromi, G., Gamez, P., & Reedijk, J. (2008). Poly beta-diketones: Prime ligands to generate supramolecular metalloclusters. *Coordination Chemistry Reviews*(252), 964-989. doi:10.1016/j.ccr.2007.07.008

Bartlett, R. J., Grabowski, I., Hirata, S., & Ivanov, S. (2005). The exchange-correlation potential in ab initio density functional theory. *The Journal of Chemical Physics*(122), 034104.

Bascomb, C. L., & Thanigasalam, K. (1978). COMPARISON OF AQUEOUS ACETYLACETONE AND POTASSIUM PY ROPHOSPHATE SOLUTIONS FOK SELECTIVE EXTRACTION OF ORGANIC-BOUND Fe FROM SOILS. *Journal of Soil Science, 29*(3), 382-387.

Basova, T., Hassan, A., & Morozova, N. (2019). Chemistry of gold(I, III) complexes with organic ligands as potential MOCVD precursors for fabrication of thin

metallic films and nanoparticles. *Coordination Chemistry Reviews*, 58-82. doi:10.1016/j.ccr.2018.09.005

Cao, Z., Zhang, L., Guo, C.-Y., Gong, F.-C., Long, S., Tan, S.-Z., . . . Sun, L.-X. (2009). Evaluation on corrosively dissolved gold induced by alkanethiol monolayer withatomic absorption spectroscopy. *Materials Science and Engineering C*, 1051-1056. doi:10.1016/j.msec.2008.09.010

Carmerman, A., Mastropaolo, D., & Camerman, N. (1983). Molecular Structure of Acetylacetone. A Crystallographic Determination. *Journal of the American Chemical Society*, 1584-1586.

Chaudhuri, M. K., & Ghosh, S. K. (1983). Novel Synthesis of Tris(acetylacetonato) iron(II). *Journal of the Chemical Society, Dalton Transactions*, 839-840. doi:10.1039/DT9830000839

Choudhury, T., & Lin, M. (1990). Homogeneous Pyrolysis of Acetylacetone at High Temperatures in Shock Waves. *International Journal of Chemical Kinetics, 20*, 491-504. doi:10.1002/kin.550220506

Claisen, L., & Erhardt, E. F. (1889). Ueber die Darstellung des Acetylacetons und seiner Homologen. *Berichte der deutschen chemischen Gesellschaft*, 1009-1019. doi:10.1002/cber.188902201220

Crundwell, F. K., & Godorr, S. A. (1997). A mathematical model of the leaching of gold in cyanide solutions. *Hydrometallurgy*(44), 147-162.

Das, D., Das, A. K., Sarkar, B., Mondal, T. K., Mobin, S. M., Fiedler, J., . . . Lahiri, K. (2009). The Semiquinone-Ruthenium Combination as a Remarkably Invariant Feature in the Redox and Substitution Series [Ru(Q)n(acac)3-n] , n = 1-3; m = (-2), -1, 0, +1, (+2); Q = 4,6-Di-tert-butyl-N-phenyl-o-iminobenzoquinone. *Inorganic Chemistry*, 11853-11864. doi:10.1021/ic901900g

Donato, D. B., Nichols, O., Possingham, H., Moore, M., Ricci, P. F., & Noller, B. N. (2007). A critical review of the effects of gold cyanide-bearing tailings solutions on wildlife. *Environmental International, 33*, 974-984. doi:10.1016/j.envint.2007.04.007

Dong, Z., Jiang, T., Xu, B., Yang, Y., & Li, Q. (2017). Recovery of Gold from Pregnant Thiosulfate Solutions by the Resin Adsorption Technique. *Metals, 7*(12), 555. doi:10.3390/met7120555

Ellis, S., & Senanayake, G. (2004). The effects of dissolved oxygen and cyanide dosage on gold extraction from a pyrrhotite-rich ore. *Hydrometallurgy*(72), 39-50. doi:10.1016/S0304-386X(03)00131-2

Falagán, C., Grail, B. M., & Johnson, D. B. (2017). New approaches for extracting and recovering metals from mine tailings. *Mining Engineering*(106), 71-78. doi:10.1016/j.mineng.2016.10.008

Fleming, C. A. (1992). Hydrometallurgy of precious metals recovery. *Hydrometallurgy*(30), 127-162.

Fraser, K. S., Walton, R. H., & Wells, J. A. (1991). Processing of refractory gold ores. *Minerals Engineering, 4*(7-11), 1029-1041.

Frisch, M., Trucks, G., Schlegel, H., Scuseria, G., Robb, M., Cheeseman, J., . . . Fox, D. (2019). Gaussian 16, Rev C.01. Conneticut: Gaussian Inc.

Frisch, M., Trucks, G., Schlegel, H., Scuseria, G., Robb, M., Cheeseman, J., . . . Pople, J. (2004). Gaussian 03, Revision C.01. Wallingford, Connecticut: Gaussian Inc.

Gökelma, M., Birich, A., Stopic, S., & Friedrich, B. (2016). A Review on Alternative Gold Recovery Reagents to Cyanide. *Journal of Materials Science and Chemical Engineering, 4*, 8-17. doi:10.4236/msce.2016.48002

Ha, V. H., Lee, J. C., Jeong, J., Hai, H. T., & Jha, M. K. (2010). Thiosulfate leaching of gold from waste mobile phones. *Journal of Hazardous Materials, 178*(3-Jan), 1115-1119. doi:10.1016/j.jhazmat.2010.01.099

Henderson, M. S. (2022). *The development of a supercritical extraction method to extract zero valent gold.* The University of the Witwatersrand, School of Chemical and Metallurgical Engineering. Johannesburg, South Africa: The University of the Witwatersrand.

Huber, J. F., & Kraak, J. C. (1972). Rapid Separation of Metal Chelates by Column Liquid-Liquid Chromatography Using Ultraviolet Detection. *Analytical Chemistry, 44*(9), 1544-1559.

John Wiley & Sons, Inc. SpectraBase. (2022, 1 7). SpectraBase Compound ID=8jvSi6rDKgq SpectraBase Spectrum ID=5AnwrxH5xTL. Retrieved 1 7, 2022, from https://spectrabase.com/spectrum/5AnwrxH5xTL

Kabemba, M. A. (2005). *Recovery of valuable metals from solid compounds by gas phase extraction*. Tswane, South Africa: Tswane University of Technology.

Katsuta, S., Imura, H., & Suzuki, N. (1992). NOVEL ENHANCEMENT EFFECT OF A PROTON DONOR ON CHELATE EXTRACTION: EXTRACTION OF IRON(III) WITH ACETYLACETONE AND 3,5-DICHLOROPHENOL. *Journal of Radioanalytical and Nuclear Chemistry, 157*(2), 255-264.

Komiya, S., & Kochi, J. K. (1977). Reversible Linkage Isomerisms of ß-Diketonato Ligands. Oxygen-Bonded and Carbon-Bonded Structures in Gold(III) Acetylacetonate Complexes Induced by Phosphines. *Journal of the American Chemical Society*, 3695-3704.

Kundu, S., Pal, A., Ghosh, S. K., Nath, S., Panigrahi, S., Praharaj, S., . . . Pal, T. (2005). Shape-controlled synthesis of gold nanoparticles from gold(III)-chelates of b-diketones. *Journal of Nanoparticle Research*, 641-650. doi:10.1007/s11051-005-3475-z

Lever, G., Cole, D. J., Hine, N. D., Haynes, P. D., & Payne, M. C. (2013). Electrostatic considerations affecting the calculated HOMO–LUMO gap in protein molecules. *Journal of Physics Condensed Matter*(25), 152101 . doi:10.1088/0953-8984/25/15/152101

Li, H., Ma, A., Srinivasakannan, C., Zhang, L., Li, S., & Yin, S. (2018). Investigation on the recovery of gold and silver from cyanide tailings using chlorination roasting process. *Journal of Alloys and Compounds*(763), 241-249. doi:10.1016/j.jallcom.2018.05.298

Li, H., Peng, J., Long, H., Li, S., & Zhang, L. (2020). Cleaner process: Efficacy of chlorine in the recycling of gold from gold-containing tailings. *Journal of Cleaner Production*. doi:10.1016/j.jclepro.2020.125066

Lottering, M. J., Lorenzen, L., Phala, N. S., Smit, J. T., & Schalkwyk, G. A. (2008). Mineralogy and uranium leaching response of low grade South African ores. *Minerals Engineering*(21), 16-22. doi:10.1016/j.mineng.2007.06.006

Machiba, M. D. (2020). *The recovery of gold from tailings material by means of an organic ligand in a gas phase.* Johannesburg, South Africa: The University of the Witwatersrand.

Malloum, A. (2021). *Molecular Physics - ATR523/SMA513.* The University of Maroua, Department of Physics, Faculty of Science. Maroua: Alhadji Malloum, The University of Maroua.

Marcon, G., Carotti, S., Coronnello, M., Messori, L., Mini, E., Orioli, P., . . . Minghetti, G. (2002). Gold(III) Complexes with Bipyridyl Ligands: Solution Chemistry, Cytotoxicity, and DNA Binding Properties. *Journal of Medicinal Chemistry, 45*(8), 1672-1677. doi:10.1021/jm010997w

Mariba, E. R. (2010). *Gas phase extraction of metals from oxides using the ligand acetylacetone.* The University of the Witwatersrand, Engineering and the Built Environment. Johannesburg, South Africa: The University of the Witwatersrand.

Masłowska, J., & Starzyński , S. (1989). Separation of metal acetylacetonates by reversed-phase high-performance liquid chromatography. *Chromatographia*(28), 519-522. doi:10.1007/BF02261075

Meerwein, H. (1933). Über Borfluorid-Verbindungen und die Verwendung des Borfluorids für Synthesen (Vorläuf. Mitteil.)1). *Berichte der deutschen chemischen Gesellschaft (A and B Series)*, 411-414. doi:10.1002/cber.19330660321

Mohammed, F. A., & Abbood, H. I. (2017). Structural and Electronic Properties of Cisplatin Metal Complex: B3LYP-SDD/DFT. *International Journal of Advanced Engineering Research and Science (IJAERS), 4*(7), 82-86. doi:10.22161/ijaers.4.7.12

Muller, A. J. (2021, 8 19). Single Crystal X-Ray Diffraction Image. Gauteng, South Africa: University of Johannesburg.

National Institute of Standards and Technology. (2021). *NIST Chemistry WebBook: NIST Standard Reference Database Number 69.* National Institute of Standards and Technology. doi:10.18434/T4D303

Nunan, T. O., Viana, I. L., Peixoto, G. C., Ernesto, H., Verster, D. M., Pereira, J. H., . . . Teixeira, L. A. (2017). Improvements in gold ore cyanidation by pre-oxidation

with hydrogen peroxide. *Minerals Engineering*(108), 67-70. doi:10.1016/j.mineng.2017.01.006

Ojeda, M. W., Perino, E., & del C. Ruiz, M. (2009). Gold extraction by chlorination using a pyrometallurgical process. *Minerals Engineering*(22), 409-411. doi:10.1016/j.mineng.2008.09.002

Olehile, O. D. (2017). *GAS PHASE EXTRACTION OF VANADIUM FROM SPENT VANADIUM CATALYST AND TANTALUM FROM TANTALUM OXIDE.* Johannesburg, South Africa: The University of the Witwatersrand.

Panias, D., & Neou-Syngouna, P. (1990). Gold extraction from pyrite cinders by high temperature chlorination. *Erzmetall*(43), 41-44.

Pople, J. A., & Beveridge, D. L. (1970). *Approximate Molecular Orbital Theory.* New York: McGraw-Hill.

Potgieter, J. H., Kabemba, M. A., Teodorovic, A., Potgieter-Vermaak, S. S., & Augustyn, W. G. (2006). An investigation into the feasibility of recovering valuable metals from solid oxide compounds by gas phase extraction in a fluidised bed. *Minerals Engineering*(19), 140-146. doi:10.1016/j.mineng.2005.08.002

Qi, S.-C., Hayashi, J.-i., & Zhang, L. (2016). Recent application of calculations of metal complexes based on density functional theory. *RSC Advances*(6), 77375-77395.

Shemi, A., Mpana, R. N., Ndlovu, S., van Dyk, L. D., Sibanda, V., & Seepe, L. (2012). Alternative techniques for extracting alumina from coal fly ash. *Minerals Engineering*(34), 30-37. doi:10.1016/j.mineng.2012.04.007

Sievers, R. E., Ponder, B. W., Morris, M. L., & Moshier, R. W. (1963). Gas Phase Chromatography of Metal Chelates of Acetylacetone, Trifluoroacetylacetone, and Hexafluoroacetylacetone. *Inorganic Chemistry, 2*(4), 693-698.

Skopenko, V. V., Amirkhanov, V. M., Yu Silva, T., Vasilchenko, I. S., Anpilova, E. L., & Garnovskii, A. D. (2004). Various types of metal complexes based on chelating b-diketones and their structural analogues. *Russian Chemical Reviews, 8*(73), 737-752. doi:10.1070/RC2004v073n08ABEH000909

Teimouri, S., Potgieter, J. H., Simate, G. S., Van Dyk, L., & Dworzanowski, M. (2020). Oxidative leaching of refractory sulphidic gold tailings with an ionic liquid. *Minerals Engineering*(156), 106484. doi:10.1016/j.mineng.2020.106484

Tshofu, G. S. (2014). *GREEN EXTRACTION TECHNOLOGY FOR THE EXTRACTION OF IRON FROM IRON ORE FINES.* Johannesburg: The University of the Witwatersrand.

Van Dyk, L., Mariba, E. R., Chen, Y., & Potgieter, J. H. (2010). Gas phase extraction of iron from its oxide in a fluidized bed reactor. *Minerals Engineering*(23), 58-60. doi:10.1016/j.mineng.2009.09.017

Van Mourik, T., Bühl, M., & Gaigeot, M.-P. (2014). Density functional theory across chemistry, physics and biology. *Philosophical Transactions of The Royal Society*, A 372:20120488.

Von Hoene, J., Charles, R. G., & Hickam, W. M. (1958). Thermal Decomposition of Metal Acetylacetonates Mass Spectrometer Studies. *Journal of Physical Chemistry, 62*, 1098-1101.

Wai, C. M., & Wang, S. (2000). Separation of metal chelates and organometalliccompounds by SFC and SFE / GC. *Journal of Biochem. Biophys. Methods*(43), 273-293.

Warneke, J., Van Dorp, W. F., Rudolf, P., Stano, M., Papp, P., Matejc˘´ık, S., . . . Swiderek, P. (2015). Acetone and the precursor ligand acetylacetone: distinctly different electron beam induced decomposition. *Physical Chemistry Chemical Physics - PCCP*(17), 1204-1216. doi: 10.1039/c4cp04239e

Weigend, F., & Ahlrichs, R. (2005). Balanced basis sets of split valence, triple zeta valence and quadruple zeta valence quality for H to Rn: Design and assessment of accuracy. *Pysical Chemistry and Chemical Pysics*(18), 3297-3305. doi:10.1039/B508541A

Whitehead, J. A., Zhang, J., McCluskey, A., & Lawrance, G. A. (2009). Comparative leaching of a sulfidic gold ore in ionic liquid and aqueous acid with thiourea and halides using Fe(III) or HSO5- oxidant. *Hydrometallurgy*(98), 276-280. doi:10.1016/j.hydromet.2009.05.012

Xie, F., Lu, D., Yang, H., & Dreisinger, D. (2014). Solvent Extraction of Silver and Gold From Alkaline Cyanide Solution with LIX 7950. *Mineral Processing and Extractive Metallurgy*(35), 229-238. doi: 10.1080/08827508.2013.825615

Xu, B., Kong, W., Li, Q., Yang, Y., Jiang, T., & Liu, X. (2017). A Review of Thiosulfate Leaching of Gold: Focus on Thiosulfate Consumption and Gold Recovery from Pregnant Solution. *Metals, 7*(6:222). doi:10.3390/met7060222

Yang, Y., Liu, S., Xu, B., Li, Q., Jiang, T., & Lv, P. (2015). Extraction of gold from a low-grade double refractory gold ore using flotation-preoxidation-leaching process. *Rare Metal Technology*, 55-62.

Zharkova, G. I., & Baidina, I. A. (2008). Synthesis and Crystal Structure of (2,2,6,6-Tetramethyl-3-imino4-heptene-5-onata)dimethylgold(III). *Russian Journal of Coordination Chemistry, 34*(6), 395-399.

Zharkova, G. I., Baidina, I. A., & Igumenov, I. K. (2006). X-RAY DIFFRACTION STUDY OF VOLATILE COMPLEXES OF DIMETHYLGOLD(III) DERIVED FROM SYMMETRICAL B-DIKETONES. *Journal of Structural Chemistry*, 1117-1126.

Zharkova, G. I., Baidina, I. A., & Yudanova, T. S. (2010). Synthesis, properties and crystal structures of volatile dimethylgold(III) complexes based on phenyl-containing b-diketones and b-iminoketone. *Polyhedron*, 1049-1054. doi:10.1016/j.poly.2009.12.026

Zhou, Y., Ding, Y., Gao, W., Wang, J., Liu, X., Xian, M., . . . Zhao, G. (2020). Biosynthesis of acetylacetone inspired by its biodegradation. *Biotechnology for Biofuels*, 13:88. doi:10.1186/s13068-020-01725-9

APPENDIX A

Plot data for simulated extraction graphs

The randomly generated values for 'concentration' utilized the following input: =NORMINV(RAND(),5,0.5). Value for 'condensate volume' utilized =RAND(). 'Mass' was calculated as the product of 'concentration' and 'condensate volume'.

Table A-1: Random number generated plot to simulate a first order extraction.

Measurement Number	**'Concentration'**	**'Condensate Volume'**	**'Mass'**	**Cumulative 'Mass'**
1	4.652631	0.159963	0.74425	0.74425
2	4.822676	0.791178	3.815594	4.559845
3	5.281977	0.44744	2.363368	6.923213
4	5.532976	0.800323	4.428168	11.35138
5	4.857239	0.642223	3.119429	14.47081
6	4.801823	0.198163	0.951542	15.42235
7	5.242613	0.465737	2.441679	17.86403
8	5.022929	0.573123	2.878757	20.74279
9	4.293953	0.210989	0.905979	21.64877
10	5.274714	0.913524	4.818577	26.46734
11	4.139069	0.39506	1.635179	28.10252
12	4.545985	0.500629	2.27585	30.37837
13	4.659361	0.474915	2.212802	32.59117
14	4.45741	0.588602	2.623639	35.21481
15	5.469441	0.731772	4.002386	39.2172
16	5.109396	0.84505	4.317693	43.53489
17	5.837272	0.938452	5.478002	49.01289
18	4.791397	0.315379	1.511108	50.524
19	3.834786	0.74812	2.868881	53.39288
20	4.92848	0.461836	2.276148	55.66903
21	5.085162	0.197159	1.002587	56.67162

The following table was generated from raw concentration data obtained from ICP-MS of the condensates sampled for an extraction attempt using hematite with nitrogen as a carrier gas. An arbitrary 'volume collected' value was chosen so that both curves could be easily viewed on the same axis. The focus of the graph was the shape of the curve and the way in which its data was manipulated, the values behind it (except concentration and time) are not important.

Table A-2: Plot data for simulated extraction curve using ICP-MS concentrations from hematite (N_2) extraction experiment.

Metal	**Time** *(min)*	**Concentration** *(µg/L)*	**'Volume collected'**	**'Mass extracted'**	**Cumulative 'mass extracted'**
Copper	30	145.161	40	5806.435518	5806.435518
	60	126.9484047	40	5077.936188	10884.37171
	120	114.3603882	40	4574.415529	15458.78724
	180	91.05919852	40	3642.367941	19101.15518
Iron	30	22461.29065	0.3	6738.387196	6738.387196
	60	22422.65438	0.3	6726.796315	13465.18351
	120	21763.19263	0.3	6528.957788	19994.1413
	180	20921.73186	0.3	6276.519559	26270.66086

APPENDIX B

Density functional theory data

All coordinates presented (Å) were calculated using Gassian16 package (Frisch *et al.* 2019) using generalized-gradient approximation (GGA) function with Perdew-Burke-Ernzerhof (PBEPBE) and triple zeta valence plus smaller sets of polarization functions (Def2TZVP) for all atoms. Atoms are labelled according to their atomic number.

Au(acac) – Au (I) acetylacetonate

6	2.048743000	-0.000002000	0.000015000
6	1.506678000	-1.310245000	0.000005000
6	1.506681000	1.310243000	0.000002000
6	2.482085000	-2.470342000	-0.000013000
6	2.482092000	2.470336000	-0.000002000
8	0.278421000	-1.698915000	0.000014000
8	0.278426000	1.698916000	-0.000007000
1	3.528737000	-2.144502000	-0.000032000
1	2.297364000	-3.098153000	-0.884009000
1	2.297398000	-3.098156000	0.883988000
1	3.528743000	2.144494000	-0.000055000
1	2.297428000	3.098120000	0.884027000
1	2.297351000	3.098181000	-0.883970000
1	3.138606000	-0.000003000	0.000014000
79	-1.063267000	0.000001000	-0.000001000

Au(Sacac) – Au (I) thioacetyl acetonate

6	2.050190000	0.003304000	-0.010236000
6	1.589255000	1.368202000	-0.015032000
6	1.499791000	-1.279893000	0.003993000
6	2.676328000	2.424862000	0.022695000
6	2.488473000	-2.429328000	-0.019352000
8	0.404225000	1.839054000	-0.021797000
1	3.598638000	2.095049000	-0.472706000
1	2.921573000	2.653295000	1.072767000
1	2.308723000	3.347370000	-0.442580000
1	2.972184000	-2.489782000	-1.006962000
1	1.993235000	-3.389210000	0.175657000

1	3.278366000	-2.279419000	0.731107000
1	3.144491000	-0.029565000	-0.014446000
79	-1.052558000	0.185646000	-0.001928000
16	-0.132696000	-1.863066000	0.024465000

Au(Nacac) – Au (I) β-ketiminato substituted variant of acetylacetone

6	-2.010860000	0.102952000	-0.000149000
6	-1.566675000	-1.244691000	-0.000038000
6	-1.388645000	1.381970000	-0.000120000
6	-2.639007000	-2.319481000	0.000032000
6	-2.323523000	2.574808000	0.000135000
8	-0.373509000	-1.736640000	0.000032000
1	-3.656759000	-1.910935000	-0.000271000
1	-2.507770000	-2.960815000	0.884019000
1	-2.507410000	-2.961301000	-0.883543000
1	-2.975210000	2.553106000	-0.885334000
1	-1.768726000	3.523035000	-0.001586000
1	-2.972463000	2.554757000	0.887678000
1	-3.099416000	0.179296000	-0.000210000
7	-0.083109000	1.639276000	-0.000132000
79	1.043699000	-0.052602000	0.000011000
1	0.177586000	2.623235000	-0.000074000

$[Au(acac)_2]^+$ - Au (III) acetylacetonate

6	3.255539000	0.000001000	0.000020000
6	2.631379000	-1.253421000	0.000012000
6	2.631377000	1.253421000	-0.000005000
6	3.447208000	-2.513124000	-0.000004000
6	3.447207000	2.513125000	0.000077000
8	1.355310000	-1.484111000	-0.000004000
8	1.355309000	1.484111000	-0.000042000
1	4.520431000	-2.297936000	0.000215000
1	3.191424000	-3.114985000	-0.884387000
1	3.191092000	-3.115249000	0.884099000
1	4.520429000	2.297937000	-0.000646000
1	3.191799000	3.114668000	0.884790000
1	3.190714000	3.115567000	-0.883695000
1	4.343148000	0.000002000	0.000038000
6	-3.255534000	-0.000001000	0.000017000
6	-2.631375000	-1.253422000	0.000009000
6	-2.631377000	1.253421000	-0.000007000
6	-3.447210000	-2.513122000	0.000068000
6	-3.447212000	2.513120000	0.000008000
8	-1.355306000	-1.484114000	-0.000018000
8	-1.355308000	1.484114000	-0.000033000
1	-3.190913000	-3.115409000	-0.883870000

1	-4.520431000	-2.297931000	-0.000397000
1	-3.191609000	-3.114823000	0.884616000
1	-4.520434000	2.297929000	-0.000135000
1	-3.191156000	3.115202000	-0.884142000
1	-3.191371000	3.115027000	0.884344000
1	-4.343143000	-0.000003000	0.000034000
79	0.000000000	0.000000000	-0.000016000

$Au(acac)_3$ – Au (III) acetylacetonate

6	3.472634000	-0.000682000	-0.000034000
6	2.848959000	-0.599342000	1.105227000
6	2.849158000	0.598205000	-1.105286000
6	3.691053000	-1.205179000	2.198939000
6	3.691453000	1.203737000	-2.199011000
8	1.587751000	-0.708744000	1.322895000
8	1.587986000	0.708068000	-1.322929000
1	4.762070000	-1.067209000	2.014844000
1	3.467922000	-2.279515000	2.272590000
1	3.420784000	-0.749694000	3.162157000
1	4.762421000	1.065301000	-2.014978000
1	3.468778000	2.278173000	-2.272590000
1	3.420938000	0.748422000	-3.162239000
1	4.560710000	-0.000882000	-0.000045000
6	-2.016871000	2.678646000	-0.305727000
6	-1.012266000	3.113298000	0.643098000
6	-2.049482000	1.589122000	-1.153254000
6	-1.362495000	4.379462000	1.417634000
6	-3.200994000	1.442286000	-2.126489000
8	0.082335000	2.564632000	0.852593000
8	-1.218572000	0.582658000	-1.304529000
1	-2.258850000	4.214241000	2.035902000
1	-1.592588000	5.209478000	0.732146000
1	-0.521970000	4.657692000	2.063256000
1	-3.883917000	2.298124000	-2.074897000
1	-3.754223000	0.516250000	-1.910252000
1	-2.808542000	1.353270000	-3.149991000
1	-2.882864000	3.336823000	-0.392913000
79	0.212113000	-0.000064000	0.000009000
6	-2.018054000	-2.677782000	0.305736000
6	-2.050137000	-1.588280000	1.153310000
6	-1.013667000	-3.112862000	-0.643125000
6	-3.201559000	-1.440946000	2.126575000
6	-1.364492000	-4.378835000	-1.417704000
8	-1.218750000	-0.582214000	1.304608000
8	0.081183000	-2.564692000	-0.852615000
1	-3.884861000	-2.296482000	2.074994000

1	-3.754386000	-0.514664000	1.910360000
1	-2.809042000	-1.352110000	3.150068000
1	-2.260781000	-4.213177000	-2.035951000
1	-1.594956000	-5.208771000	-0.732244000
1	-0.524105000	-4.657426000	-2.063350000
1	-2.884352000	-3.335561000	0.392914000

$Au(Sacac)_3$ – Au (III) thioacetyl acetonate

6	2.276423000	2.575186000	0.314382000
6	2.591282000	1.512156000	1.138962000
6	1.012488000	2.947353000	-0.267515000
6	4.004941000	1.405637000	1.667189000
6	0.991685000	4.223824000	-1.085037000
8	-0.066893000	2.316035000	-0.167658000
1	4.578810000	2.319489000	1.461777000
1	4.517196000	0.552600000	1.195860000
1	4.006631000	1.219051000	2.750487000
1	1.650321000	4.995428000	-0.663801000
1	-0.034995000	4.599978000	-1.159454000
1	1.348687000	3.997542000	-2.103436000
1	3.094679000	3.269407000	0.104655000
6	-3.857043000	0.129087000	0.372556000
6	-3.055779000	0.247041000	1.544497000
6	-3.512998000	0.052801000	-0.971769000
6	-3.780484000	0.313314000	2.876765000
6	-4.651946000	-0.061769000	-1.965828000
1	-3.634353000	-0.640332000	3.407462000
1	-4.856170000	0.493155000	2.761941000
1	-3.334046000	1.101903000	3.496888000
1	-5.592233000	0.312115000	-1.538118000
1	-4.794375000	-1.118053000	-2.243524000
1	-4.431097000	0.488765000	-2.889636000
1	-4.930637000	0.108743000	0.572343000
79	-0.216509000	-0.058782000	-0.019858000
6	2.447795000	-2.116970000	-0.602299000
6	1.458348000	-2.860406000	0.091499000
6	2.409762000	-0.953646000	-1.412307000
6	1.814581000	-4.182293000	0.721256000
6	3.626414000	-0.573385000	-2.221544000
8	1.398002000	-0.142817000	-1.582261000
1	2.879786000	-4.408894000	0.568350000
1	1.228305000	-5.013667000	0.292391000
1	1.620125000	-4.184570000	1.806796000
1	3.385247000	-0.575379000	-3.297050000
1	4.462154000	-1.264526000	-2.051642000
1	3.948352000	0.450694000	-1.969432000

1	3.432116000	-2.596890000	-0.593592000
16	-0.232494000	-2.481895000	0.134992000
16	1.569196000	0.244366000	1.675219000
16	-1.985387000	0.037956000	-1.723746000
8	-1.795375000	0.299631000	1.633820000

$Au(Nacac)_3$ – Au (III) β-ketiminato substituted variant of acetylacetone

6	1.381638000	-3.108815000	0.017850000
6	0.320272000	-2.875922000	0.910171000
6	1.828413000	-2.290290000	-1.042992000
6	0.033881000	-3.919653000	1.973088000
6	3.058971000	-2.751633000	-1.798538000
8	-0.468036000	-1.870160000	0.947151000
1	0.677486000	-4.802767000	1.877557000
1	-1.019879000	-4.227273000	1.910883000
1	0.181380000	-3.469243000	2.965847000
1	3.108709000	-3.847107000	-1.850262000
1	3.963540000	-2.399090000	-1.278432000
1	3.076314000	-2.349714000	-2.821188000
1	1.936469000	-4.033975000	0.169266000
6	2.383802000	2.488667000	0.245640000
6	2.479316000	1.391870000	1.168210000
6	1.451421000	2.797788000	-0.771035000
6	3.588422000	1.373785000	2.187730000
6	1.562582000	4.066267000	-1.569143000
8	1.643104000	0.388361000	1.250734000
1	3.179576000	1.427673000	3.211888000
1	4.286558000	2.210969000	2.050546000
1	4.157102000	0.430452000	2.126785000
1	2.440977000	4.652369000	-1.266579000
1	0.672993000	4.710969000	-1.438984000
1	1.653259000	3.865212000	-2.652843000
1	3.168796000	3.238930000	0.377291000
79	-0.065559000	0.048642000	-0.161827000
6	-3.530521000	0.492098000	0.148068000
6	-2.751881000	1.034438000	1.183095000
6	-3.096579000	-0.169492000	-1.023838000
6	-3.468051000	1.674790000	2.358535000
6	-4.170544000	-0.786106000	-1.898854000
8	-1.477026000	1.065937000	1.285132000
1	-4.558372000	1.664550000	2.238718000
1	-3.123595000	2.712507000	2.475496000
1	-3.198445000	1.138663000	3.280226000
1	-5.077504000	-0.167041000	-1.909961000
1	-4.447330000	-1.775347000	-1.502112000
1	-3.821190000	-0.917675000	-2.932250000

1	-4.609617000	0.562431000	0.279623000
7	-1.840821000	-0.308301000	-1.395320000
7	1.270404000	-1.152710000	-1.409348000
7	0.391113000	1.967164000	-1.032745000
1	-0.295852000	2.344782000	-1.688845000
1	1.768402000	-0.649632000	-2.144506000
1	-1.696641000	-0.886259000	-2.223959000